MIXED GAS
PLASTICIZATION PHENOMENA
IN ASYMMETRIC MEMBRANES

The research described in this thesis was supported by the Dutch Technology Foundation STW, applied science division of NWO and the Technology Program of the Ministry of Economic Affairs.

Mixed Gas Plasticization Phenomena in Asymmetric Membranes
T. Visser, PhD Thesis, University of Twente, The Netherlands

ISBN: 90-365-2418-0

Cover: Bundle of P84/Matrimid hollow fiber membranes photographed from above.

Printed by Wöhrmann Print Service, Zutphen, The Netherlands.

MIXED GAS PLASTICIZATION PHENOMENA IN ASYMMETRIC MEMBRANES

PROEFSCHRIFT

ter verkrijging van
de graad van doctor aan de Universiteit van Twente,
op gezag van de rector magnificus,
prof. dr. W.H.M. Zijm,
volgens besluit van het College van Promoties
in het openbaar te verdedigen
op vrijdag 24 november 2006 om 15.00 uur

door

Tymen Visser

geboren op 10 december 1977
te Zevenaar

Dit proefschrift is goedgekeurd door de promotor Prof. Dr.-Ing M. Wessling

Table of contents

Chapter 3

Hollow fiber membranes for gas separation prepared from a P84/Matrimid-blend

Chapter 4

Materials dependence of mixed gas plasticization behavior in asymmetric membranes

Chapter 7

Outlook

Chapter 1

Introduction

Abstract

Membrane-based gas separation applications have a huge market potential for separation of gas streams containing plasticizing gases and vapors. This market will expand when membranes with better stability to these plasticizing gases are developed. However, the phenomenon of plasticization in polymer membranes is not unambiguous yet. Better understanding of the complex behavior of plasticization is highly required to be able to develop more stable membranes, which is the motivation for the research presented in this thesis.

1.1. The market of membrane gas separation

The potential for membranes to effectively separate gas mixtures has been known since the 1940s [1, 2]. Nevertheless, the employment of gas separation membranes in industrial applications has become viable only during the last 25 years. In 1980, Monsanto was the first company to launch a commercial application concerning the recovery of hydrogen in the production of ammonia (H_2/N_2-purge gas separation). Grace, Separex and Cynara followed in the mid 1980s with membrane plants removing CO_2 from natural gas using cellulose acetate (CA) membranes [3], although on a relatively small scale. Other important commercialized membrane gas separation applications are the recovery of

hydrogen in refineries (H_2/CH_4 or H_2/CO) and the enrichment of nitrogen in air (O_2/N_2). Nowadays this latter application comprises about one-half of the total nitrogen production market with around 10.000 membrane systems installed [3]. In the nineties, some small membrane applications such as the dehydration of air or organic vapor removal from air and nitrogen streams were employed in industry as well.

The polymer synthesis community has been heavily involved in synthesizing new polymers in order to tailor mass transport properties. Surprisingly, only 8 or 9 different polymers are used for the currently established membrane-based applications, although many potentially interesting new polymers exist, having much higher permeability and selectivity [3]. However, high intrinsic permeability and selectivity are not the only keys to practical viability. Another important factor is the production of membranes at low costs. Currently used commercial membranes excel in this category due to highly efficient process design and the use of asymmetric or composite asymmetric membranes. To provide economical viable fluxes, the active separation layer should be as thin as possible. This is generally achieved by using asymmetric membranes ideally consisting of an ultra-thin skin layer supported by a highly porous substructure. Typically, asymmetric membranes are prepared using phase separation processes, although other techniques, such as interfacial polymerization, plasma deposition or dip coating are used as well. Nowadays, state of the art asymmetric membranes have skin layers with a thickness less than 1000 Å.

Two-thirds of the total gas separation market is based on only a small number of applications and are generally involving the separation of clean gas streams free of components that may deteriorate the membrane separation performance. However, only small incremental improvements in performance are foreseen in these membrane systems in the next years. A large market potential is predicted for applications involving the separation of gas streams containing high levels of plasticizing, condensable gases and vapors, which are in high levels present in natural gas treatments, refineries and petrochemical plants [4], but typically degrade the membrane performance. The number of applications in this market only expands when better membranes with improved stability to feed streams containing plasticizing gases and vapors are developed.

1.2. The phenomenon of plasticization

In glassy polymers, the phenomenon of plasticization can be attributed to swelling stresses on the polymer network. The addition or sorption of species causes an enhancement of local segmental motion of the polymer chains. On the macro-scale, the polymer glass experiences a weakening or softening effect, which is characterized by a reduction in glass transition temperature and modulus [5]. In polymer science, plasticization is generally considered as a positive and useful feature. The addition of plasticizers (low molecular weight additives) to poly(vinyl chloride) (PVC) depresses the glass transition temperature below room temperature which enables the processing of PVC [6]. In the pharmaceutical world, drug release is enhanced due to plasticization of the polymer matrix as a result of large interactions between the polymer and the drug (e.g. ibuprofen or methylparaben) [7, 8]. Furthermore, high pressure carbon dioxide can be used to impregnate or entrap solutes (e.g. dyes, metal complexes, medicines) in the highly swollen polymer [9-11]. Properties of immiscible blends are often improved by adding compatibilizers to stabilize the interface between the phases. Due to its plasticizing strength, supercritical carbon-dioxide can fulfill the same role as it affects viscosity, swelling and interfacial tension of a polymer melt [12]. It even acts as a highly volatile organic solvent near critical conditions when interacting with polymers.

In membrane science and in particular in gas separation, the phenomenon of penetrant-induced plasticization is generally considered as an undesired, 'negative' feature since it represents losses in membrane performance [13-16]. The increase in local segmental motion of the polymer chains results in enhanced transport rates of all penetrants to be separated. Since the transport rate of a 'slow' penetrant is more affected than that of a 'fast' component, plasticization typically results in a loss of membrane selectivity. For example in CO_2/CH_4-separation, the overall selectivity decreases as the transport rate of the 'slower' component CH_4 is significantly more affected than that of the 'faster' component CO_2 as a result of CO_2-plasticization [13, 17, 18]. In the same way, the C_3H_6/C_3H_8-selectivity drastically decreases as the mobility of the 'slower' component C_3H_8 is significantly more altered [19]. Drastic loss in separation performance can also be caused by the presence of significant amounts of C_{3+}-hydrocarbons (toluene, hexane) or water vapor in the feed gas mixture [20].

1.3. Transport behavior in glassy polymer membranes upon plasticization

1.3.1. Introduction

The analysis of transport behavior in glassy polymer membranes upon plasticization is often complicated, because its effects are often not unambiguous. The presence of plasticization causes clear changes in results obtained from permeation and sorption measurements and therefore these techniques can analyze the transport behavior in polymer membranes very well. To demonstrate the transport behavior upon penetrant-induced plasticization, this section illustrates different effects of plasticization typically observed during gas transport experiments. Many parameters may alter the plasticization behavior of polymer membranes, like for example temperature, pressure, membrane thickness, sample history, feed gas composition and type of gases used [13, 21, 22]. Since this thesis focuses on mixed gas plasticization behavior of asymmetric membranes, this section will only focus on changes due to plasticization in the transport behavior in glassy polymer membranes upon decreasing the membrane thickness and upon the use of single or mixed gas conditions.

1.3.2. Transport behavior in thick dense polymer membranes upon plasticization

Single gas conditions

In gas permeation experiments with dense glassy polymer membranes, the CO_2-permeability decreases with increasing feed pressure due to a faster decrease in solubility than an increase in diffusivity with increasing pressure [23]. At a certain CO_2-pressure, the permeability shows an upward inflection in permeability due to plasticization of the polymer matrix [14, 15]. At this point the increase in diffusivity is stronger than the decrease in solubility, due to highly altered polymer chain mobility. This inflection point – a minimum in the CO_2-permeability as a function of pressure – is often called the plasticization pressure. Above the plasticization pressure, the gas permeability becomes highly time-dependent due to irreversible relaxation of the glassy polymer chains [24]. The plasticization pressure highly depends on the type of polymer used, but one critical gas concentration is required to induce plasticization effects for many different polymers [13].

Since penetrant-induced relaxation of the glassy polymer chain is a very slow process, hysteresis is observed in permeation and sorption experiments upon depressurization in a pressurization/depressurization cycle, because the polymer glass can not relax back to a denser state within the time-scale of the experiment. The magnitude of hysteresis highly depends on the applied maximum pressure [25]. At higher pressures and thus higher concentrations of sorbed gas, the magnitude of hysteresis will be more significant. In sorption experiments, penetrant-induced polymer chain relaxation is observed as additional weight uptake [26] and also requires a critical concentration sorbed gas [27]. Above this gas concentration, the sorption of gas may continue to increase for a very long time. Up to now, the measurement and analysis of sorption-induced relaxations is only reported for vapor sorption [28].

Mixed gas conditions

Mostly, mixed gas transport behavior in polymer membranes can be predicted for rubbery polymers from single gas conditions. However, it generally does not hold for transport behavior in glassy polymer membranes. The use of gas mixtures generally results in significant deviations from ideal transport behavior, due to competition effects between gases permeating through the membrane. Competition results in reduced gas transport compared to single gas experiments because gases compete for sorption sites in the glassy polymer matrix [29-32]. With increasing feed gas concentration of the second component, the magnitude of the reduction increases. On the other hand, penetrant-induced plasticization causes increasing transport rates of all penetrants present in the mixture to separate [13, 33]. Mixed gas transport behavior in glassy polymer membranes will therefore be highly dependent on the used feed gas conditions. Frequently, researchers analyze membrane separation performance by performing single gas experiments only. Since the separation performance will be significantly different using gas mixtures, it is more appropriate to study membrane separation properties using mixed gas conditions.

1.3.3. Plasticization effects in asymmetric or thin film composite membranes

Single gas experiments

Transport behavior in glassy polymer membranes is highly thickness dependent, as these membranes tend to show an accelerated physical aging rate with decreasing thickness, which results in a significant flux reduction [34-37]. Physical aging is often interpreted as a

reduction of the amount of excess free volume in a glassy polymer over time and is therefore related to a suppression of both diffusivity and solubility [38]. The physical aging rate is similar in an integrally skinned asymmetric membrane and composite membrane with thin dense top layer [39]. Generally, physical aging is traced by following gas permeation over time. Recently, sorption experiments with thin glassy polymer films revealed that these thin films indeed have lower solubility than thick films when equally aged [40].

The effects of plasticization are highly thickness dependent as well. The CO_2-plasticization pressure shifts to lower pressures with decreasing top layer thickness using composite membranes with polyimide top layers, as illustrated in Figure 1 [41].

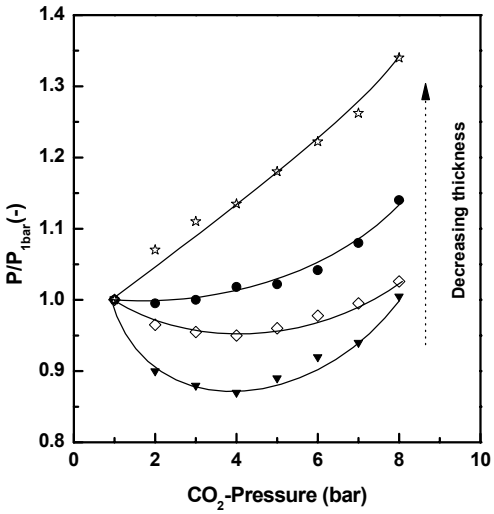

Figure 1: CO_2-permeance, normalized for the initial value at p = 1 bar, as a function of pressure for composite membranes with varying polyimide top layer thicknesses. Data are replotted from [41].

At a certain top layer thickness, no minimum in the CO_2-permeability with increasing pressure is observed anymore. By further decreasing the top layer thickness a continuously increasing CO_2-permeability with increasing pressure is obtained (upper line in Figure 1). Others confirmed this accelerated plasticization effect by using freestanding ultra-thin polyimide films [42]. A continuous increasing CO_2-permeance with increasing pressure is a typical behavior of integrally skinned asymmetric membranes [43-47]. The accelerated plasticization effect is also observed in sorption experiments. Punsalan and Koros found that thin glassy polymer films recover much faster from CO_2-conditioning when compared

to thick glassy polymer films [40], as sorption induced relaxations disappeared much faster after removing the conditioning agent.

Up to the present day, a physical explanation for the accelerated aging and plasticization effect is not found, although some have proposed possible explanations. It is for example proposed that the fractional free volume may be lower or distributed different in dense films than in asymmetric membranes due to a faster aging rate [45], while others suggest that a difference in orientation in the separation layer may exist between membranes made by phase separation or solvent evaporation [48]. Further research is required to uncover the exact physical reasons for these phenomena.

Mixed gas experiments

The mixed gas transport behavior in asymmetric membranes upon plasticization is not often reported. In the few studies existing, asymmetric membranes of cellulose acetate (CA) are usually investigated in the separation of natural gas (CO_2/CH_4) [17, 18, 49, 50]. The accelerated CO_2-plasticization effect, as described previously, is also observed for mixed gas experiments in asymmetric membranes. With increasing CO_2-feed gas concentration, the magnitude of the relative change in CO_2-permeance with increasing pressure becomes larger. Furthermore, the accelerated plasticization effect causes a continuous increase in the permeance of the second component (CH_4) with increasing pressure as well. Consequently, the effects on the mixed gas selectivity in asymmetric membranes are more severe than for thick dense films. Due to the strong effect of plasticization, competition effects hardly influence mixed gas transport behavior in asymmetric CA membranes.

Recently, Kapantaidakis et al. [43] and Barsema et al. [44] showed that CO_2-plasticization appears to be suppressed when using asymmetric membranes based on polyimides in the separation of CO_2/N_2. The CO_2-permeance decreased as a function of pressure, while maintaining high selectivities. This effect was related to competition effects, but was not verified with systematical studies. An explanation for the observed differences in the transport behavior in cellulose acetate and polyimide membranes was also not given.

1.4. Motivation

The motivation to perform the research presented in this thesis is based on the currently published scientific literature. Starting from the year 1960 until present day, over 2700 scientific papers (full papers, communications, reviews, notes, etc.) have been published in many different journals on topics related to transport of gas in a polymer membrane (Table 1, source: www.scopus.com).

Table 1: Papers published on relevant topics in gas separation (source: Scopus).

Topic	# of papers
Gas transport in polymer membranes	> 2700
Mixed gas transport in polymer membranes	772
Gas transport in polymer membranes upon plasticization	91
Mixed gas transport in polymer membranes upon plasticization	49
Mixed gas transport in asymmetric polymer membranes upon plasticization	10

This number would be much higher if the years before 1960 could be included. Out of these 2700 scientific papers, a substantial amount of papers (772) reports the separation performance of polymer membranes using gas mixtures. Only 91 papers are related to plasticization phenomena, while 49 investigate its effects in the mixed gas transport behavior in polymer membranes. Just 2% out of 2700 papers present mixed gas transport behavior in asymmetric polymer membranes in the presence of plasticizing gases, while it resembles real-life (industrial) conditions most and can not be predicted or estimated from single gas experiments or the behavior of thick dense membranes.

Of the papers published on mixed gas plasticization phenomena in asymmetric membranes, just four have systematically studied the effect of feed composition and pressure [17, 18, 49, 50]. However, this was done on asymmetric cellulose acetate membranes and in CO_2-separations only. A thorough study, which systematically investigates the influence of feed composition and pressure on the mixed gas transport behavior of other asymmetric membranes in the presence of plasticizing gases, is highly required. Besides, other feed gas mixtures containing different plasticizing gases (CO_2, C_3H_6, C_3H_8, n-C_4H_{10}, etc.) should be considered as well.

1.5. Scope of this thesis

In **Chapter 2, 'On the subtle balance between competitive sorption and plasticization effects in asymmetric hollow fiber gas separation membranes'**, the mixed gas transport behavior of asymmetric PES/Matrimid hollow fiber membranes in CO_2/CH_4- and CO_2/N_2-separations is studied. Different CO_2/CH_4- and CO_2/N_2-feed compositions are used in order to analyze effects of plasticization and competitive sorption as caused by methane and nitrogen.

Chapter 3, 'Hollow fiber membranes for gas separation prepared from a P84/Matrimid-blend', describes the preparation of a highly selective asymmetric hollow fiber membrane with an ultra-thin skin layer. The ideal separation performance of the prepared fibers is determined and the effect of physical aging is investigated measuring the O_2- and N_2-permeance during several months.

Chapter 4, 'Materials dependence of mixed gas plasticization behavior in asymmetric membranes', investigates and compares the CO_2/CH_4-separation performance of different asymmetric membranes (PPO, CA, Matrimid and blends of Matrimid with PES and P84) at different feed gas compositions. The separation performance is analyzed in terms of CO_2- and CH_4-permeance and mixed gas selectivity and the effect of CO_2-conditioning is identified.

Chapter 5, 'Plasticization of asymmetric P84/Matrimid membranes in C_3-separation', discusses the separation performance of asymmetric P84/Matrimid and Matrimid hollow fibers in the separation of C_3-hydrocarbon feed gas mixtures. The permeance and mixed gas selectivity of a 50/50 vol.% C_3H_6/C_3H_8- and a 50/10/40 vol.% $CH_4/C_3H_8/C_3H_6$-feed gas mixture are measured at different feed gas pressures. The mixed gas results are supported by single gas C_3H_6- and C_3H_8-permeation and sorption experiments.

Chapter 6, 'Sorption-induced relaxations in Matrimid polyimide', finally presents the sorption kinetics of six gases (C_3H_6, C_3H_8, CO_2, Xe, Kr and Ar) in Matrimid polyimide films. Mass uptake is recorded using a gravimetric sorption balance which is able to accurately record the small weight changes induced upon polymer chain relaxation. From the sorption data and values for partial molar volume, dilation isotherms are estimated.

Ultimately, **Chapter 7, 'Outlook',** suggests future research directions based on the findings presented in this thesis. Some preliminary results of scouting experiments support the proposed research directions.

1.6. References

1. R.M. Barrer, *Diffusion in and through solids*, 1941, New York: The University press; Macmillan.
2. G.J. van Amerongen, *The permeability of different rubbers to gases and its relation to diffusivity and solubility*, Rubber Chemistry and Technology **20** (1947), 494-511.
3. R.W. Baker, *Membrane Technology and Applications*, 2nd ed., 2002: Wiley.
4. R.W. Baker, *Future directions of membrane gas separation technology*, Industrial Engineering and Chemical Research **41** (2002), 1393-1411.
5. T.S. Chow, *Molecular interpretation of the glass transition temperature of polymer-diluent systems*, Macromolecules **13** (1980), 362-364.
6. Y. Maeda and D.R. Paul, *Effect of antiplasticization on selectivity and productivity of gas separation membranes*, Journal of Membrane Science **30** (1987), 1-9.
7. C. Wu and J.W. McGinity, *Non-traditional plasticization of polymeric films*, International Journal of Pharmaceutics **177** (1999), 15-27.
8. P.B. O'Donnell, et al., *Aqueous pseudolatex of zein for film coating of solid dosage forms*, European Journal of Pharmaceutics and Biopharmaceutics **43** (1997), 83-89.
9. A.I. Cooper, *Polymer synthesis and processing using supercritical carbon dioxide*, Journal of Materials Chemistry **10** (2000), 207.
10. D.L. Tomasko, et al., *A Review of CO_2 Applications in the Processing of Polymers*, Industrial and Engineering Chemistry Research **42** (2003), 6431-6456.
11. S.G. Kazarian, et al., *In situ spectroscopy of polymers subjected to supercritical CO_2: Plasticization and dye impregnation*, Applied Spectroscopy **51** (1997), 491-494.
12. D.R. Paul and C.B. Bucknall, *Polymer blends*, 2000: John Wiley & Sons.
13. A. Bos, et al., *CO_2-induced plasticization phenomena in glassy polymers*, Journal of Membrane Science **155** (1999), 67-78.
14. E.S. Sanders, *Penetrant-induced plasticization and gas permeation in glassy polymers*, Journal of Membrane Science **37** (1988), 63-80.
15. M. Wessling, et al., *Plasticization of gas separation membranes*, Gas Separation & Purification **5** (1991), 222-228.
16. J.S. Chiou, J.W. Barlow, and D.R. Paul, *Plasticization of glassy polymers by carbondioxide*, Journal of Applied Polymer Science **30** (1985), 2633-2642.
17. M.D. Donohue, B.S. Minhas, and S.Y. Lee, *Permeation behaviour of carbon dioxide-methane mixtures in cellulose acetate membranes*, Journal of Membrane Science **42** (1989), 197-214.

18. E. Sada, et al., *Permeation of pure carbon-dioxide and methane and binary-mixtures through cellulose-acetate membranes*, Journal of Polymer Science Part B-Polymer Physics **28** (1990), 113-125.
19. C. Staudt-Bickel and W.J. Koros, *Olefin/paraffin gas separations with 6FDA-based polyimide membranes*, Journal of Membrane Science **170** (2000), 205-214.
20. L.S. White, et al., *Properties of a polyimide gas separation membrane in natural gas streams*, Journal of Membrane Science **103** (1995), 73-82.
21. A.F. Ismail and W. Lorna, *Penetrant-induced plasticization phenomenon in glassy polymers for gas separation membrane*, Separation and Purification Technology **27** (2002), 173-194.
22. D.W. Wallace, et al., *Characterization of crosslinked hollow fiber membranes*, Polymer **47** (2006), 1207.
23. D.R. Paul and Y. Yampolskii, *Polymeric Gas Separation Membranes*, 1994, Boca Raton: CRC Press.
24. M. Wessling, et al., *Time-dependent permeation of carbon-dioxide through a polyimide membrane above the plasticization pressure*, Journal of Applied Polymer Science **58** (1995), 1959-1966.
25. S.M. Jordan, G.K. Fleming, and K.J. Koros, *Permeability of carbon dioxide at elevated pressures in substituted polycarbonates*, Journal of Polymer Science, Part B: Polymer Physics **28** (1990), 2305-2327.
26. H.L. Frisch, *Sorption and transport in glassy polymers - a review*, Polymer Engineering and Science **20** (1978), 2-13.
27. M. Wessling, et al., *Dilation kinetics of glassy, aromatic polyimides induced by carbon-dioxide sorption*, Journal of Polymer Science Part B-Polymer Physics **33** (1995), 1371-1384.
28. A.R. Berens and H.B. Hopfenberg, *Diffusion and relaxation in glassy polymer powders: 2. Separation of diffusion and relaxation parameters*, Polymer **19** (1978), 489-496.
29. P.C. Raymond, W.J. Koros, and D.R. Paul, *Comparison of mixed and pure gas permeation characteristics for CO_2 and CH_4 in copolymers and blends containing methyl methacrylate units*, Journal of Membrane Science **77** (1993), 49-57.
30. E.S. Sanders, S.M. Jordan, and R. Subramanian, *Penetrant-plasticized permeation in polymethylmethacrylate*, Journal of Membrane Science **74** (1992), 29-36.
31. R.T. Chern, et al., *Selective Permeation of CO_2 and CH_4 through Kapton Polyimide: Effects of Penetrant Competition and Gas-Phase Nonideality*, Journal of Polymer Science: Polymer Physics Edition **22** (1984), 1061-1084.
32. W.J. Koros, et al., *Model for permeation of mixed gases and vapors in glassy polymers*, Journal of Polymer Science, Polymer Physics Edition **19** (1981), 1513-1530.
33. J.D. Wind, D.R. Paul, and W.J. Koros, *Natural gas permeation in polyimide membranes*, Journal of Membrane Science **228** (2004), 227-236.

34. P.H. Pfromm and W.J. Koros, *Accelerated physical ageing of thin glassy polymer films: evidence from gas transport measurements*, Polymer **36** (1995), 2379-2387.
35. M.S. McCaig and D.R. Paul, *Effect of film thickness on the changes in gas permeability of a glassy polyarylate due to physical aging Part I. Experimental observations*, Polymer **41** (2000), 629-637.
36. K.D. Dorkenoo and P.H. Pfromm, *Experimental evidence and theoretical analysis of physical aging in thin and thick amorphous glassy polymer films*, Journal of Polymer Science Part B-Polymer Physics **37** (1999), 2239-2251.
37. K.D. Dorkenoo and P.H. Pfromm, *Accelerated physical aging of thin poly 1-(trimethylsilyl)-1- propyne films*, Macromolecules **33** (2000), 3747-3751.
38. Y. Huang, X. Wang, and D.R. Paul, *Physical aging of thin glassy polymer films: Free volume interpretation*, Journal of Membrane Science **277** (2006), 219-229.
39. M.E. Rezac, et al., *Aging of thin polyimide-ceramic and polycarbonate-ceramic composite membranes*, Industrial & Engineering Chemistry Research **32** (1993), 1921-1926.
40. D. Punsalan and W.J. Koros, *Thickness-dependent sorption and effects of physical aging in a polyimide sample*, Journal of Applied Polymer Science **96** (2005), 1115-1121.
41. M. Wessling, M. Lidon Lopez, and H. Strathmann, *Accelerated plasticization of thin-film composite membranes used in gas separation*, Separation and Purification Technology **24** (2001), 223-233.
42. C. Zhou, et al., *The accelerated CO_2 plasticization of ultra-thin polyimide films and the effect of surface chemical cross-linking on plasticization and physical aging*, Journal of Membrane Science **225** (2003), 125-134.
43. G.C. Kapantaidakis, et al., *CO_2 plasticization of polyethersulfone/polyimide gas-separation membranes*, Aiche Journal **49** (2003), 1702-1711.
44. J.N. Barsema, et al., *Preparation and characterization of highly selective dense and hollow fiber asymmetric membranes based on BTDA-TDI/MDI co-polyimide*, Journal of Membrane Science **216** (2003), 195-205.
45. P.H. Pfromm, I. Pinnau, and W.J. Koros, *Gas-Transport through Integral-Asymmetric Membranes - a Comparison to Isotropic Film Transport-Properties*, Journal of Applied Polymer Science **48** (1993), 2161-2171.
46. T.-S. Chung, et al., *Development of asymmetric 6FDA-2,6DAT hollow fiber membranes for CO2/CH4 separation: Part 2. Suppression of plasticization*, Journal of Membrane Science **214** (2003), 57-69.
47. E. Sada, H. Kumazawa, and P. Xu, *Permeation of carbon dioxide through homogeneous and asymmetric polysulfone membranes*, Journal of Polymer Science part B: Polymer Physics **27** (1989), 919-927.
48. I. Pinnau and W.J. Koros, *A Qualitative Skin Layer Formation Mechanism for Membranes Made by Dry Wet Phase Inversion*, Journal of Polymer Science Part B-Polymer Physics **31** (1993), 419-427.

49. S.Y. Lee, B.S. Minhas, and M.D. Donohue, *Effect of gas composition and pressure on permeation through cellulose acetate membranes*, AiChE Symposium Series **84** (1989), 93-99.
50. R. Wang, et al., *Characterization of hollow fiber membranes in a permeator using binary gas mixtures*, Chemical Engineering Science **57** (2002), 967-976.

Chapter 2

On the Subtle Balance between Competitive Sorption and Plasticization Effects

Abstract

The paper describes the influence of a varying feed composition of CO_2/CH_4- and CO_2/N_2-mixtures on the gas separation performance of integrally skinned asymmetric PES/PI hollow fibers with an effective skin thickness of 0.27 μm. Normally, thin membrane structures (< 3 μm) show accelerated plasticization behavior induced by CO_2 in pure gas measurements. This study shows that introducing an inert gas to the CO_2 feed mixture apparently suppresses plasticization. This effect is more pronounced at higher concentrations inert gas, supported by a continuous drop in CO_2-permeance as a function of CO_2-partial pressure. At a concentration of 80% inert gas in the feed mixture, the CO_2-permeance reduces more than 35% from its initial value, whereas the reduction is 8-10% with 2% inert gas in the feed mixture. However, a mixed gas permeation model predicts for all experimentally used gas compositions similar decreases in CO_2-permeance. Plasticization effects seem to be counterbalanced by competitive sorption. This effect becomes larger with increasing inert gas concentration. At 80% inert gas the plasticization appear to be completely counterbalanced by

competitive sorption. Besides that, for all gas compositions, the separation factor decreases with increasing feed pressure, generally assumed as an indication of plasticization. However, such a selectivity decrease is also predicted by the dual mode sorption model, which neglects effects of plasticization.

More pronounced indication of plasticization effects is observed when the N_2-permeance decay is followed in time after the membrane has been in contact with CO_2 at elevated CO_2-partial pressures. A significant enhanced N_2-permeance is observed due to polymer network dilation, which decreases very slowly in time. There seems to be a subtle balance between plasticization and competitive sorption during mixed gas experiments with integrally skinned asymmetric hollow fibers, which results in the observed phenomenon.

Keywords: Gas separation, hollow fiber membranes, carbon dioxide, plasticization, natural gas

2.1. Introduction

Over the last fifteen years polymeric gas separation membranes have demonstrated to be a viable separation medium contributing to sustainable chemical engineering [1]. However, the operating range and diversity of membrane materials remain limited; only eight or nine different polymers are used for 90% of all gas separation applications [1]. Many more high performance polymers have been tailor-made, but are often too expensive to produce on a commercial scale. On the other hand, plasticization resistance is needed for industrial application of potential separations such as CO_2/CH_4, propylene/propane or other higher hydrocarbon mixtures. For example, cellulose acetate membranes are frequently used for natural gas applications, but plasticize under operating conditions resulting in very low separation factors (α_{CO_2/CH_4} = 12-15). The presence of highly sorbing condensable gases results in loss of product and selective properties, caused by an enhanced mobility of the polymeric membrane matrix. The development of stable polymeric membrane materials with separation factors of 40 under operating conditions would definitely boost the number of commercial natural gas applications [1].

Typically, a minimum in the CO_2-permeance versus CO_2-feed pressure is considered as a characteristic behavior for plasticization. At elevated feed pressures, the permeability increases since the diffusion coefficient increases due to a higher concentration of CO_2 in

the polymeric matrix, whereas the solubility coefficient does not change much with pressure. The pressure at which the minimum occurs is called the plasticization pressure [2]. Most papers studying plasticization use thick dense films and mostly pure gas experiments to characterize the phenomenon of plasticization in their membranes. Bos et al. [2] suggested that glassy polymers plasticize at about the same CO_2-concentration, but need different partial pressures to reach it.

Others describe plasticization effects in thick films in the presence of a second inert component (gas mixtures) and show that the permeation rates of both gases are affected. Bos et al. [3] showed that Matrimid (a commercial polyimide) is plasticized by CO_2 in a mixture of 55/45 mol% CO_2/CH_4. Due to swelling of the polymer matrix and the associated local polymer mobility, the permeability of the slower component CH_4 increases to a larger extent than CO_2, leading to decreasing (diffusivity) selectivity. Therefore, pure gas measurements greatly over-predict the real selectivity due to plasticization. This is in agreement with data from Raymond et al. [4] who investigated the separation of CO_2 and CH_4 using pure gases as well as gas mixtures in copolymers and methyl methacrylate containing blends. All blends were plasticized after reaching a certain CO_2-partial pressure, which always resulted in lower separation factors compared to pure gas measurements. Staudt-Bickel and Koros [5] reported a CO_2/CH_4-separation factor of 4 under mixed gas conditions at a feed pressure of 17.5 atm using an aromatic polyimide (6FDA-mPD), whereas the ideal separation factor of this polymer was about 60, calculated from pure gas permeances. They also found a drastic decreasing selectivity in the case of the separation of propylene/propane mixtures in 6FDA-based polyimide (PI) membranes [6]. Sada et al. [7], Lee et al. [8] and Donohue et al.[9] studied the effect of feed pressure and gas composition on the CO_2/CH_4-separation performance of homogeneous and asymmetric dense cellulose acetate membranes. They all reported an increase in CH_4-permeability with increasing feed mixture pressure for all used gas compositions, indicating plasticization effects for all gas mixtures. Upon increasing the CH_4-concentration of the gas mixture, the CO_2-permeance is reduced as a result of competitive sorption. Furthermore, the separation factor decreased drastically with increasing feed mixture pressure, which was most significant for the mixture containing the highest concentration CO_2.

Industrial gas separation applications require composite membranes with thin dense top layers or integrally skinned asymmetric hollow fibers. However, the behavior of integrally thin-skinned (δ < 0.5 μm) or thin dense (δ < 3 μm) polymer films may be different from thick dense polymer films, as the physicochemical properties are different from polymer bulk properties. One example is the thickness dependence of the glass transition temperature in thin polymer films. Forrest and Dalnoki-Veress [10] observed a T_g-reduction with decreasing polymer film thickness (δ < 0.3 μm), which was explained by polymer chain confinement [11].

In membrane gas separation experiments also evidence was found for difference in polymer properties between thick and thin polymer films. Jordan et al. [12] used CO_2 as a conditioning agent to enhance the transport of O_2 and N_2 in thick dense films and asymmetric hollow fibers and recognized that lower CO_2-pressures were needed to induce swelling effects for asymmetric hollow fibers than for thick dense films. They hypothesized that the dense skin of an asymmetric hollow fiber consists of layers of nodules that are interconnected by polymer chains. These loosely packed chains are susceptible to movement and structural change by the highly sorbing CO_2. However, Shishatskii et al. [13], who investigated the effect of film thickness on material density, showed that a decreasing thickness resulted in an increase of cohesive energy density (CED) and consequently a higher gas solubility and lower gas diffusivity for the thin material. This was verified by Dorkenoo and Pfromm [14], who characterized physical aging by gas permeation experiments in poly[1-(trimethylsilyl)-1-propyne] films. The activation energies for permeation were often significantly higher for thin-skinned membranes, implying higher cohesive energy densities (CED), due to a lower free volume in comparison to the bulk polymer. Besides that, Pfromm et al. [15] observed an increased permselectivity for O_2 and N_2 in asymmetric PSf films compared to the isotropic properties due to increased activation energies for permeation. Furthermore, Pfromm and Koros [16] found proof from permeation experiments that physical ageing in thin glassy polysulfone and polyimide membranes (0.5 μm) is accelerated. Possibly, non-equilibrium excess free volume of the glassy polymeric material might eliminate over time at the surface of the films like a diffusion-like process [17].

Besides physical ageing and other physicochemical properties, also plasticization behavior is thickness dependent, as observed by Wessling et al. [18]. They showed that the CO_2-permeability in composite membranes, consisting of PI top layers (thickness between 1.5 and 4 microns) and a PDMS support film continuously increased with feed pressure, and became more pronounced with decreasing PI layer thickness. It was hypothesized by Pfromm and Koros [16] that, due to elimination of Langmuir sorption sites as a consequence of accelerated aging (the polymer may be locally more ordered due to aging), there is less CO_2 needed to induce plasticization. On the other hand, Shishatskii et al. [13] reported an increasing solubility with increasing density (as a consequence of decreasing film thickness). They suggested that this was due to increases in the cohesion energy density. The inverted pressure dependence on CO_2-permeability was also found by Pfromm et al. [15] in an asymmetric PEC film. A combination of factors would explain the unusual shape of this curve, such as a different distribution of free volume, a different orientation of the polymer molecules in the skin layer, a lower free volume in the skin layer and a smaller number/size of hypothetical Langmuir sites.

Generally, all known methods to suppress plasticization (annealing [19], thermally or chemically cross-linking [20],[21]), inter-penetrating networks [22] or polymer blending [23],[24]) lead to reductions in permeability, due to densification of the material. However, depending on the experimental conditions, plasticization may also be suppressed by using a gas mixture as touched upon by Kapantaidakis [25] and Barsema [26]. They found that plasticization of integrally skinned asymmetric hollow fibers of polyethersulfone/polyimide (Matrimid 5218) and P84 (co-PI, Lenzing) seems to be suppressed when CO_2/N_2-mixtures of 55/45 wt.% and 80/20 wt.% are used. The CO_2- and N_2-permeability decreased slightly as a function of the CO_2-partial pressure over the whole pressure range (1-20 bar) studied, both in the same order, leading to a constant separation factor. This observed phenomenon was hypothesized to be based on competitive sorption. The same explanation was given by Vu et al. [27] for the observed depression of the CO_2-permeance as a function of pressure (7-55 bar) using Matrimid polyimide hollow fibers in a 10% CO_2/90% CH_4 gas mixture. Their CO_2/CH_4 separation factor kept nearly constant up to 40 bar. Yoshino et al. [28] performed gas separation experiments in integrally skinned asymmetric hollow fibers with 50/50 mol% binary mixtures of C_3H_6/C_3H_8 and C_4H_6/C_4H_{10} and observed no plasticization effects for the first mixture, but strong plasticization effects for the second (pressure range 1-5 bar). On

the other hand, Wang et al. [29] investigated the true separation performance of 6FDA-based polyimide hollow fiber membranes in a binary (40/60 mol%) gas mixture of CO_2 and CH_4 and did observe plasticization effects. They hypothesized that plasticization, which increased the permeability, offsets the combined effects of competitive sorption and non-ideal gas behavior (especially in a gas mixture), which normally both decrease the permeability. However, their gas permeation results were reported at one partial CO_2-pressure (13.9 bar) and were compared to pure gas permeation results at the accompanying partial pressure (5.5 bar).

Some publications report no plasticization for CO_2/N_2-mixtures, whereas for CO_2/CH_4-mixtures proof of plasticization was reported by other researchers. It is clear that a detailed investigation is required to quantify the effect of the presence of an inert gas (N_2 and CH_4) on plasticization in asymmetric integrally-skinned membranes. Besides that, it has to be investigated whether any indication of plasticization can be found. Possibly, plasticization effects are masked or need higher partial CO_2-pressure to induce it, as competitive sorption results in lower CO_2-concentrations in the polymer. Therefore, the main objective of this paper is to investigate thoroughly the influence of the inert gas concentration in several CO_2-mixtures on the plasticization effect of polyethersulfone/polyimide integrally skinned asymmetric hollow fibers.

2.2. Experimental

2.2.1. Hollow fiber preparation

Asymmetric hollow fibers were prepared by a dry/wet spinning technology, of which details can be found in literature [30]. An 80/20 wt. % blend of polyimide (PI, Matrimid 5218, Vantico AG) and polyethersulfone (PES, Sumikaexcel, Sumitomo) was dissolved in a mixture of NMP and acetone (45 and 29 wt. % respectively). The polymer blend concentration in the spinning dope was 26 wt. %. The volatile component acetone was added to obtain a defect-free top layer structure [19]. A mixture of NMP/H_2O (80/20 wt. %) was used as the internal coagulant, leading to an open internal structure. Furthermore, the spinning dope was kept constant at a temperature of 50°C to promote acetone evaporation in the air gap by using a chimney. Due to the chimney, the air gap was fixed at a height of 20 cm. The coagulation bath consisted of tap water (T=23°C) and the

relative humidity in the spinning room was 68%. A tube-in-orifice spinneret was used with an outer diameter of 0.5 mm and an inner diameter of 0.2 mm.

2.2.2. Hollow fiber structure analysis

The prepared fibers' geometry and morphology were determined by using scanning electron microscopy (SEM, Jeol JSM-T220). Samples were prepared by freeze fracturing pieces of fibers using liquid nitrogen and subsequently sputtering a thin layer of gold using a Balzer Union SCD 040 sputtering device. Figure 1 shows cross-sections of the prepared hollow fibers by SEM, indicating that the fibers are free of macro-voids and have uniform geometry with an outside diameter of 550 μm and a wall thickness of 80 μm. Furthermore, the morphology is clearly asymmetric with a dense skin at the outside of the fiber. The fibers withstand a maximum pressure difference of 20 bar. Above this pressure difference the fiber wall collapses.

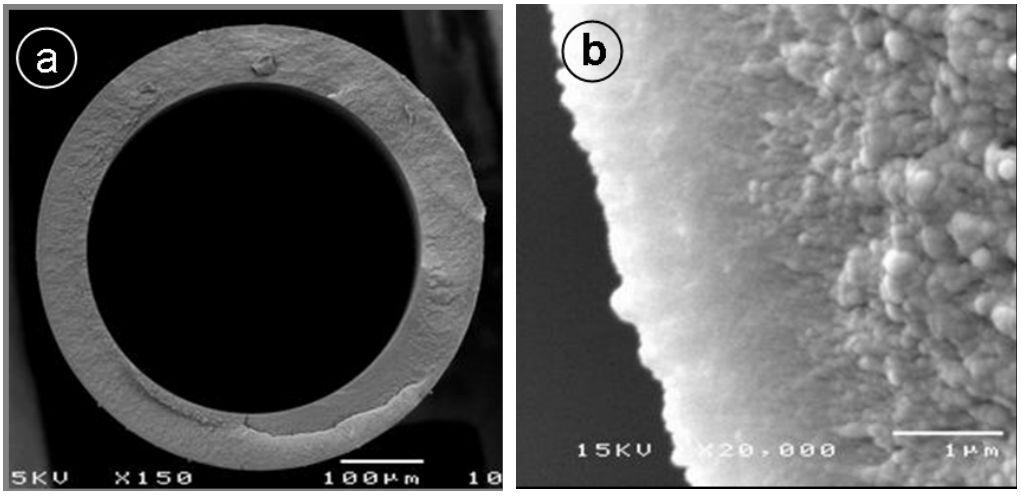

Figure 1: SEM-pictures of (a) geometry and (b) morphology of integrally skinned asymmetric PES/PI hollow fibers.

2.2.3. High pressure gas sorption

Gas sorption isotherms at 35°C of N_2, CH_4 and CO_2 in a thick dense PES/PI film (a piece of 0.3 g, 30 μm thick) were determined by a magnetic suspension balance (MSB, Rubotherm). High accuracies can be reached, as the microbalance is separated from the sample and measuring atmosphere [31]. The mass change of samples in the measuring cell is transmitted through the wall of the pressure vessel by an electromagnet/permanent

magnet pair. The microbalance operates at ambient conditions, as it is located outside the measuring cell, whereas the pressure vessel can be used at a wide range of pressures and temperatures (vacuum < p < 150 bar, -40°C < T < 150°C). The measuring principle contains two steps or two positions of the permanent magnet. In the first position, the zero-point position, only the permanent magnet is freely suspended. The sample rests on a fixed support in the cell. In this position, the balance is set to the tare (empty weight) and is calibrated. In the second position, the sample is picked up towards a controlled position change of the permanent magnet and the mass change can be weighed in time. The measurement procedure can be divided into five steps:

1) Evacuating of pressure vessel and sample for at least 24 hours;
2) Increasing gas pressure to desired value;
3) Waiting until equilibrium in mass change is reached;
4) Record equilibrium mass, temperature and pressure;
5) Repeating step 2 and 3 or if the maximum pressure is reached: evacuate sample (step 1) and start measurement with new gas or new sample.

According to Archimedes' principle, the equilibrium mass increase has to be corrected for buoyancy. This is done by subtracting the weight at zero sorption at a certain pressure from the vacuum weight of the sample. The density of the sample is determined at room temperature using a Micromeritics AccuPyc 1330 pycnometer. With the corrected equilibrium weight increase and the density of the polymer the solubility and solubility coefficient are calculated.

The sorbed amount of gas (C) of pure gases in polymers as function of the pressure (p) can be represented by the dual mode sorption model [32], based on Henry's law and the Langmuir model, and can be written as

$$C = k_D p + \frac{C_H' \cdot b \cdot p}{1 + b \cdot p} \qquad (1)$$

where k_D, C_H', and b are the pure component values of the Henry's law, Langmuir capacity and Langmuir affinity parameter, respectively. These parameters can be

determined from the measured sorption data. The sorption of gas mixtures is more complex as competitive sorption occurs. Nonetheless, the dual mode sorption parameters can be used to estimate its behavior and are used to model permeation trends. The model does not correct for plasticization phenomena.

2.2.4. Gas permeation

Single gas experiments

The permeation characteristics of the prepared hollow fibers were determined in a thermostated high pressure set up (up to 60 bar) by using the variable pressure method as described by Kapantaidakis and Koops [33]. Five fibers of each 15 cm long were potted into 3/8 inch stainless steel holders, while sealing the other side by using an epoxy resin. Gas permeance values of successively N_2, CH_4, O_2 and CO_2 were determined at a pressure of 4 bar and a temperature of 35°C. All gases were obtained from Praxair. The hollow fiber membrane modules were pressurized from the shell side. The gas permeance (P/l) values were calculated from the steady-state pressure increase in time in a calibrated volume at the permeate side. The thickness of the asymmetric skin was calculated by dividing the intrinsic permeability coefficients of the blended material by the determined permeance value for the asymmetric fiber. The intrinsic permeation properties were obtained by measuring the gas permeance of 20-25 μm thick dense films, cast on a glass plate using a solution of 15 wt.% (80/20 wt.%) PES/PI in NMP and a casting knife of 0.3 mm. The ideal selectivity was determined from the ratio of pure gas permeance values obtained at 4 bar. The ideal separation factor of O_2 and N_2 was used to determine whether the membranes were defect-free. Only defect-free membranes were used in this study. Furthermore, the pressure dependence on the pure gas permeance of N_2, CH_4 and CO_2 in the prepared hollow fibers was determined up to 20 bar feed pressure. To identify hysteresis effects for pure CO_2, pressurization and depressurization steps were taken with two new membrane modules, in which the permeance was always measured after conditioning the membranes for 90 minutes. The membrane module was kept at the highest pressure (16 bar) for 16 hours to check time dependency of conditioning. Subsequently, the N_2-permeance was measured overnight, where after the CO_2-permeance at 4 bar was measured again.

Mixed gas experiments

For experiments with gas mixtures new membrane modules were prepared to guarantee having membranes without permeation history [16], [34]. Two different CO_2-mixtures (N_2 and CH_4) were used to investigate the influence of the type of inert gas. Four different inert gas/CO_2-compositions (98/2, 80/20, 50/50 and 20/80) were used in these experiments. The gas mixtures were all obtained from Praxair. The concentrations of the gas mixtures were analyzed by Praxair and had relative errors of less than 2%. In every gas separation experiment two similar membrane modules were measured simultaneously. The gas separation performance was determined according to the following protocol:

1) Thorough degassing and evacuation;
2) Determination of permeance properties with successively N_2 and O_2 at 4 bar to check for defects;
3) Degassing for at least one hour;
4) Determination of separation performance of CO_2/inert gas mixture at 4 bar for at least 6 hours;
5) Measuring N_2-permeance decay overnight (about 16 hours);
6) Thorough degassing and evacuation for at least 30 minutes;
7) Increasing CO_2/inert gas-pressure to next pressure (e.g. 8 bar);
8) Repeating step 5, 6 and 7 up to the maximum pressure (16 or 20 bar depending on the condition of the fibers in the membrane module).

The retentate flow rate was kept constant between 50 and 100 ml/min to prevent influence of stage-cut (lower than 0.01) and to ensure a constant feed composition across the membranes. The hollow fiber membrane modules were always pressurized from the shell side. The feed and permeate compositions were analyzed by means of a Perkin-Elmer gas chromatograph (GC) equipped with a HayeSep Q column. The GC was calibrated with the gas mixtures obtained from Praxair. The separation factor (⟨) was calculated according to:

$$\alpha = \frac{y_A / y_B}{x_A / x_B} \qquad (2)$$

where x and y are the feed and permeate side and A is CO_2 and B is N_2 or CH_4, respectively. The temperature was kept constant at a temperature of 35°C. To take into account the time dependency of conditioning and guarantee the consistency of the permeance data, permeance values were collected after measuring for six hours. Due to this conditioning effect by CO_2, the polymer loses the ability to return into the original state within relatively short time scales after degassing [34]. Therefore, an additional indication for plasticization can be found by measuring the N_2-permeance decay in time directly after a gas separation experiment with CO_2. When plasticization has occurred, the N_2-permeance should be significantly higher than its original value and decrease very slowly in time [26].

2.2.5. Non-ideality

When working with gas mixtures at elevated pressures, one needs to take into account the non-ideal behavior of these mixtures. It is more appropriate to express the permeation driving force in terms of a fugacity rather than a partial pressure difference. Therefore, CO_2-fugacity coefficients were calculated for pure CO_2 and mixtures of CO_2/CH_4 and CO_2/N_2 with the process simulator program Hysys® using Equation-of-States (EoS). The EoS of Peng-Robinson [35] and Soave Redlich Kwong [36] were used for these calculations. Both models gave similar results. The CO_2-fugacity coefficient deviates more than 20% from the ideal values in the pressure range used. The two inert gases CH_4 and N_2 behave only slightly different from ideal gas behavior (maximum of 5% for CH_4 and 2% for N_2). Furthermore, the CO_2-fugacity coefficient (derived from the compressibility factor) in CO_2-mixtures increases with increasing content of inert gas. The CO_2/CH_4 gas mixtures behave more non-ideal than the CO_2/N_2 mixtures, especially at higher concentrations inert gas. However, as the difference is not that large, the driving force will not vary much for the gas compositions. The partial pressure differences used in the experiments are corrected for the calculated non-ideality and will be expressed in terms of fugacities.

2.3. Results and Discussion

2.3.1. Single gas experiments

High pressure gas sorption

The sorption isotherms at 35°C of CO_2, CH_4 and N_2 in a 80/20 wt.% PES/PI film are shown in Figure 2. The maximum pressure used was 50 bar. Clearly, CO_2 has the highest solubility in PES/PI, whereas CH_4 is sorbing more than N_2. The polymer will be significantly dilated by the sorbed CO_2. Subsequent stepwise desorption leaves extra free volume in the polymer matrix. The polymer chains can not relax back to a denser matrix in the time scale of these measurements, causing hysteresis between sorption (closed stars in Figure 2) and desorption (open stars in Figure 2) [37]. The obtained sorption isotherms were fit by the dual mode sorption model [32], of which the parameters can be found in Table 1. (For CO_2, also the desorption curve was fitted according to this model.) The model parameters are used later to estimate permeation properties as a function of feed pressure.

Table 1: Dual mode sorption parameters for CO_2, CH_4 and N_2 in a film of a 80/20 wt.% PES/PI-blend.

Gas	$k_D \left(\frac{cm^3(STP)}{cm^3 bar}\right)$	$C'_H \left(\frac{cm^3(STP)}{cm^3}\right)$	$b\ (bar^{-1})$
CO_2	0.73	32.31	0.17
CH_4	0.177	11.5	0.055
N_2	0.13	3.19	0.23

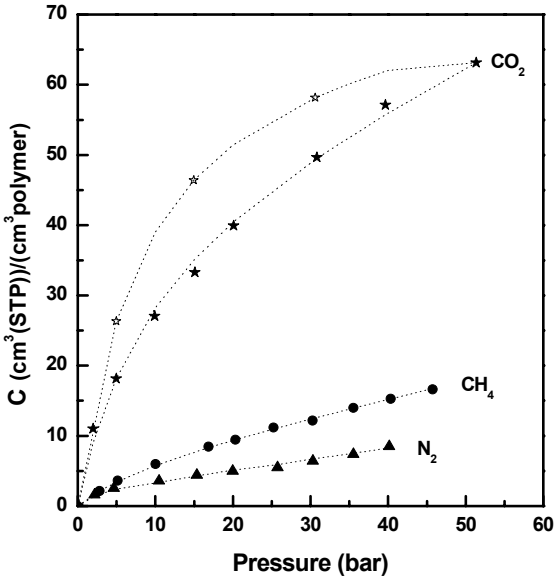

Figure 2: Sorption isotherms at 35°C of CO_2, N_2 and CH_4 in a film of PES/PI. The dotted lines are model lines, which are fitted according to the dual mode sorption model. The open stars represent the solubility during desorption.

Single gas permeation performance

Permeation properties were measured with three different dense thick films and integrally skinned asymmetric hollow fiber membrane modules. Table 2 shows the average results from these gas permeation experiments (1 GPU (gas permeation unit) is 10^{-6}·cm^3(STP)/cm^2·s·cmHg or 7.610^{-12}·m^3(STP)/m^2·s·Pa). Fibers were taken as defect-free when the O_2/N_2-separation factor was $\alpha \geq 6.7$. This value has been reported in literature for defect-free asymmetric hollow fibers prepared according to the same spinning procedure and dope properties [19]. Therefore, the results in Table 2 show that the used hollow fibers have a defect-free skin and do not have to be coated or cured afterwards. From the permeation values the skin thickness has been calculated to be 0.27 µm. Furthermore, it can be seen that this material has an ideal selectivity of 30 for CO_2/N_2 and 40 for CO_2/CH_4.

Table 2: Gas permeation properties (at 4 bar) of 80/20 wt.% PES/PI dense films and asymmetric hollow fibers.

Membrane structure	P_{N_2}	P_{O_2}	P_{CH_4}	P_{CO_2}	α_{O_2/N_2}	α_{CO_2/N_2}	α_{CO_2/CH_4}	Δx *(μm)*
Dense film (P in Barrer)	0.11	0.86	0.08	3.44	6.8	31	40	20-50
Hollow fibers (P in GPU)	0.38	2.6	0.29	11.5	6.7	30	40	0.27

Furthermore, the pressure dependence of the CO_2-, N_2- and CH_4-permeance was measured of the prepared asymmetric hollow fibers (Figure 3). The CO_2-permeance was always measured after six hours of conditioning in agreement with the mixed gas measurements. Figure 3 shows clearly accelerated plasticization by pure CO_2, which is typical for thin dense films [18] and asymmetric membranes [15]. No permeability decrease or minimum can be observed; instead it increases immediately. The N_2- and CH_4-permeance decrease as a function of pressure, where the decrease is the largest for N_2. This is in accordance with the trends predicted by the dual-mode sorption model. When the hypothetical CO_2/N_2- and CO_2/CH_4-separation factors are plotted as a function of pressure (Figure 3), a sharp increase in separation factor is observed. These curves show the typical over-prediction of the real mixed gas separation factor when using single gas permeances.

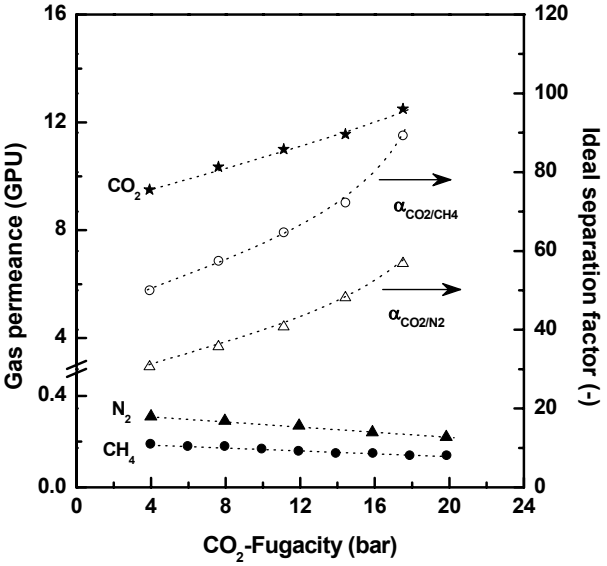

Figure 3: Single gas permeance and ideal separation factor as a function of pressure for N_2, CH_4 and CO_2.

Figure 4 shows the gas permeation results of increasing and subsequently decreasing the CO_2-pressure. Again, a typical upward curvature is observed when the pressure is increased stepwise. As the CO_2-conditioning time for each pressure was only 90 minutes, the absolute increase in permeance is lower than the one observed in Figure 3. Furthermore, significant conditioning effects are observed when the permeance is measured for 16 hours at 16 bar CO_2-pressure. In the depressurization part considerably higher permeances are observed for both hollow fiber membrane modules, indicating hysteresis effects. Surprisingly, the permeance increases when the pressure is lowered. This could be explained by the alterations of the polymer matrix induced by CO_2 not able to relax back in the time scale of the measurements. The extra created free volume at the previous higher pressures results in higher permeances upon depressurization. After measuring the N_2-permeance of both modules overnight, the CO_2-permeance has partly recovered to the initial value at 4 bar, indicating reversibility of the CO_2-induced dilation effect.

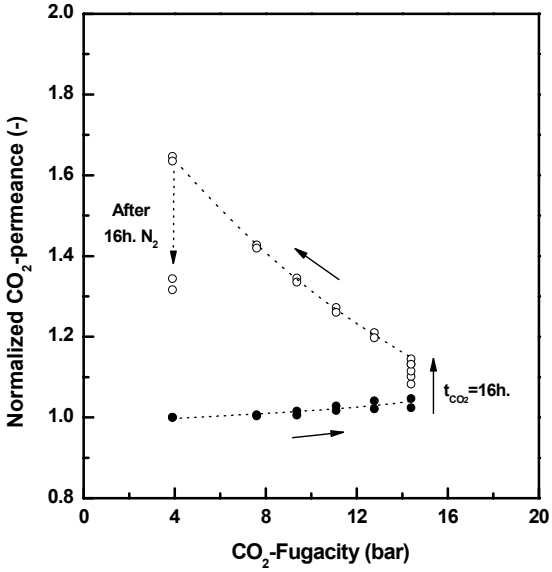

Figure 4: Hysteresis in normalized CO_2-permeance as a function of pressure for two hollow fiber membrane modules.

N_2-permeance decay in time

Conditioning of the glassy polymeric matrix would yield higher diffusion coefficients due to plasticization processes going on during CO_2-exposure. Therefore, additional indication for plasticization or polymer network dilation effects is gathered by following the N_2-permeance decay in time immediately after an experiment is carried out with a gas mixture containing CO_2. Figure 5a and 5b show N_2-permeance decays in time for the applied feed pressures for pure CO_2 and the 80/20 wt.% CO_2/N_2-mixture.

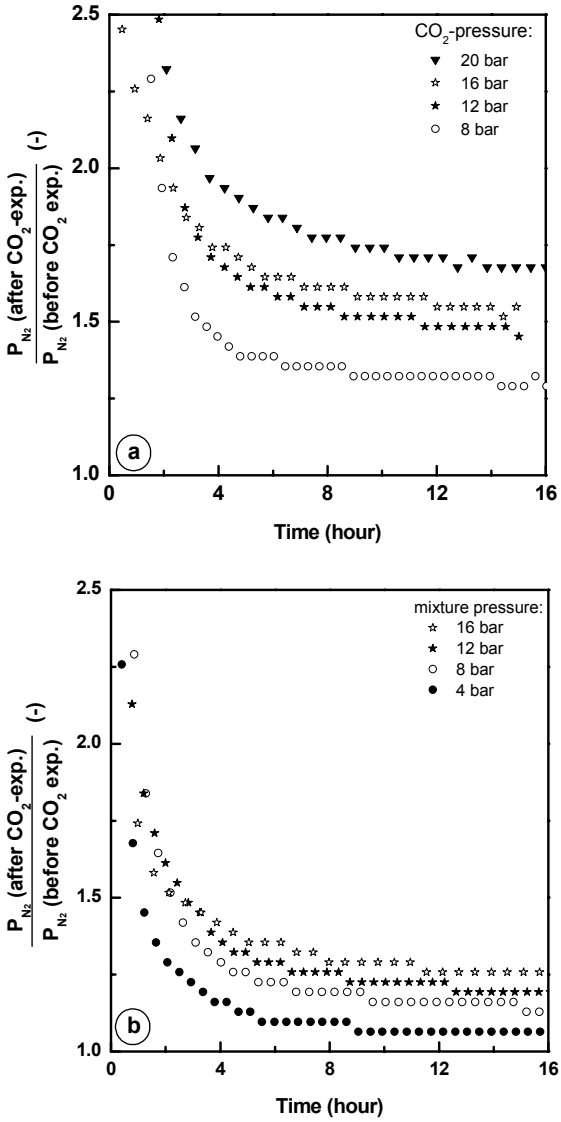

Figure 6: N_2-Permeance decay in time after exposure to (a) pure CO_2 and (b) 80/20 wt.% CO_2/N_2 gas mixture for different feed pressures.

The measured N_2-permeances are divided by the initial N_2-permeance that is determined before the membranes have been in contact with CO_2 (fibers without permeation history). Consequently, a value of one would suggest no occurrence of plasticization, whereas a value above one suggests plasticization. Physical aging effects of the hollow fibers will not

have a significant influence anymore on these measurements as the fibers were used 3 months after spinning.

For pure CO_2 (Figure 5a), the N_2-permeance starts at more than 3 times higher than the initial value and decreases slowly in time as was expected. However, on the experimental time-scale, the membrane does not consolidate towards its original structure. Instead, a higher permeance remains, indicating permanent polymer network dilation. At higher CO_2-pressures, the remaining N_2-permeance increases, indicating larger extents of dilation. After using a mixture of 80% CO_2 and 20% N_2 (Figure 5b), similar trends are observed as for pure CO_2, although the extent of membrane swelling is smaller. Clearly, the use of CO_2-mixtures results in significant polymer network dilation. The extent of membrane swelling seems to be dependent on the pressure of the feed mixture.

When the N_2-permeance decay in time is plotted at one feed pressure (16 bar) for all used gas compositions (Figure 6), a smaller extent of membrane swelling is observed for an increasing inert gas content in the feed mixture. At 80% inert gas in the feed gas mixture, the N_2-permeance decay in time reaches a value of one rather quickly, indicating absence of polymer network dilation. The extent of dilation seems to be dependent on the concentration of CO_2 in the feed mixture, whereas the choice of the second component in the feed mixture (N_2 or CH_4) does not seem to have much effect.

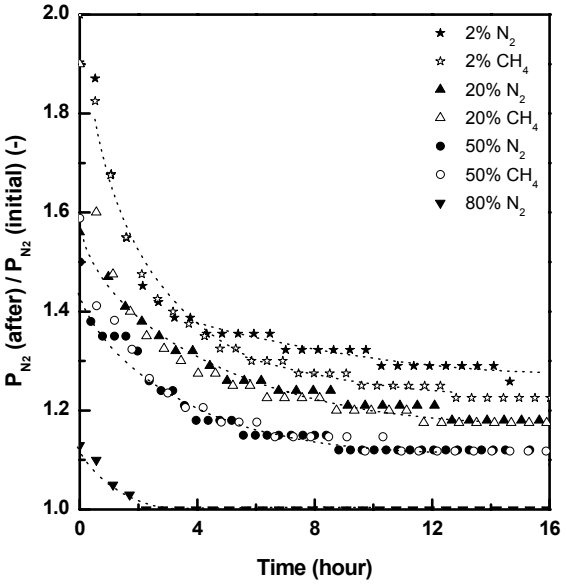

Figure 7: N_2-Permeance decays in time, measured immediately after mixed gas experiments at a feed pressure of 16 bar, for all used feed compositions.

2.3.2. Mixed gas experiments

The single gas permeation experiments showed that polyimide-based hollow fibers possess typical plasticization behavior. Plasticization is accelerated using pure CO_2 and significant polymer network dilation is observed indicated afterwards by an enhanced N_2-permeance and its decays in time. After using CO_2-containing gas mixtures, the extent of polymer network dilation is less, but still significant. However, Kapantadaikis et al. [25], Barsema et al. [26] and Vu et al. [27] observed a suppression of CO_2-plasticization in the separation of CO_2/N_2 and CO_2/CH_4 gas mixtures using polyimide-based integrally-skinned asymmetric hollow fibers. This was indicated by a continuously decreasing CO_2-permeance and an almost constant separation factor with increasing feed pressure. The suppression was explained as a competitive sorption effect that offsets or counterbalances the plasticization effect.

Modeled mixed gas separation performance

Story and Koros [32] described a mixed gas permeation model, in which competitive sorption of the gases is assumed. This model allows an estimation of the mixed gas permeabilities as a function of pressure. The model does not correct for plasticization

effects. There also exists a more complex model for competitive sorption and diffusion, but it does not give a more accurate prediction of the mixed gas permeabilities. The competitive sorption model predicts that the permeability of a gas is lowered by the presence of a second gas only by reducing the sorption level of the first component. The model is based on the Petropolous model [38], which describes gas flux in terms of the thermodynamic activity of sorbed gas. This single gas permeation model has been extended to include gas mixtures [32] and consists of the following expression for the permeability *P* of component *i* in a binary mixture of *A* and *B*:

$$P_i = k_{D_i} D_{D_i} \left\{ 1 + \frac{F_i K_i}{1 + b_A f_A + b_B f_B} \right\} \tag{3}$$

where $F_i = D_{H_i} / D_{D_i}$, $K_i = C'_{H_i} b_i / k_{D_i}$, D_H and D_D are characteristic Henry's law diffusion coefficients, f is the feed fugacity and *i* represents component *A* or *B*. The parameters k_D, C'_H and *b* were determined from sorption data. The values for D_d and D_h were estimated by changing them such that the modeled permeabilities for pure CO_2, CH_4 and N_2 and the ideal separation factors (CO_2/N_2 and CO_2/CH_4) fit the intrinsic properties of a thick dense PES/PI film (Table 2). Figure 7a shows the calculated CO_2-permeability as a function of pressure for all experimentally used gas compositions. The calculated values are normalized to the initial permeability at 4 bar, which was always the first feed pressure used in the gas separation experiments.

Decreasing trends in CO_2-permeability with pressure are observed, which is typical for gas separation in thick films in absence of plasticization. The reductions in the CO_2-permeability are almost unaffected by the type of inert gas, CH_4 or N_2. However, with increasing inert gas concentration the depression of the CO_2-permeability is larger, due to the competitive sorption effect incorporated into the model.

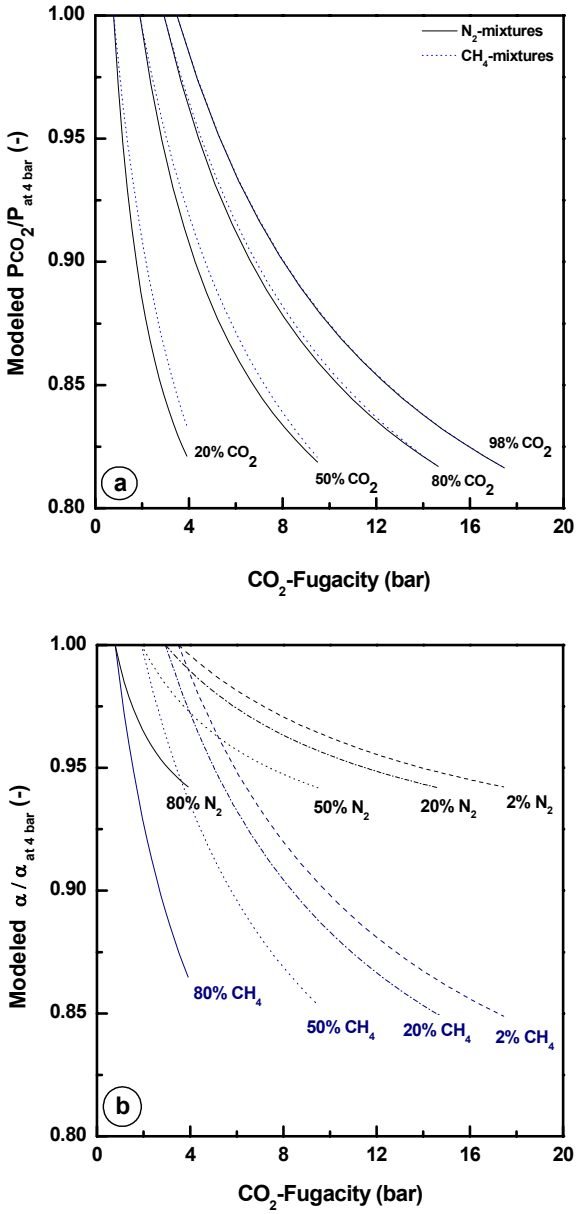

Figure 7: Permeation model for (a) normalized CO_2-permeance and (b) separation factor, both as function of partial fugacity for all used gas compositions (CH_4- and N_2-mixtures).

Figure 7b shows the modeled separation factor as a function of pressure for all experimentally used gas compositions. The pressure range for the calculations is chosen such that they agree well with the experimentally used gas compositions and pressures

reported later in this paper. The separation factor decreases in all cases as a function of pressure, due to a faster decreasing CO_2-permeance compared to the N_2 and CH_4-permeances. The reduction in separation factor is larger for the CO_2/CH_4 mixtures. This is due to a larger competitive sorption effect induced by CH_4, as the solubility of CH_4 is larger than N_2 in the used polymer (Figure 2), resulting in larger reductions of the CO_2-permeance. Frequently, a decreasing selectivity is taken as an indication of plasticization. However, one has to be cautious since glassy polymers show this trend anyway even if the polymer is not plasticized.

Experimental mixed gas separation performance

The gas separation performance of integrally skinned PES/PI asymmetric hollow fibers was measured for four different gas compositions with N_2 as well as CH_4 as the second (inert) component. Figure 8 shows the normalized CO_2-permeance as a function of CO_2-fugacity for all used gas compositions. Normalization is done by dividing all permeances by the initial permeance at 4 bar. Besides that, all reported values are averages of two simultaneously carried out measurements on two different modules. The dotted lines in Figure 8 are shown to guide the eye.

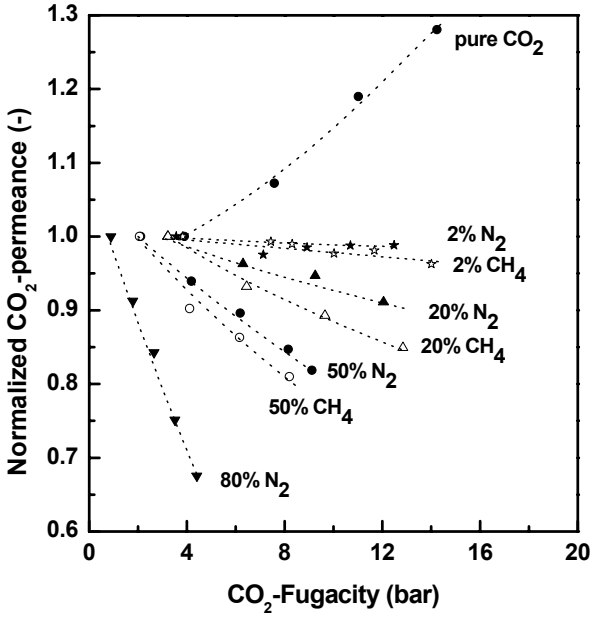

Figure 8: Normalized CO_2-permeance as a function of CO_2-partial fugacity for different feed gas mixtures and pure CO_2. The dotted lines are trend lines and only shown to guide the eye.

Surprisingly we find that introducing only 2% inert gas (N_2 or CH_4) to the feed gas mixture causes the CO_2-permeance to reduce drastically compared with exposure to pure CO_2. Plasticization seems to be suppressed, as indicated by the continuously decreasing CO_2-permeance with increasing pressure. By further increasing the inert gas concentration in the feed gas mixture, the apparent suppression of plasticization becomes more pronounced and an increasing drop in CO_2-permeance is observed. Furthermore, the decrease in CO_2-permeance seems to be almost independent of the type of inert gas. The values of the CO_2-permeances are only slightly lower with CH_4 in the gas mixture. At a concentration of 80% inert gas in the feed mixture, the reduction of the CO_2-permeance at 16 bar feed pressure is more than 30%, whereas the decrease in CO_2-permeance with 2% inert gas in the feed mixture amounts only 2-3% at the same feed pressure.

The mixed gas permeation experiments give the impression of regular transport in glassy polymers without plasticization. However, the mixed gas permeation model predicted for all experimentally used gas compositions similar decreases in CO_2-permeance (Figure 7a), viz. between 15 and 20% with an almost equal decay for the feed conditions chosen (pressure and composition). Besides that, N_2-permeance decay measurements showed significant polymer network dilation upon removing the conditioning agent. It is hypothesized that the plasticization effect is counterbalanced by competitive sorption. The competitive sorption effect seems to become stronger with increasing concentrations inert gas (less plasticization, more competition).

When the trends for the CO_2-permeability for the model and the experiments are plotted together (Figure 9), this effect is clearly observed. At 80% inert gas the plasticization effect appears to be completely counterbalanced by competition effects, whereas at 2% inert gas, plasticization effects cause the CO_2-permeance to deviate highly from the modeled permeances. In the N_2-permeance decay measurements in time (Figure 6) it was already observed that at 80% inert gas in the feed mixture polymer network dilation seemed to be absent. Thus, a subtle balance between plasticization and competitive sorption during mixed gas experiments with integrally skinned asymmetric hollow fibers explains the observed phenomena.

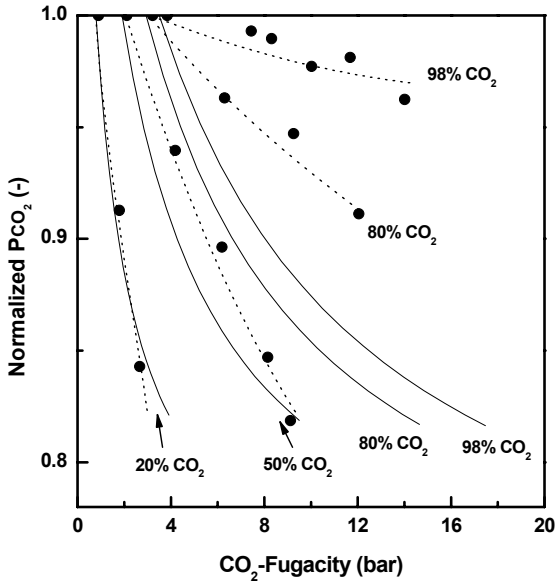

Figure 9: Normalized CO_2-permeance as a function of CO_2-fugacity according to the model (solid line) and the experiments (solid dots and dotted lines).

The total decrease in CO_2-permeance is already 8-10% by introducing 2% inert gas. Nevertheless, the hypothesis that at higher pressures the CO_2-permeance will have an upward curvature as a function of pressure could still hold. However, the hollow fiber membrane modules were only stable up to 20 bar feed pressure, while the plasticization pressure may be much higher. Gas separation experiments with hollow fiber membranes having thicker - more stable - fiber wall will be required to prove this hypothesis.

Figures 10a and 10b show the CO_2/N_2- and CO_2/CH_4-separation factors as a function of CO_2-fugacity. At a feed pressure of 4 bar, the mixed gas selectivities are similar to the ideal separation factors calculated from single gas permeation measurements. With increasing inert gas concentration the separation factors are lower, as was predicted by the mixed gas permeation model. However, the separation factor for the 98/2 wt.% CO_2/N_2-mixture is lower than expected. This might be due to the accuracy of the GC. The area measured by the GC (corresponding to the amount of gas that is permeating) is very small in the case of N_2. The obtained area is always corrected for N_2 entering the GC from the air. Logically, the correction is the most sensitive for the 98/2 wt.% CO_2/N_2-mixture.

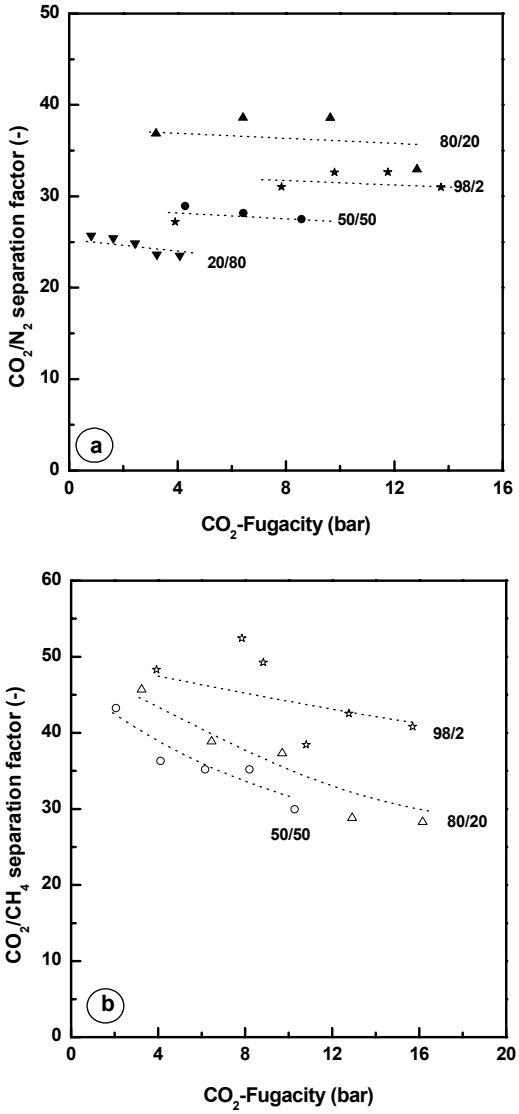

Figure 10: Separation factor as a function of pressure for three different (a) CO_2/N_2 and (b) CO_2/CH_4 gas compositions. The dotted lines are trend lines and only shown to guide the eye.

Similar to the mixed gas permeation model (Figure 7b) the separation factors decrease as a function of pressure. The CO_2/CH_4-separation factor decreases more significantly with pressure than the CO_2/N_2-separation factor, as was also expected considering the mixed gas permeation model. The selectivity is lower when the concentration of inert gas increases, but the drop in selectivity as a function of CO_2-fugacity is similar for all used gas

compositions. The CO_2/N_2- and CO_2/CH_4-separation factor reductions are slightly larger than calculated by the mixed gas permeation model. This might be a consequence of plasticization effects, but can also be due to the accuracy of the measurements as well as the estimated parameters in the used permeation model. However, when plasticization effects would have been present one would expect a steeper fall of the selectivity at higher CO_2-concentrations in the feed. The experimental results do not show such a relationship.

As observed in Figures 2 and 4, conditioning of the membrane modules by pure CO_2 resulted in hysteresis effects upon pressurization and depressurization steps in permeation or sorption measurements [3], [37]. The mixed gas experiments gave the impression of regular transport without any plasticization effect. When plasticization is indeed suppressed, no structural alterations of the polymer network should have occurred during mixed gas experiments. Therefore, it is interesting to see whether hysteresis effects appear upon pressurization and depressurization steps in mixed gas experiments. Figure 11a shows the normalized CO_2-permeance as a function of fugacity in a feed mixture of 95/5 wt.% CO_2/N_2 in such an experiment, whereas Figure 11b shows the separation factor as a function of fugacity of this measurement.

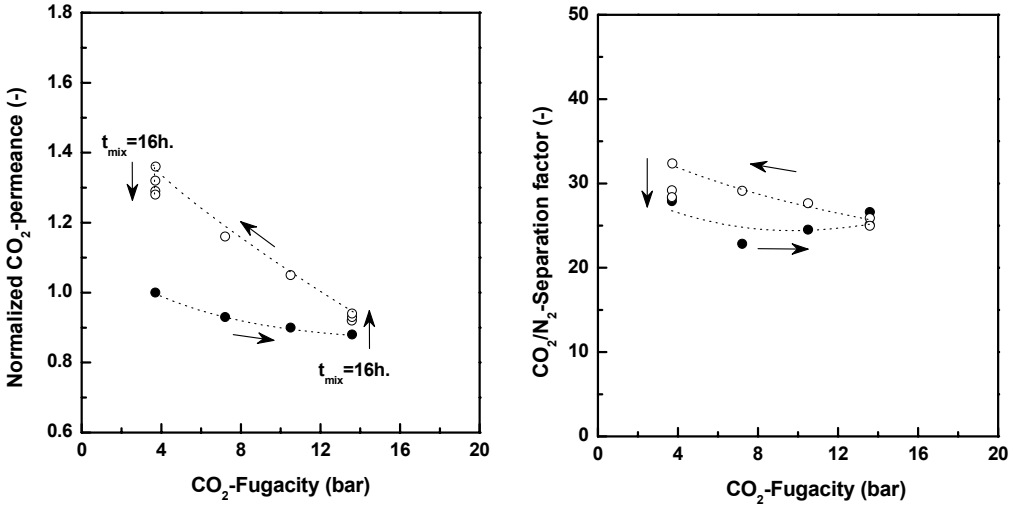

Figure 11: (a) CO_2-Permeance and (b) CO_2/N_2-separation factor as a function of CO_2-fugacity in a 95/5 wt.% CO_2/N_2-gas mixture. Black dots represent increasing pressure steps and open dots decreasing pressure steps.

The membrane module was always conditioned for 120 minutes. Before lowering the pressure stepwise, the separation performance was measured for 16 hours at 16 bar total feed pressure. After coming back to the initial pressure (4 bar), the separation performance was measured again for 16 hours. The arrows indicate the sequence of the measurement. Upon increasing the pressure stepwise, a decreasing trend is observed, similar to the trends observed in Figure 8 for the 98/2 wt.% mixtures. However, the permeance is strongly time dependent as can be seen from the data points at 16 bar. Besides that, hysteresis effects are observed upon depressurization. The increased solubility of CO_2 - as a result of extra created free volume - results in higher permeances when the pressure is lowered. However, the separation factor remains nearly constant, i.e. between 25 and 30 (Figure 11b), independent of the time or the direction of the pressurization steps. Again, this indicates that plasticization effects are counterbalanced by competitive sorption in mixed gas experiments, until the conditioning agent is removed or even partly removed.

Clearly, the mixed gas plasticization behavior of integrally skinned polyimide asymmetric hollow fibers is completely different from plasticization behavior using thick films and single gases. On the experimental level it is clear that introducing an inert gas to a CO_2-mixture appears to suppress plasticization effects during mixed gas experiments. Furthermore, increasing the inert gas concentration in the feed only strengthens this effect. Competitive sorption effects might dominate the transport behavior during mixed gas experiments, masking the polymer network dilation that is observed in N_2-permeance decay measurements. However, can competitive sorption effects depress the CO_2-permeance this much at only an inert gas concentration of 2%, especially as asymmetric hollow fibers normally do show accelerated plasticization behavior for pure CO_2? On the other hand, why do the same polyimide-based thick dense films plasticize under mixed gas conditions [21]? With the results of this work, it is not yet possible to give full explanation on all molecular events governing the subtle balance between plasticization and competitive sorption.

Plasticization is often defined as the increase in CO_2-permeance with feed pressure, due to dilation of the glassy polymeric matrix. However, this paper shows that decreasing CO_2-permeances as a function of pressure does not automatically mean that plasticization effects have to be absent. Therefore, it seems more appropriate to state that plasticization is the phenomenon of an enhanced diffusion coefficient of the component itself or other

components due to swelling-induced local segmental motion caused by the presence of a 'plasticizing' component in the polymer matrix. The identification of plasticization however requires extensive experimentation and interpretation since it may be masked by competitive sorption.

2.4. Conclusions

Integrally skinned polyimide-based asymmetric hollow fiber membranes showed to have totally different plasticization behavior compared to thick dense or integrally skinned asymmetric cellulose acetate membranes. Typical plasticization behavior was found in single gas permeation experiments, that is, plasticization was accelerated as no minimum was found in the CO_2-permeance as a function of feed pressure. Besides that, hysteresis was found in the CO_2-permeance upon pressurization and depressurization steps. Also N_2-permeance decay measurements, which were always measured after using a gas mixture, clearly indicated polymer network dilation. The extent of dilation increased with increasing concentration CO_2 in the gas mixture. The type of inert gas did not have significant influence on the N_2-permeance decay.

When an inert gas (N_2 or CH_4) was introduced to a binary gas mixture of CO_2 plasticization seemed to be suppressed. Already 2% inert gas in the feed gas mixture resulted in a continuously decreasing CO_2-permeance as a function of pressure. Increasing the inert gas concentration in the feed resulted in an enhancement of this effect. The decrease in permeance was 8-10% for the 98/2 wt.% mixture, whereas the decrease was 35% for the 20/80 wt.% mixture. A mixed gas permeation model indicated that there exists a subtle balance between competitive sorption and plasticization, which means that plasticization effects such as polymer network dilation are masked during mixed gas experiments.

Furthermore, the CO_2/N_2- and CO_2/CH_4-separation factor decreased with increasing feed mixture pressure (the most for CH_4), which is in accordance with the dual mode sorption model. Plasticization effects might still have influenced the observed experimental values. However, when plasticization effects are still present one would expect a steeper fall of the selectivity at higher CO_2-concentrations in the feed. The experimental results did not show such a relationship.

Hysteresis effects in the CO_2-permeance were observed upon performing pressurization and depressurization steps in a mixed gas experiment, indicating alterations of the glassy polymer matrix. Nevertheless, the separation factors were nearly constant, independent of the direction of the pressurization. Competitive sorption tends to reduce the solubility of CO_2 during mixed gas experiments, in this way counterbalancing the plasticization effect.

It remains unclear why the plasticization behavior of these asymmetric hollow fiber membranes during mixed gas experiments differs from typical plasticization behavior in thick films. More work has to be done to understand the physical or molecular reason for the apparent suppression of plasticization.

2.5. References

1. R.W. Baker, *Future directions of membrane gas separation technology*, Industrial Engineering and Chemical Research **41** (2002), 1393-1411.
2. A. Bos, et al., *CO_2-induced plasticization phenomena in glassy polymers*, Journal of Membrane Science **155** (1999), 67-78.
3. A. Bos, *High pressure CO_2/CH_4 separation with glassy polymer membranes - Aspects of CO_2-induced plasticization*, in *Chemical Technology*. 1996, University of Twente: Enschede. p. 144.
4. P.C. Raymond, W.J. Koros, and D.R. Paul, *Comparison of mixed and pure gas permeation characteristics for CO_2 and CH_4 in copolymers and blends containing methyl methacrylate units*, Journal of Membrane Science **77** (1993), 49-57.
5. C. Staudt-Bickel and W.J. Koros, *Improvement of CO_2/CH_4 separation characteristics of polyimides by chemical crosslinking*, Journal of Membrane Science **155** (1999), 145-154.
6. C. Staudt-Bickel and W.J. Koros, *Olefin/paraffin gas separations with 6FDA-based polyimide membranes*, Journal of Membrane Science **170** (2000), 205-214.
7. E. Sada, et al., *Permeation of pure carbon-dioxide and methane and binary-mixtures through cellulose-acetate membranes*, Journal of Polymer Science Part B-Polymer Physics **28** (1990), 113-125.
8. S.Y. Lee, B.S. Minhas, and M.D. Donohue, *Effect of gas composition and pressure on permeation through cellulose acetate membranes*, AiChE Symposium Series **84** (1989), 93-99.
9. M.D. Donohue, B.S. Minhas, and S.Y. Lee, *Permeation behaviour of carbon dioxide-methane mixtures in cellulose acetate membranes*, Journal of Membrane Science **42** (1989), 197-214.
10. J.A. Forrest and K. Dalnoki-Veress, *The glass transition in thin polymer films*, Advances in Colloid and Interface Science **94** (2001), 167-195.

11. R.L. Jones, et al., *Chain conformation in ultrathin polymer films*, Nature **400** (1999), 146-149.
12. S.M. Jordan, M.A. Henson, and W.J. Koros, *The effects of carbon dioxide conditioning on the permeation behavior of hollow fiber asymmetric membranes*, Journal of Membrane Science **54** (1990), 103-118.
13. A.M. Shishatskii, Y.P. Yampolskii, and K.-V. Peinemann, *Effects on film thickness on density and gas permeation parameters of glassy polymers*, Journal of Membrane Science **112** (1996).
14. K.D. Dorkenoo and P.H. Pfromm, *Accelerated physical aging of thin poly 1-(trimethylsilyl)-1- propyne films*, Macromolecules **33** (2000), 3747-3751.
15. P.H. Pfromm, I. Pinnau, and W.J. Koros, *Gas-Transport through Integral-Asymmetric Membranes - a Comparison to Isotropic Film Transport-Properties*, Journal of Applied Polymer Science **48** (1993), 2161-2171.
16. P.H. Pfromm and W.J. Koros, *Accelerated physical ageing of thin glassy polymer films: evidence from gas transport measurements*, Polymer **36** (1995), 2379-2387.
17. M.S. McCaig and D.R. Paul, *Effect of film thickness on the changes in gas permeability of a glassy polyarylate due to physical aging Part I. Experimental observations*, Polymer **41** (2000), 629-637.
18. M. Wessling, M. Lidon Lopez, and H. Strathmann, *Accelerated plasticization of thin-film composite membranes used in gas separation*, Separation and Purification Technology **24** (2001), 223-233.
19. J.J. Krol, M. Boerrigter, and G.H. Koops, *Polyimide hollow fiber gas separation membranes: preparation and the suppression of plasticization in propane/propylene environments*, Journal of Membrane Science **184** (2001), 275-286.
20. Y. Liu, R. Wang, and T.-S. Chung, *Chemical crosslinking modification of polyimide membranes for gas separation*, Journal of Membrane Science **189** (2001), 231-239.
21. A. Bos, et al., *Plasticization-resistant glassy polyimide membranes for CO_2/CH_4 separations*, Separation and Purification Technology **14** (1998), 27-39.
22. A. Bos, et al., *Suppression of CO_2-plasticization by semiinterpenetrating polymer network formation*, Journal of Polymer Science Part B-Polymer Physics **36** (1998), 1547-1556.
23. A. Bos, et al., *Suppression of gas separation membrane plasticization by homogeneous polymer blending*, AIChE Journal **47** (2001), 1088-1093.
24. G.C. Kapantaidakis, et al., *Gas permeation through PSF-PI miscible blend membranes*, Journal of Membrane Science **110** (1996), 239-247.
25. G.C. Kapantaidakis, et al., *CO_2 plasticization of polyethersulfone/polyimide gas-separation membranes*, Aiche Journal **49** (2003), 1702-1711.
26. J.N. Barsema, et al., *Preparation and characterization of highly selective dense and hollow fiber asymmetric membranes based on BTDA-TDI/MDI co-polyimide*, Journal of Membrane Science **216** (2003), 195-205.

27. D.Q. Vu, W.J. Koros, and S.J. Miller, *Effect of condensable impurities in CO_2/CH_4 gas feeds on carbon molecular sieve hollow-fiber membranes*, Industrial and Engineering Chemistry Research **42** (2003), 1064-1075.
28. M. Yoshino, et al., *Olefin/paraffin separation performance of asymmetric hollow fiber membrane of 6FDA/BPDA-DDBT copolyimide*, Journal of Membrane Science **212** (2003), 13-27.
29. R. Wang, et al., *Characterization of hollow fiber membranes in a permeator using binary gas mixtures*, Chemical Engineering Science **57** (2002), 967-976.
30. G.C. Kapantaidakis, G.H. Koops, and M. Wessling, *Preparation and characterization of gas separation hollow fiber membranes based on polyethersulfone-polyimide miscible blends*, Desalination **145** (2002), 353-357.
31. F. Dreisbach, R. Seif, and H.W. Losch, *Gravimetric measurement of adsorption equilibria of gas mixture CO/H_2 with a magnetic suspension balance*, Chemical Engineering & Technology **25** (2002), 1060-1065.
32. B.J. Story and W.J. Koros, *Comparison of three models for permeation of CO_2/CH_4 mixtures in poly(phenylene oxide)*, Journal of Polymer Science part B: Polymer Physics **27** (1989), 1927-1948.
33. G.C. Kapantaidakis and G.H. Koops, *High flux polyethersulfone-polyimide blend hollow fiber membranes for gas separation*, Journal of Membrane Science **204** (2002), 153-171.
34. M. Wessling, et al., *Time-dependent permeation of carbon-dioxide through a polyimide membrane above the plasticization pressure*, Journal of Applied Polymer Science **58** (1995), 1959-1966.
35. D. Peng and D.B. Robinson, *New 2-constant equation of state*, Industrial & Engineering Chemistry. Fundamentals **15** (1976), 59-64.
36. A. Bertucco, M. Barolo, and G. Soave, *Estimation of chemical-equilibria in high-pressure gaseous systems by a modified Redlich-Kwong-Soave equation of state*, Industrial & Engineering Chemistry Fundaments **34** (1995), 3159-3165.
37. M. Wessling, et al., *Dilation kinetics of glassy, aromatic polyimides induced by carbon-dioxide sorption*, Journal of Polymer Science Part B-Polymer Physics **33** (1995), 1371-1384.
38. J.H. Petropoulos, *Quantitative analysis of gaseous diffusion in glassy polymers*, Journal of Polymer Science A-2 **8** (1970), 1797-1801.

Chapter 3

Hollow fiber membranes for gas separation prepared from a P84/Matrimid-blend

Abstract

Polymer blending is a versatile method to tune gas separation properties of polymer membranes while it also can increase the chemical stability of the membranes to aggressive feed streams. This paper reports the preparation of such integrally skinned asymmetric hollow fiber membranes consisting of a 50/50 wt.% P84/Matrimid polyimide blend using a dry/wet phase separation spinning process. The spinning process was very reproducible and made it possible to prepare nearly defect-free membranes with high fluxes. The addition of a volatile component (acetone) to the spinning dope enhanced skin formation. Post-treatment with silicone rubber resulted in recovery of intrinsic selectivities and skin layers with a calculated thickness of 80 to 90 nm.

Keywords: Gas separation, dry/wet phase inversion, hollow fiber spinning, asymmetric membranes, polymer blending

3.1. Introduction

A good balance between productivity and selectivity, while having long term stability in contact with aggressive feeds, at high pressures and temperatures are critical for a successful gas separation membrane [1]. According to Robeson's trade-off relation [2], a gas separation membrane with both high productivity and a high selectivity is difficult to obtain. Polymer blending is a good opportunity to tune gas separation properties of gas separation membranes. Traditionally, polymer blending was considered not to be useful as polymer blends are rarely homogeneous [3]. However, several common glassy polymers do blend homogeneously and offer good gas separation properties. Besides, blending may reduce the membrane manufacturing costs when blending an expensive high performance polymer with a relative inexpensive polymer. Several patent applications [4-6] describe the opportunities of homogeneous polymer blending of polymers like polyethersulfones, polyimides and polyamides, which resulted in membranes having a superior combination of productivity and selectivity.

Polymer blending can improve the chemical and/or thermal stability and the resistance against aggressive gas streams of membranes. Bos et al. [7] showed that the blending of Matrimid polyimide with polysulfone (PSf), polyethersulfone or co-polyimide P84 is an effective way to suppress plasticization effects in CO_2/CH_4-separations using dense films of these polymer blends. Kapantadaikis et al. [8] and Visser et al. [9] showed that plasticization effects are also less pronounced using asymmetric hollow fiber membranes of a PES/Matrimid-blend. However, the use of PES in a Matrimid-blend reduced the maximum obtainable CO_2/CH_4-selectivity compared to plain Matrimid membranes. The use of the co-polyimide P84 seems more attractive as it is more selective to CO_2 than Matrimid, although its intrinsic gas permeability is relatively low [10]. Hollow fiber membranes consisting of a blend of P84 with the much more permeable Matrimid polyimide can result in membranes combining good productivity and selectivity with an improved resistance to plasticization.

Integrally skinned hollow fiber membranes are typically prepared using a dry/wet phase separation process. Basic requirements for these membranes are a thin, defect-free gas separation top layer (skin) and an open porous substructure with negligible gas transport resistance. These membranes are typically prepared using the process of dry/wet phase

separation. The formation of a thin gas separation skin occurs when locally, at the outer side of the nascent fiber, the polymer concentration is higher. Upon contact with the coagulant, the polymer concentration at the outside surface is too high for liquid-liquid demixing to occur [11]. This results in vitrification without initially liquid-liquid demixing [12]. A locally higher polymer concentration can be induced using solvent evaporation in the air gap [13]. For this reason, low-boiling components are often added to spinning dopes. For example, acetone and tetrahydrofuran were used as low-boiling additives for the preparation of defect-free integrally skinned asymmetric Matrimid hollow fibers [13, 14]. Variation of the amount of volatile component allows tuning the skin thickness.

It is possible to prepare integrally skinned asymmetric hollow fiber membranes having an ultra-thin skin without the addition of low-boiling components [15, 16]. Fibers have to be spun from a 'critical' concentration as at this concentration fibers theoretically exhibit the thinnest skin layer with minimum to no defects. This critical polymer concentration is determined from the intersection of two asymptotic lines of the viscosity-concentration curve and reflects the onset of chain entanglement. However, post-treatment of these membranes with a silicone rubber coating solution was always required to obtain the intrinsic selectivity of the membrane material [15, 16]. Therefore, the addition of volatile components to a spinning dope is the preferable route to enhance the formation of a defect-free skin.

In this paper we present the preparation of high-flux integrally skinned asymmetric hollow fiber membranes consisting of a P84/Matrimid-blend using dry/wet spinning technology. The influence of adding different amounts of low-boiling acetone to the spinning dope is investigated to study its effect on the skin thickness (permeance) and the ideal O_2/N_2-selectivity. Physical aging effects are investigated as well.

3.2. Experimental

3.2.1. Materials

Hollow fiber membranes were prepared using the commercially available Matrimid 5218 polyimide (BTDA-AAPTMI, Vantico AG, Switzerland) and P84 co-polyimide (BTDA-TDI/MDI, HP Polymer GmbH, Austria). Solvents (analytical grade) were purchased from Acros and Merck (The Netherlands) and were used without further purification.

The rubbery polymer polydimethylsiloxane (PDMS, Sylgard 184) was obtained from Dow Corning, The Netherlands and used as coating material to plug surface defects. Gases (purity > 99.5%) were obtained from Praxair (The Netherlands) and used as received.

3.2.2. *Viscosity measurements*

To determine the optimum polymer concentration for hollow fiber spinning the rheological behavior of a 50/50 wt.% P84/Matrimid blend was investigated. Polymer concentrations between 20 and 34 wt.% of a 1/1 P84/Matrimid blend in NMP were used. Solution viscosities at three different temperatures (40, 50 and 60 °C) were measured using a Brabender® cone and plate viscometer (Viscotron). The viscosity was determined from the magnitude of torque required to overcome the viscous resistance when a cone-shape spindle rotates in the solution. The optimum polymer concentration was estimated at the intercept of the tangent line at the lowest polymer concentration with the tangent line at the highest polymer concentration. The influence of acetone in the spinning dope was not taken into account.

3.2.3. *Membrane formation*

Dense flat-sheet membranes were prepared by casting polymer solutions of 15 or 20 wt.% in NMP on a glass plate using a 0.3 mm casting knife. Solvent was evaporated in a nitrogen atmosphere for 3 days and subsequently films were dried for at least 2 days under vacuum at 150 °C. Finally, dry films with a thickness of 30-40 μm were obtained.

Hollow fiber membranes were produced by the process of dry/wet phase separation using spinning technology. An extruded fiber passes through an air-gap where evaporation takes place before entering the coagulation bath. After leaving the air gap the fiber enters the coagulation bath where the final membrane structure is set due to phase inversion. Details on the used spinning set-up can be found in literature [14, 16].

Before use, the polymer solutions were filtered over a 15 μm metal filter and degassed for at least 48 hours. The bore liquid was a 80/20 wt.% degassed mixture of NMP/demineralized water. A tube-in-orifice spinneret was used with an inner diameter of 200 μm and an outer diameter of 500 μm. The spinning temperature was set at 50°C. The prepared fibers were rinsed in tap water for at least 16 hours to remove residual NMP

and acetone. Subsequently, the fibers were dried using a solvent exchange process to prevent pore collapse [13]. Fibers were placed successively in ethanol and n-hexane for 4 hours to displace water from the porous structure of the membranes. Finally, the fibers were dried in ambient air for at least 24 hours.

Hollow fiber membranes were prepared using two different dope compositions (Table 1) with NMP as solvent and acetone as volatile additive (non-solvent). Tap water at room temperature was used as coagulant. The P84/Matrimid blend composition (50/50 wt.%) was chosen arbitrarily. The reproducibility of the spinning process was verified by spinning hollow fiber membranes with the same recipe twice.

Table 1: Dope solution compositions used for spinning of hollow fiber membranes of a 50/50 wt.% P84/Matrimid-blend.

Dope	*% Polymer*	*% NMP*	*% Acetone*
A	32	45	23
B	30	60	10

The initial parameters of the spinning process (air-gap length, bore liquid flow rate and take up speed) were chosen according to previously published recipes [14, 16], but were slightly adjusted during spinning. Table 2 summarizes the final spinning conditions used. Dope A was spun using a chimney (fixed air gap) in which a N_2-flow of 170 ml/min (at 50°C) was introduced to decrease the humidity and to control the evaporation step. Dope B was spun without a chimney which made it possible to vary the air gap.

Table 2: Spinning conditions of dope A and B.

Parameter	*Dope A (chimney)*		*Dope B (no chimney)*	
	I	*II*	*I*	*II*
Dope fluid flow rate (ml/min)	2	1.6	1.9	1.9
Bore fluid flow rate (ml/min)	1.6	0.8	1.5	1.5
Take up speed (m/min)	8.9	8.9	8.4	8.9
Air gap length (cm)	20	20	20	10
Humidity (%)	34	77	58	55
Room temperature (°C)	22	22	22	23

3.2.4. Analysis of membrane morphology

The geometry and morphology of the prepared membranes were determined using scanning electron microscopy (SEM, Jeol JSM-T220). Samples were prepared by freeze fracturing pieces of film and fiber using liquid nitrogen and subsequently sputtered with a thin layer of gold using a Balzer Union SCD 040 sputtering device.

3.2.5. Gas permeation experiments

Pure gas permeance values were determined using a constant volume - variable pressure method as described by Kapantaidakis and Koops [16]. Typically, five fibers of 20 cm were potted into 3/8 inch stainless steel holders, while sealing the other side with an epoxy resin. The hollow fiber membranes were always pressurized from the shell side. Single gas permeance values were determined at a pressure of 4 bar and a temperature of 35°C and were calculated from the steady-state pressure increase in time in a calibrated volume at the permeate side. The intrinsic separation properties of a 50/50 wt.% P84/Matrimid-blend were determined from permeation experiments with flat sheet membranes. The thickness of the asymmetric skin was calculated from the intrinsic permeability coefficients of N_2 and O_2 and the permeance values obtained for the asymmetric hollow fiber membranes. The separation factors (ratio of O_2- and N_2-permeance values) were used to determine the quality (number of defects) of the prepared membranes. In some cases the permeance of He, H_2, CH_4 and CO_2 was measured as well. If necessary, the membranes were post-treated with a PDMS-solution (5 wt.% in n-hexane and cured at 65°C for 4 hours) to plug possible defects.

3.3. Results and discussion

3.3.1. Viscosity behavior

Figure 1 shows the viscosity behavior of a 50/50 wt.% P84/Matrimid blend in NMP at three different temperatures.

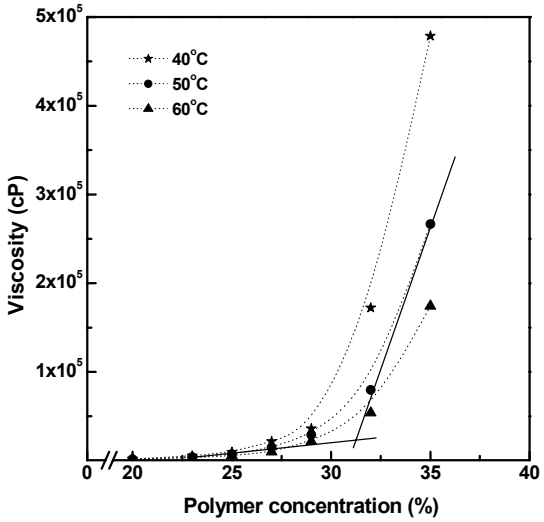

Figure 1: Viscosity-concentration curve for 50/50 wt.% P84/Matrimid solutions at 40, 50 and 60°C. The dotted lines are trend lines and only used to guide the eye.

At a certain point on the concentration axis the viscosity rapidly increases, suggesting the onset of significant chain entanglement. The magnitude of the slope of the curve is highly dependent on the temperature of the polymer solution: with increasing solution temperature chain entanglement occurs at higher polymer concentrations. The intersection of the tangent lines at low and high polymer concentration indicates the polymer concentration range suitable for membrane preparation. The exact position of the intersection is highly dependent on the amount of data points. Nonetheless, at 50°C this value is ~31.5 wt.% in NMP and provides a starting point for hollow fiber membrane preparation via dry/wet spinning.

3.3.2. Analysis of membrane morphology

Figure 2 and Table 3 show the fiber geometry and fiber dimensions, respectively, obtained with dope A (a) and dope B (b). Unfortunately, the fiber bores were not concentric due to

a slightly tilted spinneret needle. This resulted in large differences in wall thickness. Despite these differences in geometry, the morphology of fibers spun from the same dope composition (A1 vs. A2 and B1 vs. B2) is quite similar.

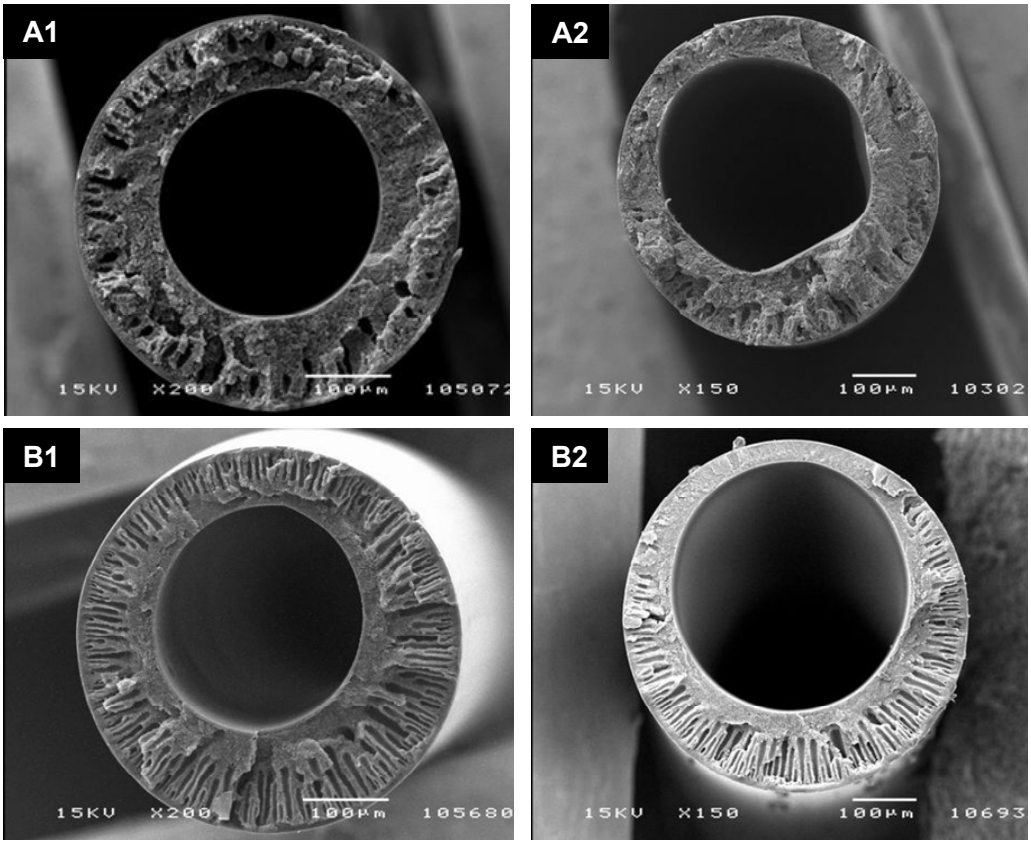

Figure 2: Geometry and morphology of the hollow fibers prepared using dope A (1 and 2) and B (1 and 2).

Table 3: Fiber dimensions of the hollow fibers prepared using dopes A and B.

	Dope A		*Dope B*	
	1	*2*	*1*	*2*
Fiber diameter (µm)	480	455	450	540
Wall thickness (µm)	50-130	80-100	70-130	30-120

Figure 2 shows that all structures have fingerlike macrovoids, which are oriented from outside to inside. This shows that precipitation occurred mainly from the outside of the

fiber, just underneath the top layer. In general, macrovoids are formed upon the onset of liquid-liquid demixing [17]. Solvent/non-solvent pairs like NMP/water have a strong mutual affinity, which favors the onset of this demixing process and hence favors the formation of macrovoids. Often, macrovoid formation can be eliminated by increasing the polymer concentration or by adding non-solvent to the spinning dope, because this suppresses liquid-liquid demixing [17]. As Figure 2 shows, higher polymer concentration (dope A) indeed reduces the amount of macrovoids. However, this can also be attributed to the higher non-solvent (acetone) concentration in dope A. On the other hand, the evaporation of acetone enhances skin formation and thus the tendency to form macrovoids, which may explain the small amount of macrovoids observed in hollow fiber membranes prepared from dope A.

Macrovoids are not observed in the first 20-40 microns of the bore side of the fibers prepared form dope B, which is probably the length of the precipitation front induced by the bore liquid. The addition of NMP to the bore liquid reduces the density of the internal skin and thus reduces the tendency to form macrovoids from the bore side. It suggests the existence of a certain critical structure-transition thickness at which the substructure changes from a fingerlike to a spongy structure, which is dependent on the velocities of the precipitation fronts from the outside and inside of the fiber. This phenomenon has been reported earlier for asymmetric flat sheet membranes prepared by wet phase separation by Vogrin et al. with cellulose acetate [18] and by Li et al. with polyethersulfone and polyimide [19].

Figures 3 and 4 show the cross-section of the fiber outside and fiber bore, respectively, at a magnification of 20.000 (A1 and A2: dope A, B1andB2: dope B). A dense skin layer with a gradual transition to a porous substructure is observed for all four batches (Figure 3). The absolute skin thickness can not be estimated. At the most inner side of the fibers, an open spongy substructure is obtained for all four batches despite the presence of fingerlike macrovoids further in the fiber wall (Figure 4).

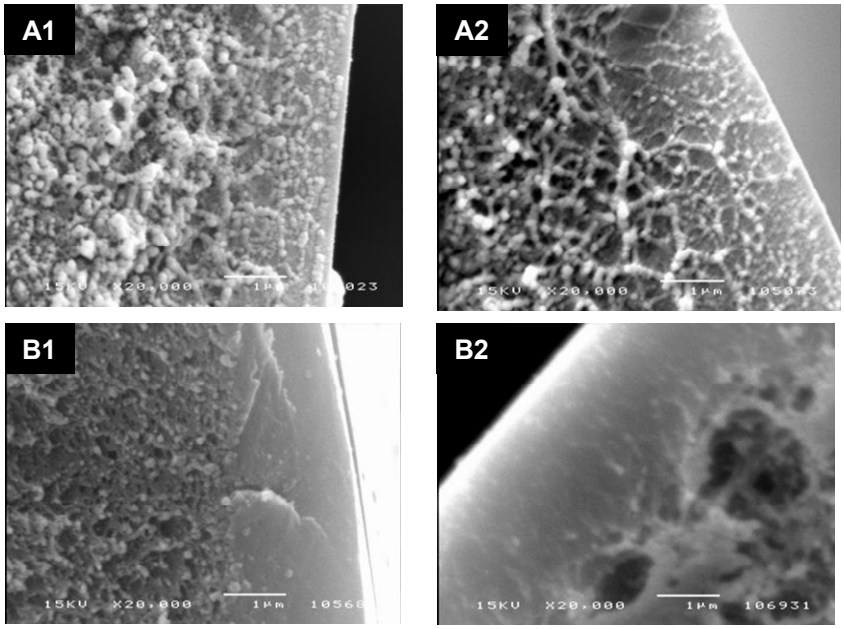

Figure 3: Cross-sections of fiber outside skins of fibers prepared from dopes A (A1 and A2) and B (B1 and B2) at a magnification of 20.000.

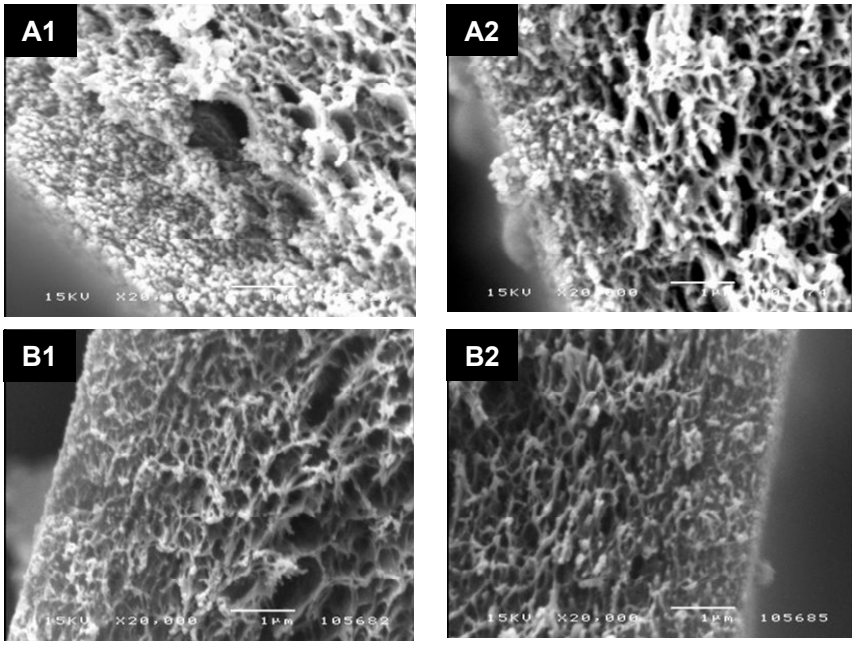

Figure 4: Cross-sections of the fiber bores prepared from dopes A (A1 and A2) and B (B1 and B2) at a magnification of 20.000.

3.3.3. Gas permeation characteristics

Intrinsic gas permeation properties

Table 4 shows the intrinsic gas permeation properties of dense films of a 50/50 wt.% P84/Matrimid-blend with a thickness of ~30 μm. The permeability (in Barrer = $1 \cdot 10^{-10}$ $cm^3 \cdot cm/cm^2 \cdot s \cdot cmHg$) was measured for five gases (N_2, O_2, He, CH_4 and CO_2).

Table 4: Intrinsic gas permeation properties of dense films of a 50/50 wt.% P84/Matrimid blend.

Permeability (Barrer)					*Separation factor (-)*		
N_2	O_2	*He*	CH_4	CO_2	O_2/N_2	He/N_2	CO_2/CH_4
0.048	0.37	9.1	0.029	1.36	7.7	190	46.5

Gas permeation results for fibers prepared from dope A

Table 5 shows the average gas permeance values for hollow fibers prepared from dope A for at least four different membrane modules (1 GPU (gas permeation unit) is $1 \cdot 10^{-6} \cdot cm^3(STP)/cm^2 \cdot s \cdot cmHg$ or $7.6 \cdot 10^{-12}$ $m^3(STP)/m^2 \cdot s \cdot Pa$). The experimental error of the measurements is less than 10%.

Table 5: Gas permeance values (in GPU) for fibers prepared from dope A1 and A2.

Dope	*Permeance (GPU)*					
	N_2	O_2	CH_4	*He*	H_2	CO_2
A1	0.17	1.20	0.11	24.9	n.a.	4.96
A2	0.16	1.00	0.12	16.7	16.5	4.68

Although the permeance values for O_2 and H_2 are slightly different for the fibers prepared from dope A1 and A2, the other values found for the other gases (N_2, CH_4 and CO_2) are almost equal. The calculated skin thickness is 340 nm (dope A1) and 360 nm (dope A2) for N_2 and 260 nm (dope A1) and 410 nm (dope A2) for O_2. The calculated skin layers are relatively thick (>260 nm), which is probably due to the relative high acetone concentration in the spinning dope. Also the use of a chimney (to obtain low humidity) probably increased the skin thickness. Krol et al. [14] obtained the same results for

asymmetric Matrimid polyimide hollow fibers using similar spinning conditions. Table 6 shows the ideal separation factors obtained for fibers prepared from dope A as calculated from the permeance values.

Table 6: Ideal separation factors for fibers prepared from dope A1 and A2 as calculated from the permeance values.

Dope	*Separation factor (-)*				
	O_2/N_2	He/N_2	H_2/CH_4	CO_2/N_2	CO_2/CH_4
A1	7.2	151	n.a.	30	45
A2	6.6	108	140	30	40

The prepared membranes are nearly defect-free as the obtained ideal selectivities are within 90% of the intrinsic values (Table 4). Overall, it can be concluded that the spinning process using dope A is well reproducible. Nearly defect-free hollow fiber membranes but low gas permeance values are obtained.

Gas permeation results for fibers prepared from dope B

Tables 7 and 8 show the (average) gas permeance values and ideal separation factors for fibers prepared from dope B for at least four different membrane modules before and after post-treatment with a silicone rubber coating. The experimental error of the measurements is within 15%. The CO_2-permeance was only measured after post-treatment to avoid the influence of CO_2-conditioning on the other gas permeance values [20].

Very high gas permeance values are obtained. The calculated skin thickness of the uncoated fibers is only 65 nm (dope B1) or 43 nm (dope B2) for N_2 and 75 nm (dope B1) or 53 nm (dope B2) for O_2. No significant differences were found in the gas permeance values obtained for fibers prepared with different air gaps (10 and 20 cm). Others [16] did find an influence of the length of the air gap on the gas permeation properties of PES/Matrimid hollow fibers, but their spinning process did not contain any volatile additives.

The ideal separation factors obtained for fibers without any post-treatment are significantly lower (~20%) than the intrinsic selectivity (Table 4). Post-treatment of the membranes with a PDMS-coating resulted in recovery of the intrinsic separation factors (Table 8) with only limited loss of productivity. The calculated skin thickness after coating increases to 79 nm (dope B1) or 90 nm (dope B2) for N_2 and 81 nm (dope B1) and 87 nm (dope B2) for O_2. It can be concluded that hollow fiber membranes with ultra-thin skins and almost intrinsic selectivity are obtained using dope B. Furthermore, it can be concluded that the reproducibility of the spinning process is good.

Table 7: Gas permeance values (in GPU) for fibers prepared from dope B1 and B2 (uncoated and coated).

Dope	*Permeance (GPU)*					
	N_2	O_2	CH_4	*He*	H_2	CO_2
B1 uncoated	0.84	5.8	n.a.	n.a.	n.a.	n.a.
B1 coated	0.70	5.1	n.a.	n.a.	n.a.	25.4
B2 uncoated	1.30	7.9	n.a.	n.a.	n.a.	n.a.
B2 coated	0.61	4.9	0.43	94.6	92.9	21.1

Table 8: Ideal separation factors for fibers prepared from dope B1 and B2 after PDMS post-treatment as calculated from the permeance values.

Dope	*Separation factor (-)*				
	O_2/N_2	He/N_2	H_2/CH_4	CO_2/N_2	CO_2/CH_4
B1 uncoated	6.9	n.a.	n.a.	n.a.	n.a.
B1 coated	7.3	n.a.	n.a.	36.3	n.a.
B2 uncoated	6.1	n.a.	n.a.	n.a.	n.a.
B2 coated	7.9	155	219	34.4	49

Effect of physical aging

Polymer membranes always experience flux reductions due to physical aging phenomena. Physical aging tends to reduce the amount of excess free volume in a glassy polymer over

time resulting in suppressed fluxes and often enhanced selectivities [21]. The rate of aging is highly thickness dependent [22]. Aging effects appear to accelerate with decreasing top layer thickness. For investigation of plasticization behavior of asymmetric membranes, it is important to work with membranes that are completely aged to not confuse observed phenomena with the effect of physical aging. Figure 5 shows (a) the O_2-permeance and (b) the O_2-permeance decay (values are normalized for initial O_2-permeance) in time for dope A2 and B2.

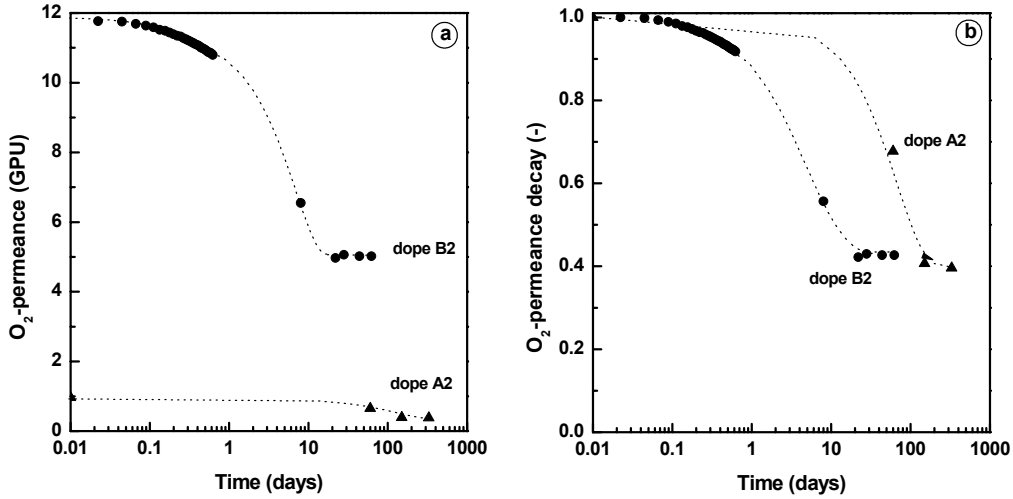

Figure 5: (a) O_2-permeance (GPU) and (b) O_2-permeance decay in time due to physical aging for fibers prepared from dopes A2 and B2.

Complete aging indeed takes place faster for fibers with a thin skin (dope B2) compared to fibers with a thick skin (dope A2) (30 days for dope B compared to 100 and 150 days for dope A). Remarkably, the ideal O_2/N_2-separation factor (uncoated) of dope B did not change, while it was expected to increase as a result of skin densification. It may be related to densification of the substructure, which generally results in a decrease of the selectivity and may have counterbalanced a potential increase in selectivity due to skin densification.

A similar extent of O_2-permeance decay is observed for dopes A2 and B2 (Figure 5b). Only 40% of the initial O_2-permeance is left after complete aging. It suggests that top layer thickness does not influence the amount of aging, but that only the physical aging rate is influenced by thickness.

3.4. Discussion

The spinning of asymmetric hollow fibers of a P84/Matrimid-blend with small amounts of acetone in the spinning dope resulted in nearly defect-free hollow fiber membranes with ultra-thin skins and very high ideal separation factors. In comparison, Ube Industries (Japan) produces polyimide hollow fiber membranes with a H_2/CH_4-selectivity of 100-200 and a H_2-permeance 80-200 GPU [23], while Air Liquide/MEDAL™ (U.S.A.) produces polyaramide fibers with a H_2/CH_4 and H_2/N_2-selectivities of more than 200 (permeance values not reported). This shows that the P84/Matrimid hollow fibers presented here potentially can be of commercial interest.

To obtain a commercially successful hollow fiber membrane for gas separation, macrovoid formation should be eliminated, as it significantly reduces the mechanical strength of the fibers. Hollow fiber membranes should be able to withstand high pressure differences. Large amounts of fingerlike macrovoids were formed when low concentrations of acetone were used in the spinning dope. Increasing the polymer concentration of the dope solution did reduce the amount of macrovoids, but resulted in lower permeation rates as well. Decreasing the hollow fiber wall thickness below 40 μm resulted in a macrovoid-free substructure (Figure 2). However, to provide sufficient mechanical stability, the fiber diameter should also be much smaller. Often swelling agents, organic or inorganic additives are used in spinning dopes to better control hollow fiber morphology [24]. These kinds of additives typically increase dope viscosity and promote pore formation. The concentration of the additive is very important as skin formation may be inhibited at too high concentrations. The addition of the polymer polyvinylpyrrolidone (PVP) for example suppresses macrovoid formation, but also results in an ultrafiltration-type skin layer [25]. Nonetheless, the use of swelling agents, organic or inorganic additives in the spinning of a P84/Matrimid blend seems to be the best solution if hollow fiber membranes with a macrovoid-free substructure have to be obtained. However, the main purpose of this paper was only to obtain defect-free gas separation membranes for investigating the transport behavior of gas mixtures through hollow fiber membranes consisting of a P84/Matrimid-blend. No effort was made to completely suppress macrovoid formation and to increase the mechanical strength.

3.5. Conclusions

High-flux and nearly defect-free integrally skinned asymmetric membranes consisting of a 50/50 wt.% P84/Matrimid-blend were prepared by dry/wet spinning. The volatile additive acetone was used in the spinning dope to enhance skin formation. At high acetone concentration (23 wt.%), hollow fiber membranes were produced having relative low gas permeance (calculated skin thickness of 350-400 nm) but ideal selectivities within 90% of the intrinsic selectivity values. At low acetone concentration (10% wt.%), ultra-thin gas separation skins were obtained (calculated skin thickness of 43-73 nm) while still having about 80% of the intrinsic selectivity of the membrane material. Intrinsic selectivity was recovered after post-treating the fibers with a silicone rubber coating. The calculated skin layer thickness after coating was 80 to 90 nm. Fibers prepared from both dopes contain macrovoids in their substructure. The amount of these fingerlike macrovoids was significantly higher at lower acetone concentrations in the spinning dope. No effort was made to eliminate macrovoid formation.

The reproducibility of the spinning process was high as the permeation properties of the fibers prepared from the same spinning dope were very similar. Fibers prepared from dopes with low acetone concentration completely aged in less than 30 days, whereas fibers prepared from dopes with high acetone concentration completely aged in 100 to 150 days. The magnitude of the O_2-permeance decay in time was similar for both dopes. The results prove that hollow fiber membranes prepared from a 50/50 wt.% P84/Matrimid-blend could be industrially interesting.

3.6. References

1. R.W. Baker, *Future directions of membrane gas separation technology*, Industrial Engineering and Chemical Research **41** (2002), 1393-1411.
2. L.M. Robeson, *Correlation of separation factor versus permeability for polymeric membranes*, Journal of Membrane Science **62** (1991), 165-185.
3. D.R. Paul and C.B. Bucknall, *Polymer blends*, 2000: John Wiley & Sons.
4. O.K. Ekiner, *Blends of polyethersulfone with aromatic polyimides, polyamides or polyamides-imides and gas separation membranes made therefrom*, EP 0,648,812 A2 (1994)
5. O.K. Ekiner, *Polyimide blends for gas separation membranes*, WO 2004/050223 A2 (2004)

6. R.S. Kohn, M.R. Coleman, and T.-S. Chung, *Gas separation membranes comprising miscible blends of polyimide polymers*, US 5.055.116 (1991)
7. A. Bos, et al., *Suppression of gas separation membrane plasticization by homogeneous polymer blending*, AIChE Journal **47** (2001), 1088-1093.
8. G.C. Kapantaidakis, et al., *CO_2 plasticization of polyethersulfone/polyimide gas-separation membranes*, Aiche Journal **49** (2003), 1702-1711.
9. T. Visser, G.H. Koops, and M. Wessling, *On the subtle balance between competitive sorption and plasticization effects in asymmetric hollow fiber gas separation membranes*, Journal of Membrane Science **252** (2005), 265-277.
10. J.N. Barsema, et al., *Preparation and characterization of highly selective dense and hollow fiber asymmetric membranes based on BTDA-TDI/MDI co-polyimide*, Journal of Membrane Science **216** (2003), 195-205.
11. J.A. Van 't Hof, et al., *Preparation of asymmetric gas separation membranes with high selectivity by a dual-bath coagulation method*, Journal of Membrane Science **70** (1992), 17.
12. S.G. Li, et al., *Physical gelation of amorphous polymers in a mixture of solvent and nonsolvent*, Macromolecules **29** (1996), 2053.
13. D.T. Clausi and W.J. Koros, *Formation of defect-free polyimide hollow fiber membranes for gas separations*, Journal of Membrane Science **167** (2000), 79-89.
14. J.J. Krol, M. Boerrigter, and G.H. Koops, *Polyimide hollow fiber gas separation membranes: preparation and the suppression of plasticization in propane/propylene environments*, Journal of Membrane Science **184** (2001), 275-286.
15. T.S. Chung, S.K. Teoh, and X.D. Hu, *Formation of ultrathin high-performance polyethersulfone hollow-fiber membranes*, Journal of Membrane Science **133** (1997), 161-175.
16. G.C. Kapantaidakis and G.H. Koops, *High flux polyethersulfone-polyimide blend hollow fiber membranes for gas separation*, Journal of Membrane Science **204** (2002), 153-171.
17. C.A. Smolders, et al., *Microstructures in phase-inversion membranes. Part 1. Formation of macrovoids*, Journal of Membrane Science **73** (1992), 259-275.
18. N. Vogrin, et al., *The wet phase separation: The effect of cast solution thickness on the appearance of macrovoids in the membrane forming ternary cellulose acetate/acetone/water system*, Journal of Membrane Science **207** (2002), 139-141.
19. D. Li, et al., *Thickness Dependence of Macrovoid Evolution in Wet Phase-Inversion Asymmetric Membranes*, Industrial and Engineering Chemistry Research **43** (2004), 1553-1556.
20. M. Wessling, et al., *Plasticization of gas separation membranes*, Gas Separation & Purification **5** (1991), 222-228.
21. Y. Huang, X. Wang, and D.R. Paul, *Physical aging of thin glassy polymer films: Free volume interpretation*, Journal of Membrane Science **277** (2006), 219.

22. P.H. Pfromm and W.J. Koros, *Accelerated physical ageing of thin glassy polymer films: evidence from gas transport measurements*, Polymer **36** (1995), 2379-2387.
23. R.W. Baker, *Membrane Technology and Applications*, 2nd ed., 2002: Wiley.
24. O.M. Ekiner and G. Vassilatos, *Polyaramide hollow fibers for hydrogen/methane separation - spinning and properties*, Journal of Membrane Science **53** (1990), 259-273.
25. R.M. Boom, et al., *Microstructures in phase inversion membranes. Part 2. The role of a polymeric additive*, Journal of Membrane Science **73** (1992), 277-292.

Chapter 4

Materials dependence of mixed gas plasticization behavior in asymmetric membranes

Abstract

A subtle balance exists between competitive sorption and plasticization effects in the separation of CO_2/CH_4-mixtures using PES/Matrimid asymmetric hollow fiber membranes. To study the materials dependence of this subtle balance, the mixed gas permeation behavior of five different asymmetric membranes (PES/Matrimid, P84/Matrimid, Matrimid, PPO and CA) was investigated using four different CO_2/CH_4-feed compositions (20/80, 50/50, 80/20 and 98/2 vol.% CO_2/CH_4) up to feed gas pressures of 20 bar. Typically, plasticization effects or competitive sorption effects dominate the mixed gas separation performance. The CO_2-concentration or pressure at which plasticization starts to dominate the separation performance is different for every membrane material. The mixed gas permeation results show that plasticization effects dominate the mixed gas separation performance of asymmetric Matrimid and CA membranes, resulting in a relative large loss of selectivity. PPO membranes appear to be less susceptible to plasticization, but possess low mixed gas CO_2/CH_4-selectivities. The mixed gas separation performance of asymmetric

PES/Matrimid membranes is not very sensitive for CO_2-plasticization due to relative strong competitive sorption effects. However, the incorporation of PES into a Matrimid-blend results in membranes with less selectivity. On the other hand, incorporating P84 to a Matrimid-blend appears to result in increased selectivity and more plasticization resistance. However, this is only valid for CO_2-feed gas concentrations below 80 vol.%. Plasticization effects start to dominate the mixed gas separation performance of P84/Matrimid membranes above this CO_2-feed gas concentration. Although glassy polymer membranes can be very susceptible to plasticization effects, the results obtained with the Matrimid-blends show that the separation performance is still superior compared with rubbery polymer membranes.

Keywords: Gas separation, asymmetric membranes, carbon dioxide, plasticization, competitive sorption

4.1. Introduction

In natural gas separations glassy polymer gas separation membranes are often preferred above rubbery polymer membranes due to their much higher CO_2/CH_4-selectivity. However, glassy polymers generally loose this high (diffusion) selectivity due to gas induced plasticization of the polymer matrix [1]. Sorption of CO_2 into the polymer causes an enhanced polymer chain segmental mobility, resulting in enhanced mass transport of all components to separate. Staudt-Bickel et al. [2] reported an almost complete loss of selectivity in the separation of a 50/50 vol.% CO_2/CH_4-mixture with dense films of a typical 6FDA-polyimide.

Generally, plasticization phenomena observed in glassy polymer gas separation membranes are complex due to the non-equilibrium state of the polymer glass. Effects of plasticization may highly vary depending on factors like the membrane material, the membrane morphology (integrally skinned asymmetric or dense membranes), the feed composition, pressure and temperature, and the types of penetrants permeating. Furthermore, the onset of plasticization effects may differ with the method of investigation [3]. However, recent gravimetric sorption studies suggest that there exists a critical volume dilation threshold above which relaxational sorption occurs indicating, what is frequently coined, the phenomenon of plasticization [3]. Ongoing research is focused on gaining more insights concerning the complex transport behavior in the presence of strong plasticizing components. Strong plasticizing penetrants are for example present in the separation of

natural gas with high CO_2-concentrations or the separation of higher hydrocarbons (e.g. C_3H_6/C_3H_8). Especially in these areas a large market potential is predicted for polymer gas separation membranes [4].

Often plasticization is said to occur when the presence of a strong plasticizing component causes a diffusion and thus permeation enhancement of another non-plasticizing component compared to its transport rate without that component. Often this results in drastically decreasing mixed gas selectivities with increasing partial pressure of the plasticizing component. For integrally skinned asymmetric or thin film composite membranes plasticization is typically characterized as a continuously increasing CO_2-permeance with increasing pressure, also called accelerated plasticization [5]. In principle, this holds for both pure and mixed gas experiments.

There exists a phenomenon counteracting plasticization: the presence of a second component typically causes the permeability of the first component to reduce in glassy polymer membranes [6]. This may be explained in terms of the dual mode sorption model: penetrants compete for sorption sites which are associated with the non-equilibrium free volume in glassy polymers [6]. Chern et al. [7] showed that by adding small amounts of water vapor the CO_2-permeance in Kapton polyimide was significantly suppressed due to competitive sorption. Furthermore, Sada et al. [8], Lee et al. [9] and Donohue et al. [10] demonstrated that the addition of CH_4 to the feed suppressed the CO_2-permeability in cellulose acetate membranes.

In summary, competitive sorption effects cause the permeability of penetrants to decrease with increasing feed pressure, while plasticization effects cause a permeability increase with increasing feed pressure (see Table 1). A larger permeability reduction is obtained with increasing CH_4- feed concentration (more competition, less plasticization), while a larger permeability increase is obtained with increasing CO_2-feed concentration (less competition, more plasticization).

Table 1: Effect of competitive sorption and plasticization effects on CO_2-permeability.

CO_2-Permeability	*Upon*	*With*
↓	Competitive sorption	Increasing CH_4-feed concentration
↑	Plasticization	Increasing CO_2-feed concentration

It is important to point out that the decrease in the separation factor due to these effects is difficult to attribute to one of these effects as both effects can cause a decrease in the separation factor. It is known that asymmetric cellulose acetate membranes are very susceptible to CO_2-plasticization resulting in strongly decreasing CO_2/CH_4-selectivities with increasing CO_2-feed content [9]. Recently it was found that the presence of CO_2-plasticization does not always result in lower separation performances [11]. For PES/Matrimid asymmetric hollow fiber membranes it was shown that with increasing CO_2-feed concentrations higher CO_2/CH_4-selectivities were obtained. These two examples show that a subtle balance between competitive sorption and plasticization effects can turn into an undesired decrease as well as a desired increase in separation performance.

Thus, literature shows that in CA membranes, plasticization effects dominate the mixed gas separation performance [9], while competition effects dominate the transport behavior of asymmetric PES/Matrimid membranes [11]. A significant difference exists with respect to the susceptibility of a material towards both plasticization and competition. For this reason it is desirable to investigate the balance between competition and plasticization effects in other membrane materials and to identify which effect is the most dominating.

The paper will show the mixed gas transport behavior of five different membrane materials using three different CO_2/CH_4-feed compositions for studying the 'subtle balance' behavior in these materials.

4.2. Experimental

4.2.1. Materials

Like the blending of Matrimid with PES, blending it with the co-polyimide P84 appeared to be an effective way to suppress CO_2-induced plasticization effects in dense thick films for CO_2/CH_4-separation [12]. Besides, P84/Matrimid membranes intrinsically have a

much higher CO_2/CH_4-selectivity and may therefore be more interesting for these kinds of separations. Therefore, P84/Matrimid hollow fiber membranes were produced to make a comparison with hollow fiber membranes consisting of a PES/Matrimid blend and pure Matrimid. The polyimides, Matrimid 5218 (BTDA-AAPTMI) and P84 (BTDA-TDI/MDI), were purchased from Vantico AG (Switzerland) and HP Polymer GmbH (Austria), respectively, while PES (Sumikaexcel) was purchased from Sumitomo (Belgium).

To obtain a more comprehensive overview, the mixed gas permeation behavior of cellulose acetate (CA) and poly(2,6-dimethyl-1,4-phenylene oxide) (PPO) asymmetric membranes was investigated. PPO is known for its extremely high permeability [13, 14], while cellulose acetate is the most commonly used material in natural gas membrane separations [4]. The used cellulose acetate asymmetric membranes were prepared in house to guarantee consistency of the permeation experiments. Cellulose acetate, (CA-398-3) with a molecular weight M_w of 100,000 g/mol and an acetyl content of 39.8%, was purchased from Eastman Company (the Netherlands). Integrally skinned asymmetric poly(2,6-dimethyl-1,4-phenylene oxide) (PPO) hollow fibers were kindly provided by Parker Gas Separation (the Netherlands).

All solvents (N-methyl pyrrolidon (NMP), acetone, ethanol, methanol and n-hexane, analytical grade) were purchased from Acros (the Netherlands) and were used as received. Pure gases (purity > 99.5%) and pre-calibrated gas mixtures were obtained from Praxair (the Netherlands) and used without further purification.

4.2.2. Membrane preparation

Preparation of asymmetric flat sheet membranes

Integrally skinned asymmetric cellulose acetate flat sheet membranes were prepared by dry/wet phase inversion following a recipe using acetone and methanol as the solvent and non-solvent [15]. After filtration of the polymer solution (0.15 μm metal filter), wet films were cast on glass plates at room temperature using 0.3 and 0.5 mm casting knifes. After an evaporation step of 20 seconds, the membranes were immersed into a methanol coagulation bath. After coagulation the membranes were rinsed for 24 hours with fresh methanol. Subsequently the membranes were solvent exchanged in n-hexane for at least 4

hours and slowly dried in air (in a nearly closed container). Finally the membranes were dried in a 100°C vacuum oven for at least for 24 hours to remove residual solvent. Critical in the reproducible preparation of asymmetric CA membranes appeared to be the drying procedure, as too fast drying resulted in excessive shrinkage and poor mechanical stability.

Preparation of asymmetric hollow fiber membranes

Integrally skinned asymmetric hollow fibers were prepared by dry/wet spinning following a recipes described in literature [16, 17]. Table 1 shows the compositions of the polymer dopes and bore liquids used in the spinning process. Acetone was added to the spinning dope to enhance the formation of a defect-free top layer [16]. In both cases, the spinning process was carried out a temperature of 50°C and a tube-in-orifice spinneret with an outer diameter of 0.5 mm and an inner diameter of 0.2 mm was used.

Table 2: Dope and bore liquid compositions used in spinning process.

	P84/Matrimid	*Matrimid*
Polymer (wt.%)	30	25
Solvent (NMP, wt.%)	60	45
Additive (acetone, wt.%)	10	30
Bore liquid (NMP/H_2O, wt.%)	80/20	70/30

4.2.3. Membrane structure analysis

The geometry and morphology of the prepared membranes were determined using scanning electron microscopy (SEM, Jeol JSM-T220). Samples were prepared by freeze fracturing pieces of film and fiber using liquid nitrogen and subsequently covered with a thin layer of gold using a Balzer Union SCD 040 sputtering device.

4.2.4. Pure gas permeation characteristics

All permeation characteristics were determined by using the variable pressure method as described by Kapantaidakis and Koops [18]. In the case of hollow fiber membranes, five fibers of each 20 cm long were potted into 3/8 inch stainless steel holders, while sealing the other side with an epoxy resin. The hollow fiber membrane modules were pressurized from the shell side. In the case of flat sheet membranes, films were cut in circles (surface area of 11.95 cm^2) and pressurized from the dense (skin) side.

Single gas permeance values of N_2 and O_2 were determined at a pressure of 4 bar and a temperature of 35°C and were calculated from the steady-state pressure increase in time in a calibrated volume at the permeate side. The thickness of the asymmetric skin was calculated from the of intrinsic permeability coefficient for a certain gas and its permeance for the asymmetric membrane. The ideal separation factor (the ratio of the pure gas permeances) was used to determine whether the prepared membranes were defect-free. If needed, defects and pinholes were plugged by dip coating the membranes with a 5 wt.% PDMS-solution in n-hexane [19].

Besides the ideal O_2/N_2-separation performance, the pure gas CO_2-permeance was measured as a function of pressure to observe the difference in strength of CO_2-plasticization for the used materials. Permeance values were always recorded after 3 hours of measuring.

4.2.5. Mixed gas separation performance

Mixed gas separation experiments were always conducted using membrane modules without permeation history [20, 21]. Consequently, the mixed gas separation performance may fluctuate slightly from module to module. Four different CO_2/CH_4-compositions (20/80, 50/50, 80/20 and 98/2 vol.% CO_2/CH_4) were investigated at a temperature of 35°C. In every gas separation experiment two similar membrane modules were measured simultaneously. The gas separation performance was determined according to the following protocol:

1) Determination of permeance properties with successively N_2 and O_2 at 4 bar to check quality of membranes;
2) Degassing for at least half an hour;
3) Determination of separation performance of CO_2/CH_4 gas mixture at 4 bar for approximately 6 hours;
4) Tracing residual conditioning by measuring N_2-permeance decay overnight (16 hours);
5) Degassing and evacuation for 30 minutes;
6) Increasing mixed gas pressure;
7) Repeating step 5, 6 and 7 up to the maximum pressure (depending on the mechanical stability of the membranes).

Feed and permeate compositions were analyzed using a Perkin-Elmer gas chromatograph (GC) equipped with a HayeSep Q column. The GC was calibrated with the pre-calibrated feed mixtures. In principle, low stage-cuts (ratio of permeate to feed flow, Q_p/Q_f) are preferred in mixed gas permeation experiments. However, low stage-cuts could not be maintained in experiments with high-flux membranes (P84/Matrimid and PPO). Therefore, a linear cross-flow model was used to define the CO_2- and CH_4-permeabilities [22]. The model assumes a linear profile for the feed concentration. Accordingly, the permeability '*P*' of component '*i*' is defined as:

$$P_i = y_i Q_p / (A(p_f \bar{x}_i - p_p y_i) \quad (1)$$

Where

$$\bar{x}_i = (Q_f x_f - Q_r x_r)/(Q_f + Q_r) \quad (2)$$

where x and y are the feed and permeate concentrations, respectively, A the surface area, p_f and p_p the feed and permeate pressure (bar), and Q_f, Q_r and Q_p the feed, retentate and permeate flow (ml/min). The mixed gas selectivity is defined as the ratio of permeance values:

$$\alpha_{i/j} = \frac{Pi}{Pj} \quad (3)$$

The permeation driving force is expressed in terms of fugacity to take into account non-ideal behavior of gas mixtures at elevated pressures. Fugacities were calculated using the Peng-Robinson equation-of-state [11]. To take into account the time dependency of conditioning and to guarantee the consistency of the permeance data, permeance values were collected in all cases after six hours measuring time [21]. CO_2-conditioning causes subtle packing disruptions in the non-equilibrium polymer matrix. Within the relative short time scales of the experiments the polymer chains can not relax back into their original state [21]. Therefore, an additional indication for plasticization can be obtained by measuring the N_2-permeance decay in time directly after a CO_2-mixed gas experiment. When plasticization has occurred, the N_2-permeance will be significantly higher than its original value and will decrease very slowly in time [11, 23].

4.3. Results and discussion

4.3.1. Asymmetric membrane structure analysis

Figure 1a-1e shows the cross-sections of the asymmetric membranes used in the gas permeation experiments. All hollow fiber membranes (1a-1d) have a typical asymmetric structure; a dense thin top layer at the outside supported by a spongy porous substructure. The P84/Matrimid and Matrimid hollow fiber membranes show large amounts of fingerlike macrovoids that are oriented from outside to inside, whereas the PES/Matrimid and PPO membranes have not. The CA asymmetric membranes (1e) have a more symmetric geometry with a macrovoid-free morphology. The presence of macrovoids is not detrimental as it will not influence the separation performance but only decrease the mechanical resistance of the membrane. Therefore, for industrial high-pressure gas separation processes macrovoid formation should be avoided.

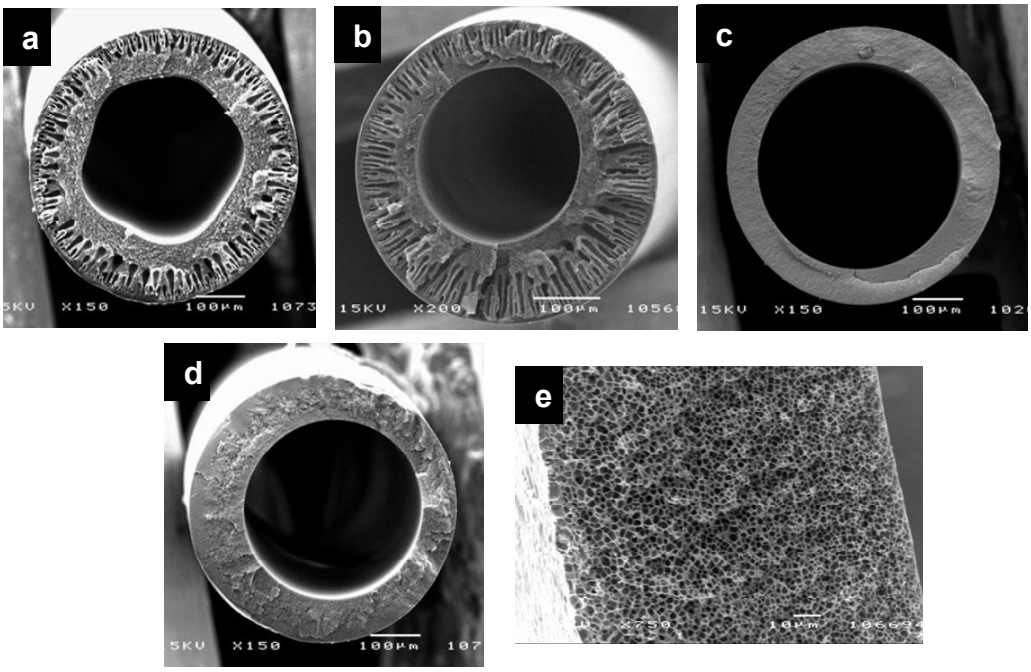

Figure 1: Cross-sections of prepared asymmetric membranes: (a) Matrimid, (b) P84/Matrimid, (c) PES/Matrimid, (d) PPO and (e) CA.

4.3.2. Pure gas permeation characteristics

Table 2 shows the pure gas permeation characteristics of the different membranes. The permeance values (1 GPU (gas permeation unit) is $1 \cdot 10^{-6}$ $cm^3(STP)/cm^2 \cdot s \cdot cmHg$ or $7.6 \cdot 10^{-12}$ $m^3(STP)/m^2 \cdot s \cdot Pa$) are an average of three to four different membranes. The standard deviation in the gas permeation measurements was less than 10% for PPO and the Matrimid-based hollow fiber membranes. However, the CA membranes were very difficult to reproduce, which resulted in a significantly larger standard deviation (~25%). Furthermore, the developed P84/Matrimid membranes have much thinner separating layer compared to the other four materials, which have a more or less equal top layer thickness.

Except for the PES/Matrimid membranes, all membranes were post-treated by applying a PDMS coating to recover the intrinsic selectivity of the material. P84/Matrimid possesses the highest ideal O_2/N_2-selectivity, PPO the lowest. The obtained selectivity for PPO does not completely correspond to the intrinsic selectivity (α = 4.7), even after coating with PDMS. The ideal selectivity can be negatively influenced by the rubber coating, according to the resistance-in-series model of Henis and Tripodi [24]. However, the PDMS-coating is approximately 1 to 2 micron thick. It was calculated that a PDMS-layer with this thickness can not significantly influence the selectivity of the skin layer. Probably, the PPO surface defects are just too large to completely recover the intrinsic selectivity.

Table 3: Pure gas permeation characteristics of the asymmetric membranes used in the mixed gas permeation experiments.

	P/l (N_2) (GPU)	P/l (O_2) (GPU)	(O_2/N_2) (-)	l (N_2) (μm)
CA	0.32	1.7	5.2	0.43
P84/Matrimid	0.61	4.9	7.9	0.09
Matrimid	0.42	2.8	6.8	0.35
PES/Matrimid	0.38	2.6	6.7	0.27
PPO	4.8	20	4.1	0.43

Figures 2a and 2b show the absolute and normalized pure gas CO_2-permeance as a function of pressure for the used membranes. CA and Matrimid membranes show the

strongest increase in CO_2-permeance, which stands for the strongest effect of plasticization. PPO membranes seem to experience the smallest effect of plasticization.

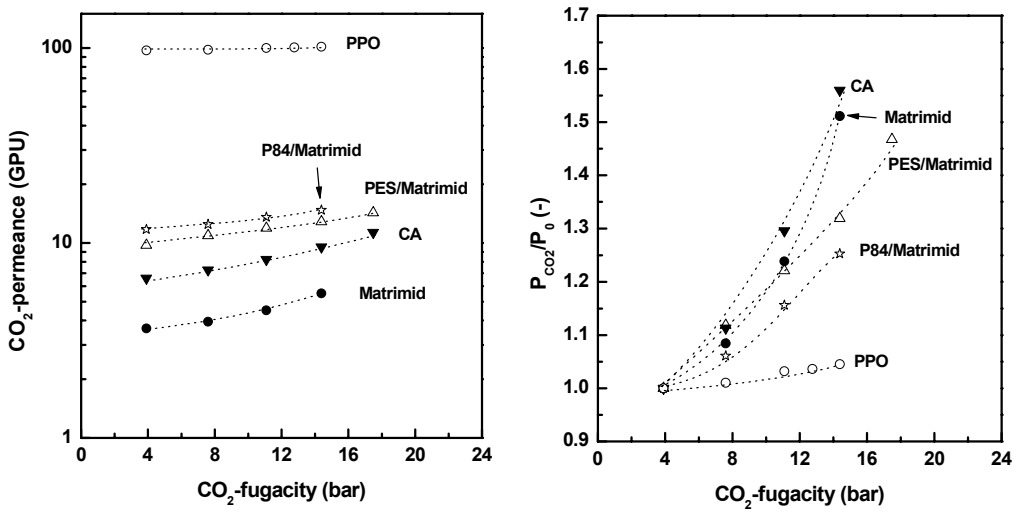

Figure 2: (a) Absolute (in GPU) and (b) normalized pure gas CO_2-permeance as function of CO_2-fugacity.

4.3.3. Mixed gas separation performance

The results will be discussed in terms of the CO_2-permeance (absolute and normalized values), the N_2-permeance decay (tracing the residual conditioning), the mixed gas CO_2/CH_4-separation factor and the normalized CH_4-permeance. The normalized CO_2- and CH_4-permeances are the ratio of the permeance at each pressure (P_{CO2} and P_{CH4}) to the permeance at a feed pressure of 4 bar (P_0) and gives the opportunity to compare the separation performance of the different membrane materials. The dotted lines presented in figures are only used to guide the eye. The results shown of PES/Matrimid membranes have been recently reported [11], but are added to the other results in order to make a more comprehensive comparison.

20/80 vol.% CO_2/CH_4-separation

Figures 3a and 3b show the absolute and the normalized CO_2-permeance, respectively, as a function of CO_2-fugacity for the different membranes using a feed gas of 20/80 vol.% CO_2/CH_4. All membranes show a continuous decrease in the CO_2-permeance with increasing fugacity. The largest total permeance reduction is observed for PPO and the

smallest for Matrimid (Figure 3b). This can be explained by stronger competitive sorption effects or smaller plasticization effects.

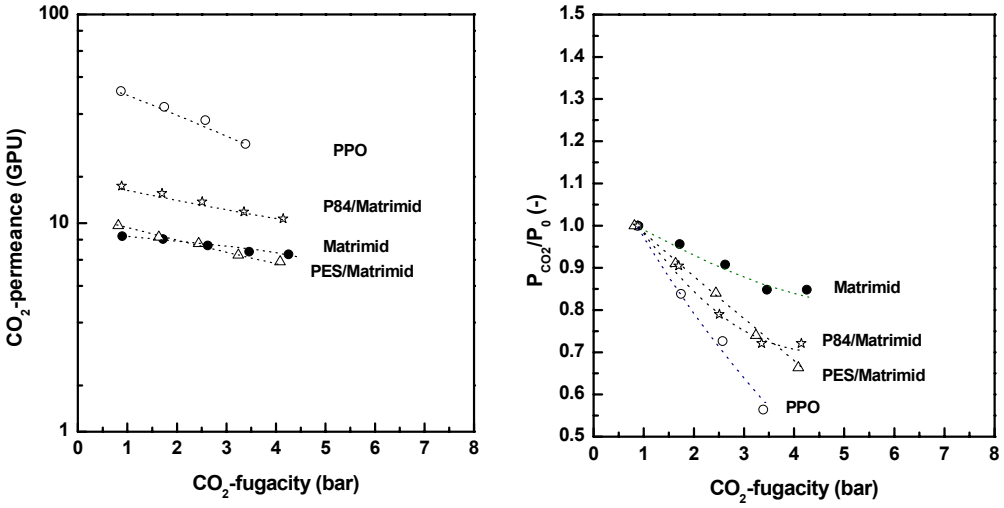

Figure 3: (a) Absolute (in GPU) and (b) normalized CO_2-permeance as a function of the CO_2-fugacity using a 20/80 vol.% CO_2/CH_4-feed gas mixture.

The amount of residual conditioning is determined from the N_2-permeance decay in time (Figure 4). Figure 4 shows that almost no (PPO and the Matrimid blends) or only minor residual conditioning (Matrimid) has occurred for all membranes. The small amount of residual conditioning for Matrimid can be correlated to the smaller reduction in CO_2-permeance with increasing fugacity observed in Figure 3b. While the CO_2-permeance reduction for PPO, P84/Matrimid and PES/Matrimid is only caused by competition effects, plasticization effects have slightly counterbalanced these competition effects in the case of Matrimid.

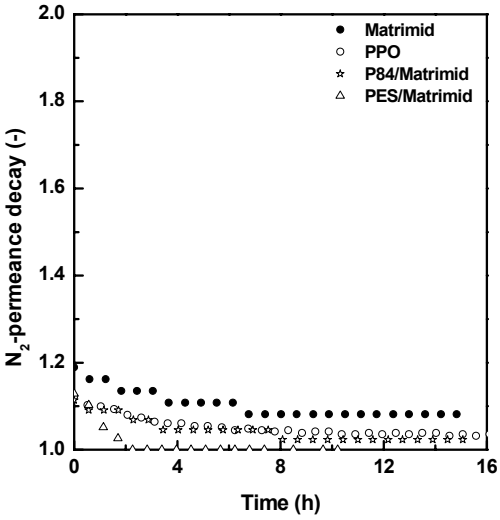

Figure 4: N_2-permeance decay after 20/80 vol.% CO_2/CH_4-separation at a feed pressure of 16 bar (CO_2-fugacity of 3.3 bar).

Figures 5a and 5b show the obtained mixed gas CO_2/CH_4-separation factors and normalized CH_4-permeance as a function of CO_2-fugacity. All membranes exhibit a continuous decrease in separation factor with increasing fugacity. This is a result of a stronger decrease in the CO_2-permeance compared to the CH_4-permeance which is a typical behavior of glassy polymer membranes [25]. However, the decreasing separation factor of Matrimid membranes may be slightly influenced by plasticization effects which were already observed in Figure 4. Al-Juaied and Koros [26] observed no plasticization effects using a feed composition of 10/90 CO_2/CH_4 up to a fugacity of ~14 bar in similar Matrimid hollow fiber membranes. The obtained results for Matrimid show that at 20 vol.% CO_2 plasticization effects are present, but have only a minor effect of the mixed gas separation performance. It may be suggested that at this CO_2-feed gas concentration (20 vol.%) a threshold value for CO_2 sorption is reached, sufficient to induce plasticization effects.

PPO membranes give by surprisingly low mixed gas selectivity, as ideal CO_2/CH_4-separation factors of more than 20 have been reported [13]. The low selectivity may be caused by strong competition effects, which generally decrease mixed gas selectivity compared to ideal (pure gas) selectivity. Furthermore, the PPO membranes were not

100% defect-free, even after post-treatment with silicone rubber, logically lowering the maximum achievable CO_2/CH_4-mixed gas selectivity. Nonetheless, the asymmetric Matrimid-based membranes have significant higher mixed gas selectivity than PPO. Blending Matrimid with P84 gives higher separation factors compared to pure Matrimid, while blending with PES results in less selective membranes.

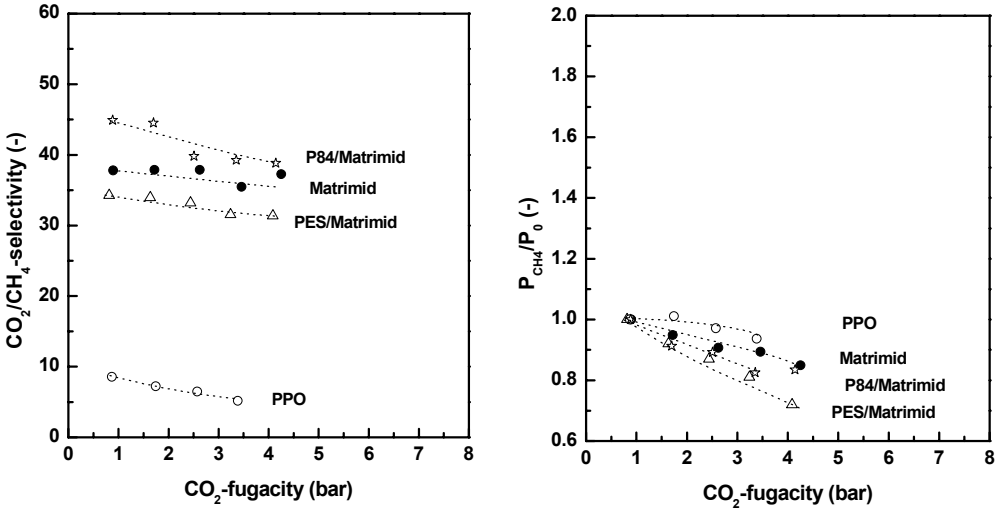

Figure 5: (a) CO_2/CH_4-selectivity and (b) normalized CH_4-permeance as a function of CO_2-fugacity using a 20/80 vol.% CO_2/CH_4-feed gas mixture.

Summarizing, the separation performance of all membrane materials investigated is fully determined by competitive sorption effects because plasticization effects are (almost) absent. The CO_2-permeance and the separation factor decrease with increasing feed fugacity for all membranes investigated, which is consistent with the effects expected upon competitive sorption.

50/50 vol.% CO_2/CH_4-separation

Figure 6 shows (a) the absolute and (b) the normalized CO_2-permeance as a function of the CO_2-fugacity for CA, P84/Matrimid and PES/Matrimid membranes in the separation of a 50/50 vol.% CO_2/CH_4-gas mixture. All three membrane materials show a continuous decrease in the CO_2-permeance with increasing CO_2-fugacity, with the strongest permeance reduction for PES/Matrimid (Figure 6b).

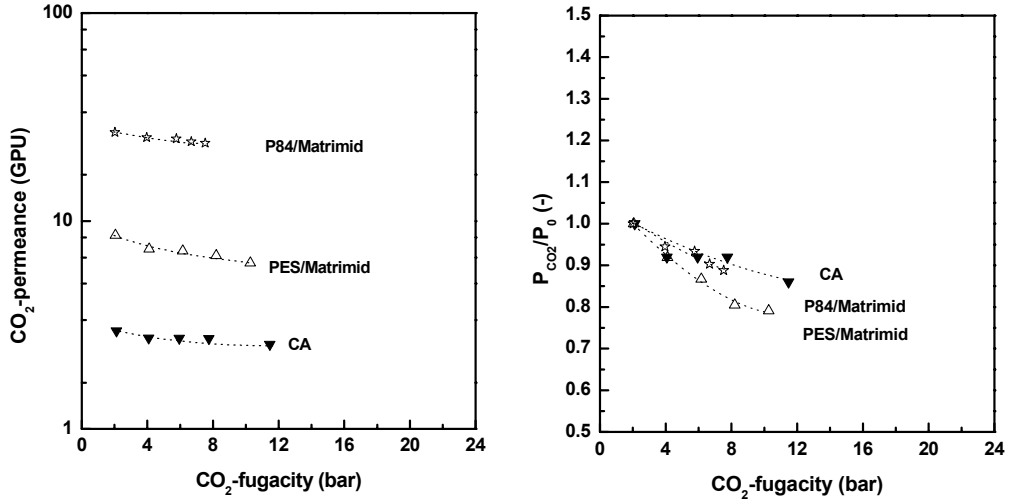

Figure 6: (a) Absolute (in GPU) and (b) normalized CO_2-permeance as a function of CO_2-fugacity using a 50/50 vol.% CO_2/CH_4-feed gas mixture.

However, the N_2-permeance decay measurements (Figure 7) show that P84/Matrimid and PES/Matrimid membranes exhibit the largest extent of residual conditioning. CA membranes seem to recover considerably faster to their original N_2-permeance (before the permeation experiment), while PES/Matrimid and P84/Matrimid membranes end up with ~15% residual conditioning.

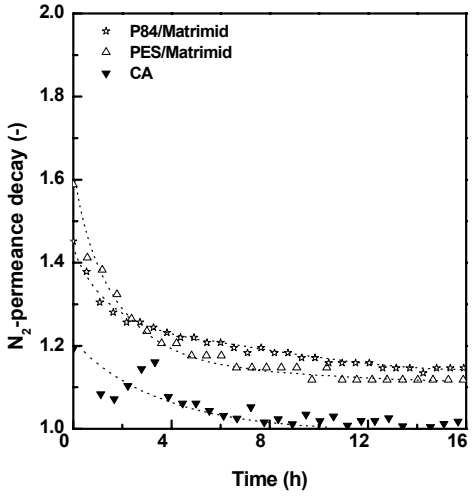

Figure 7: N_2-permeance decay after 50/50 vol.% CO_2/CH_4-separation at a feed pressure of 16 bar (CO_2-fugacity of 8.2 bar).

Donohue et al. [10] reported that plasticization induced changes in CA membranes seem to recover relative fast after the separation of CO_2/CH_4-mixtures. The polymer chains of CA apparently relax very fast back to a compactly dense packed state upon release of the CO_2-mixture. This can be interpreted in terms of the fact that CA has the lowest T_g of all membranes investigated [27]. As the magnitude of the T_g is a measure for chain stiffness, CA will have the highest polymer chain mobility to relax.

Figure 8 shows (a) the CO_2/CH_4-separation factor and (b) the normalized CH_4-permeance as a function of CO_2-fugacity. All membrane materials show a relative strong decrease in separation factor with increasing CO_2-fugacity. The CH_4-permeance shows a significant increase in fugacity for CA membranes, while it is more or less unchanged for PES/Matrimid and P84/Matrimid membranes.

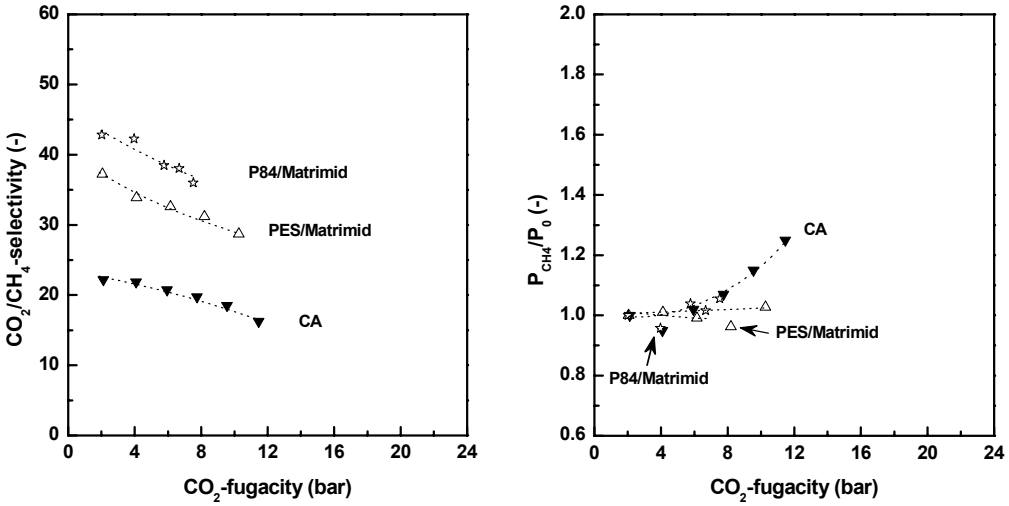

Figure 8: (a) CO_2/CH_4-selectivity and (b) normalized CH_4-permeance as a function of CO_2-fugacity using a 50/50 vol.% CO_2/CH_4-feed gas mixture.

The strong increase in CH_4-permeance and consequently decreasing separation factor for CA membranes is caused by plasticization effects. Therefore, it can be concluded that plasticization effects dominate the mixed gas transport behavior of CA membranes. As the CH4-permeance does not change much with increasing fugacity, the decrease in mixed gas selectivity for PES/Matrimid and P84/Matrimid membranes can be attributed to competition effects. It can be concluded that the mixed gas transport behavior for

PES/Matrimid and P84/Matrimid membranes is dominated by competition effects using a 50/50 vol.% CO_2/CH_4-feed gas mixture.

Summarizing, CA, PES/Matrimid and P84/Matrimid membranes show a *decreasing* CO_2-permeance with increasing fugacity. Nevertheless, plasticization effects dominate the separation performance of CA membranes. The CH_4-permeance *increases* with increasing fugacity, which gives a strong decrease in separation factor. On the other hand, the separation performance of PES/Matrimid and P84/Matrimid membranes is dominated by competition effects, although plasticization effects are not completely absent as was shown by the N_2-permeance decay measurements.

80/20 vol.% CO_2/CH_4-separation

Figure 9 shows (a) the absolute and (b) the normalized CO_2-permeance as a function of the CO_2-fugacity for all membranes in the separation of a 80/20 vol.% CO_2/CH_4-feed gas mixture. The absolute CO_2-permeances (in GPU) are somewhat higher for all membranes compared to the previous described gas mixtures (20/80 and 50/50). Because the CH_4-feed gas concentration is decreased, competition effects will be smaller. On the other hand, plasticization effects will be stronger due to a higher CO_2-feed gas concentration. Both effects will result in a higher (absolute) CO_2-permeance.

Figure 9b shows that the normalized CO_2-permeance increases significantly with increasing CO_2-fugacity for Matrimid and CA, suggesting a much stronger plasticization effect compared to the previous described gas mixtures. Although less strong, P84/Matrimid and PPO membranes show an increase in CO_2-permeance with fugacity as well. On the other hand, a continuous decrease in CO_2-permeance with increasing fugacity is still observed for PES/Matrimid membranes, suggesting relative strong competition effects.

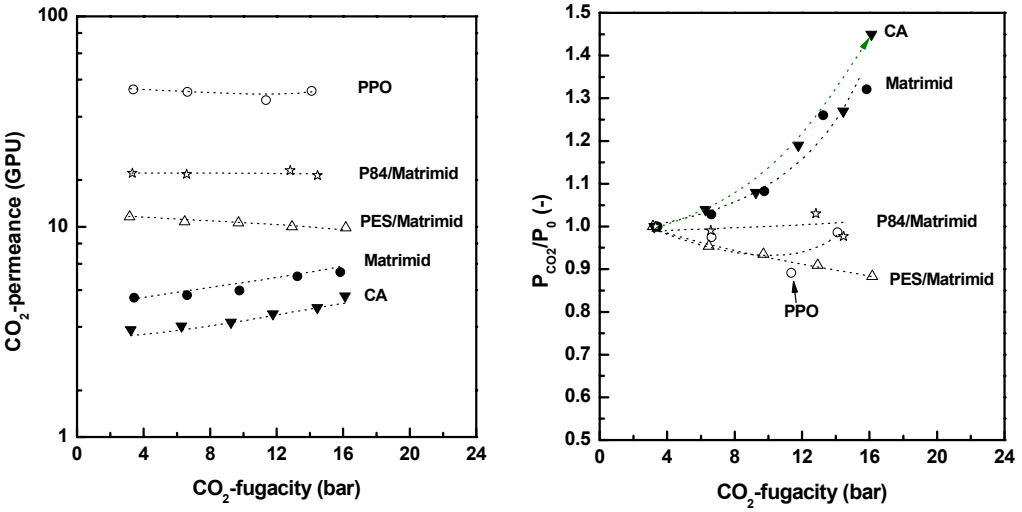

Figure 9: (a) Absolute (in GPU) and (b) normalized CO_2-permeance as a function of the CO_2-fugacity using a 80/20 vol.% CO_2/CH_4-feed gas mixture.

Figure 10 shows the N_2-permeance decay measurements for all membranes after the separation of a 80/20 vol.% CO_2/CH_4-feed gas mixture. Again, the N_2-permeance decay for CA membranes show a relative fast decrease towards the initial N_2-permeance, although the increase in the normalized CO_2-permeance with increasing CO_2-fugacity (Figure 9b) suggested a large effect of plasticization. This was explained in the previous section (50/50 vol.%) by the larger polymer chain mobility of CA compared to the other membrane materials. On the other hand, the CO_2-permeance behavior of PPO and the Matrimid-based membranes are confirmed by these experiments (Figure 10). Matrimid membranes show the highest amount of CO_2-induced residual conditioning (>40%) and thus the strongest effect of plasticization. The other materials appeared to be less susceptible to plasticization looking at the trends in CO_2-permeance. They show significantly less residual conditioning after the mixed gas permeation experiment (~20%). Furthermore, the two polyimide blends experience a similar extent of residual conditioning, suggesting a similar magnitude of CO_2-induced plasticization effects. This was also observed in the permeation experiments with pure CO_2 (Figure 2). However, the mixed gas CO_2-permeance shows a permeance reduction for PES/Matrimid membranes and a permeance increase for P84/Matrimid membranes with increasing fugacity. Probably, the observed difference in the CO_2-permeance behavior may be attributed to a

more pronounced competitive sorption effect in PES/Matrimid membranes compared to P84/Matrimid membranes.

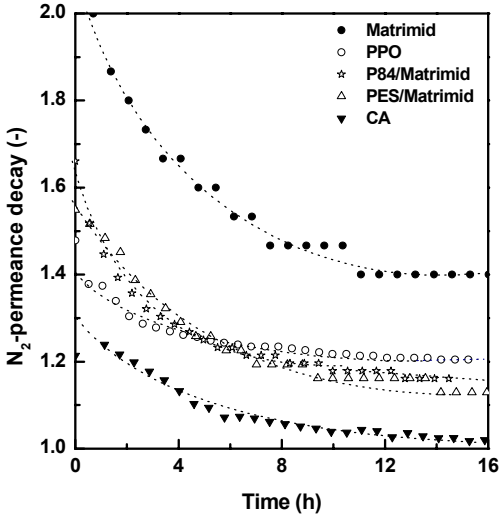

Figure 10: N_2-permeance decay after 80/20 vol.% CO_2/CH_4-separation at a feed pressure of 16 bar (CO_2-fugacity of 13.3 bar).

Figure 11 shows the (a) mixed gas CO_2/CH_4-separation factors and (b) normalized CH_4-permeance as a function of CO_2-fugacity for the different membranes investigated. Plasticization has a much stronger effect on the separation performance due to the higher CO_2-feed concentration compared to the previously described gas mixtures, as was shown by N_2-permeance decay measurements (Figure 10). Therefore, decreases in selectivity are not only caused by competitive sorption effects, but by plasticization effects as well. For example, for cellulose acetate it is reported that plasticization is the most dominating effect [8]. This is verified by looking at the CO_2/CH_4-separation factors in Figure 10. CA membranes show the largest loss in selectivity as a function of fugacity of all used materials, which is confirmed by looking at the normalized CH_4-permeance. The increase in normalized CH_4-permeance with increasing fugacity is the strongest for CA membranes.

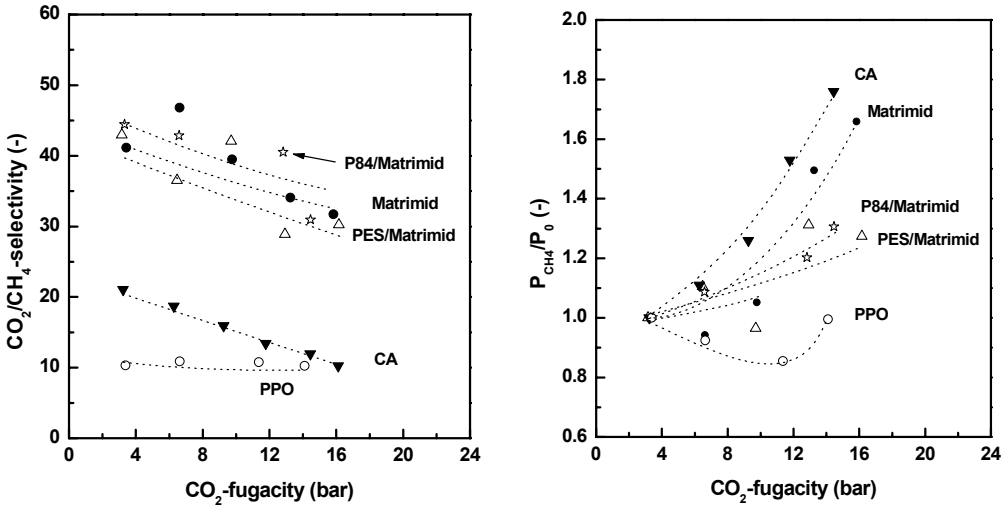

Figure 11: CO_2/CH_4-selectivity as a function of CO_2-fugacity using a 80/20 vol.% CO_2/CH_4-mixture.

For the other membranes (Matrimid, P84/Matrimid, PES/Matrimid and PPO) plasticization effects are pronounced as well, as the CH_4-permeance increases with increasing fugacity as well. However, in the case of CA membranes, the selectivity as a function of fugacity was lower at this CO_2-feed gas concentration compared to the previous described feed gas mixtures, while it increased for PPO, PES/Matrimid and P84/Matrimid membranes. It suggests that plasticization is not as dominant in these latter membranes compared to CA membranes. For Matrimid membranes similar selectivities were obtained compared to the 20/80 vol.% CO_2/CH_4-feed gas mixture, suggesting stronger plasticization effects than for PPO and the Matrimid-based blends, but weaker than for CA membranes. Typically, in the absence of plasticization, the mixed gas selectivity increases with increasing CO_2-feed gas concentration due to competition effects. Since the selectivity is higher with increasing CO_2-feed gas concentration, it can be concluded that competition effects still dominate the mixed gas separation performance of P84/Matrimid, PES/Matrimid and PPO membranes. Plasticization effects are clearly present but do not significantly influence the separation performance of these membranes, while they do for CA and Matrimid membranes.

Summarizing, at a CO_2-feed gas concentration of 80 vol.% plasticization effects start to dominate the separation performance of Matrimid membranes. CA membranes

experience a stronger effect of plasticization compared to the previous mixture, causing a decrease in selectivity with increasing CO_2-feed concentration. Competition effects are dominating the separation performance of P84/Matrimid, PPO and PES/Matrimid membranes, although plasticization effects are clearly visible.

98/2 vol.% CO_2/CH_4-separation

The trends that can be observed in the absolute and normalized CO_2-permeance (Figure 12) using a 98/2 vol.% feed gas mixture are similar to those observed using a 80/20 vol.% feed gas mixture (Figure 9). The absolute CO_2-permeances for the different materials are higher due to a decrease in competitive sorption effects (decreasing concentration of second component CH_4). Furthermore, the normalized CO_2-permeance increases with increasing fugacity for CA, Matrimid and P84/Matrimid membranes. For PES/Matrimid membranes still a slight decrease in the CO_2-permeance with increasing fugacity is observed. Due to smaller competition effects and a higher degree of plasticization at this feed gas composition, the increase in CO_2-permeance is stronger for P84/Matrimid compared to the 80/20 vol.% feed gas mixture. For the same reasons, the decrease in CO_2-permeance with increasing fugacity is less strong for PES/Matrimid membranes.

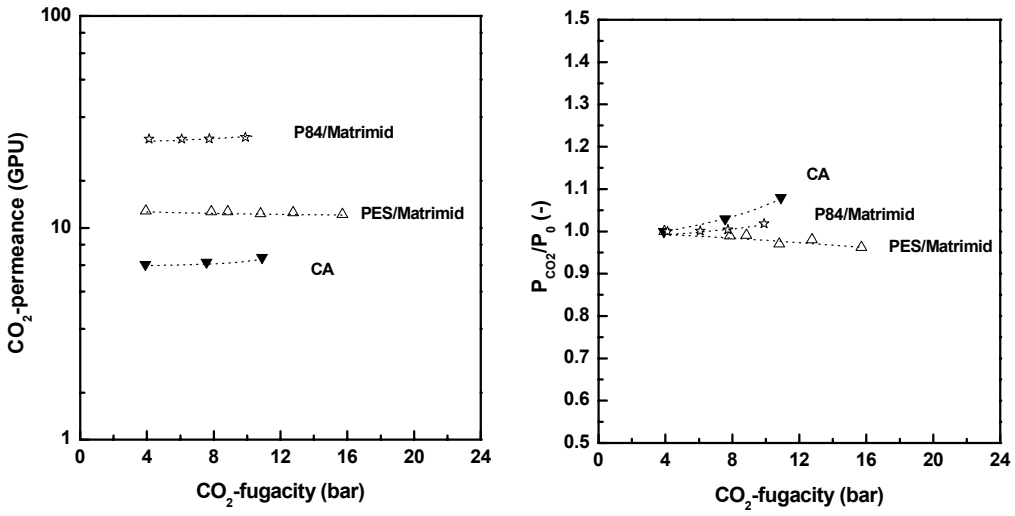

Figure 12: (a) Absolute (in GPU) and (b) normalized CO_2-permeance as a function of CO_2-fugacity using a 98/2 vol.% CO_2/CH_4-feed gas mixture.

A stronger increase in CO_2-permeance with increasing fugacity is not observed for CA membranes. The total increase in CO_2-permeance seems to be more or less unchanged. As all used membranes were completely aged before performing any mixed gas permeation experiment, a difference in the level of physical aging can be excluded as the reason for this effect. Furthermore, membranes without CO_2-permeation history were always used for a mixed gas experiment. The exact reason for the deviation in the CO_2-permeance behavior of CA membranes remains unclear.

Nonetheless, the extent of residual conditioning measured by the N_2-permeance decay (Figure 13) is significantly higher for CA membranes at this feed gas concentration compared to the 80/20 vol.% feed gas mixture.

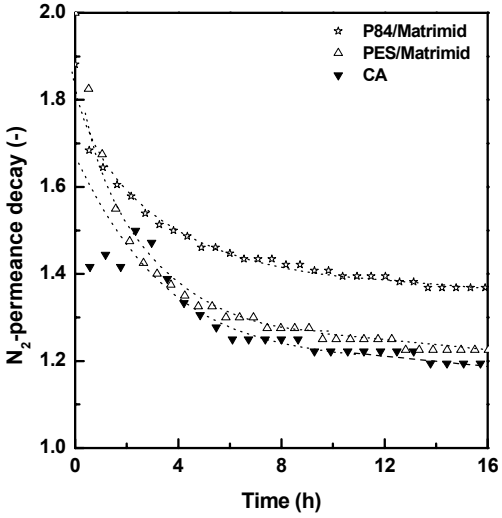

Figure 13: N_2-permeance decay after 98/2 vol.% CO_2/CH_4 separation at a feed pressure of 16 bar (CO_2-fugacity of 13.3 bar).

The degree of plasticization is that high that the initial N_2-permeance is not recovered anymore as was observed in the previously described feed gas mixtures (50/50 and 80/20 vol.% CO_2/CH_4). For the other membranes (PES/Matrimid and P84/Matrimid), a higher extent of residual conditioning is observed at this CO_2-feed concentration. The effects of plasticization appeared to be stronger for P84/Matrimid membranes compared to PES/Matrimid membranes, while the difference in pure gas CO_2-permeation behavior was very small.

Figure 14 shows (a) the mixed gas separation factor and (b) the normalized CH_4-permeance as a function of CO_2-fugacity in the separation of a 98/2 vol.% CO_2/CH_4-feed gas mixture. The separation factor of CA membranes is lower compared to the separation of the 80/20 vol.% CO_2/CH_4-feed gas mixture, which is due to strong and dominating plasticization effects. This causes also a strong increase in the normalized CH_4-permeance with increasing CO_2-fugacity. Plasticization is clearly more pronounced for P84/Matrimid membranes at a 98/2 vol.% feed gas concentration because a relative strong decrease in separation factor with increasing CO_2-fugacity is observed, while the values of the CO_2/CH_4-selectivity are lower compared to those in the separation of a 80/20 vol.% CO_2/CH_4-feed gas mixture. Besides, a large increase in the normalized CH_4-permeance with increasing fugacity is observed (Figure 14b). Therefore, it can be concluded that plasticization is dominating the separation performance of P84/Matrimid membranes at a 98/2 vol.% CO_2/CH_4-feed gas composition.

Plasticization has also a significant effect on the separation performance of PES/Matrimid membranes as the normalized CH_4-permeance is increasing with increasing CO_2-fugacity (Figure 14b). However, competitive sorption still seems to be the dominant effect, as the mixed gas selectivity values increased with increasing CO_2-feed concentration (from 80 to 98 vol.%) as a result of less competition effects.

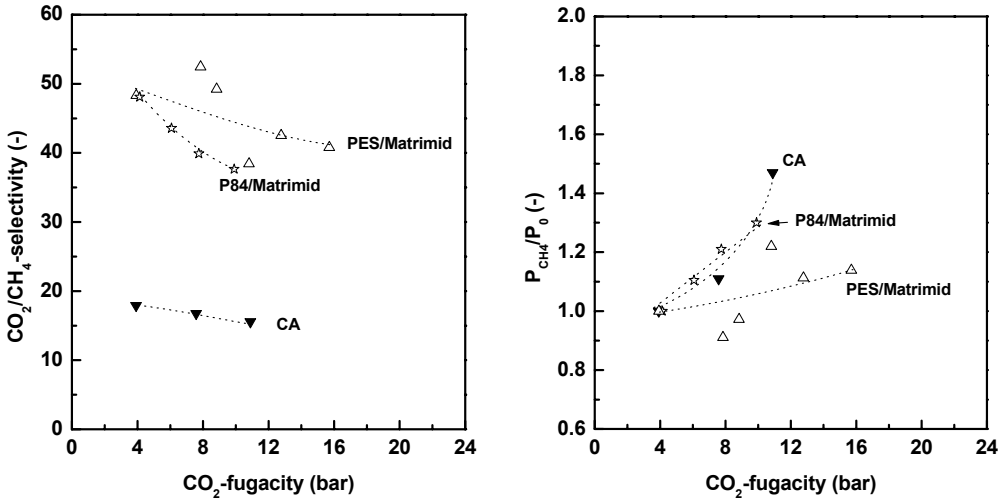

Figure 14: CO_2/CH_4-selectivity as a function of CO_2-fugacity in the separation of a 98/2 vol.% CO_2/CH_4-feed gas mixture.

Summarizing, plasticization effects are significantly stronger at a CO_2-feed concentration of 98% vol.%, as is shown by the N_2-permeance decay measurements. Furthermore, plasticization effects start to dominate the separation performance of P84/Matrimid membranes, because the mixed gas selectivity decreases with increasing CO_2-feed gas concentration (80 to 98 vol.%) and the CH_4-permeance shows a relative strong increase with increasing fugacity. Although plasticization effects are also more pronounced for PES/Matrimid membranes, the mixed gas selectivity still increases by increasing the CO_2-feed gas concentration from 80 to 98 vol.%, which suggests the mixed gas separation performance is not significantly influenced by plasticization effects over the complete concentration range investigated.

4.3.4. Discussion

Overall it can be concluded that a subtle balance between competition and plasticization effects exists in all asymmetric membranes investigated. However, depending on the material studied, plasticization or competition dominates the mixed gas transport behavior. For Matrimid membranes plasticization is dominant at high CO_2-feed gas concentrations (80 vol.% CO_2), while competition effects are dominant at low CO_2-feed gas concentrations (20 vol.% CO_2). For CA membranes, plasticization appears to be always the dominant effect (with the used feed gas compositions). Especially in the case of CA, plasticization effects can cause significant losses in selectivity with increasing CO_2-level, as was also observed by others [8-10]. PPO appeared to less susceptible to plasticization, but showed poor mixed gas selectivities probably caused by strong competition effects. Furthermore, the PPO membranes still contained some surface defects, which logically lowered the maximum achievable selectivity.

Of all asymmetric membranes investigated, PES/Matrimid and P84/Matrimid membranes have the most promising CO_2/CH_4-separation properties. Figure 15 shows the mixed gas selectivity as a function of CO_2- and CH_4-fugacity for PES/Matrimid and P84/Matrimid membranes.

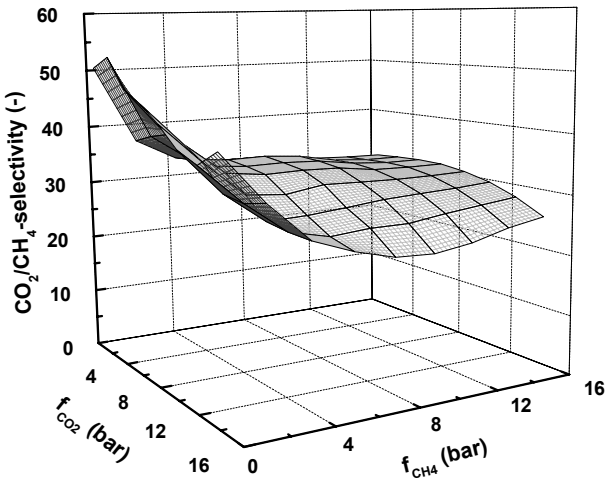

(a)

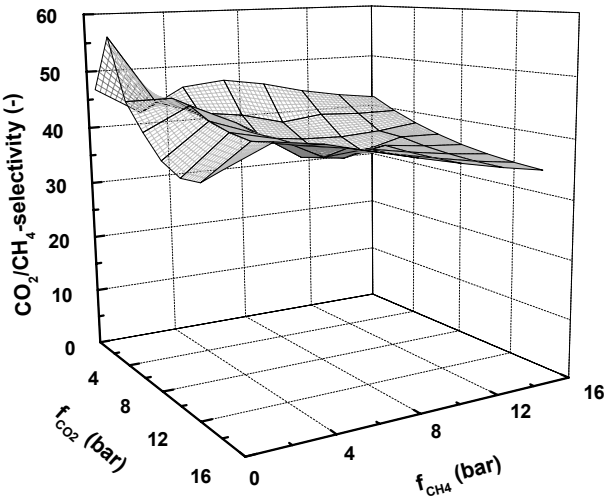

(b)

Figure 15: Contour plots of mixed gas selectivity as a function of CO_2- and CH_4-fugacity for (a) PES/Matrimid and (b) P84/Matrimid membranes.

The separation properties improve with decreasing CH_4-fugacity, which was interpreted as a result of strong competitive sorption effects in PES/Matrimid membranes. Plasticization effects seem not to influence the mixed gas separation performance much. A similar trend is observed for P84/Matrimid membranes; the separation properties become better with decreasing CH_4-fugacity. However, at the lowest CH_4-fugacity and higher

CO_2-fugacity (high CO_2-feed gas concentrations) the separation properties start to decline due to significant plasticization. Blending Matrimid with PES or P84 positively influences the plasticization resistance and thus the mixed gas separation performance, although it appears to be more effective at high CO_2-feed gas concentrations for PES/Matrimid membranes. Unless the fact that P84/Matrimid membranes seem to be slightly more susceptible to plasticization effects, they have much higher mixed gas selectivities compared to PES/Matrimid membranes.

It should be pointed out that plasticization phenomena are highly dependent on the conditions of the experiment. To allow a fair comparison, it was attempted to use membranes with a more or less similar skin thicknesses. However, the P84/Matrimid membranes possessed a thinner skin than the other four membranes. Typically, plasticization effects are more pronounced with decreasing thickness of the separation layer [5]. Furthermore, we were unable to obtain defect-free PPO membranes, which obviously influenced the maximum obtainable selectivity, while the reproducibility of the CA membranes was poor. Nevertheless, the observed trends to our opinion give a reliable view on the effects occurring in the mixed gas permeation behavior of different membrane materials based on glassy polymers.

Competitive sorption and especially plasticization effects can result in significant lower mixed gas selectivities for glassy polymer membranes. However, glassy polymer membranes may still show a much better separation performance than for example rubbery membranes which do not experience competitive sorption effects [28]. Figure 16 shows the mixed gas CO_2/CH_4-selectivity as a function of CO_2-fugacity of PES/Matrimid, P84/Matrimid membranes using a 80/20 vol.% CO_2/CH_4-feed gas mixture and a PEO-based rubbery membrane [28]. The two Matrimid-based membranes exhibit much higher CO_2/CH_4-selectivities, mainly due to high diffusion selectivities. Although for other glassy polymer membranes (6FDA-polyimide in Figure 16) the diffusion selectivity is often completely lost due to CO_2-plasticization [2], Figure 16 shows that a stable separation performance is obtained for PES/Matrimid and P84/Matrimid membranes up to at least 14 bar CO_2, which is in the range of typical CO_2-fugacities in natural gas.

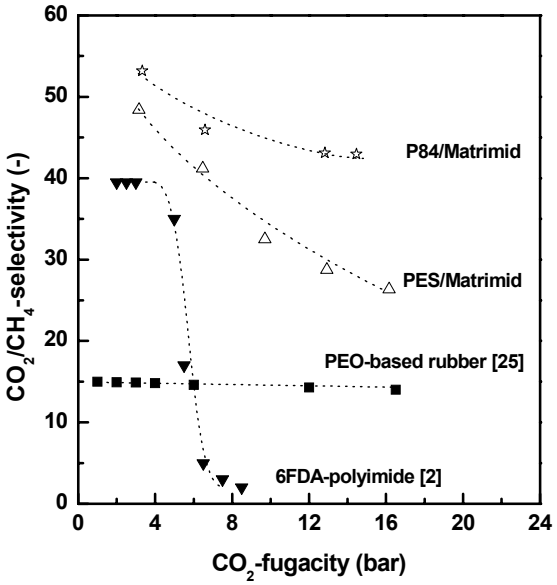

Figure 16: Mixed gas CO_2/CH_4-selectivity as a function of the CO_2-fugacity for two Matrimid-based glassy polymer membranes using a 80/20 vol.% CO_2/CH_4-feed gas mixture and a PEO-based rubbery membrane [28].

4.4. Conclusions

The results show that a subtle balance exists between competitive sorption and plasticization effects for all asymmetric membranes investigated. The magnitude of competition or plasticization effects varies depending on the materials investigated. Different levels of CO_2-concentration are required to reach the point where plasticization starts to dominate the separation performance of a certain material. The mixed gas permeation results showed that plasticization effects dominated the mixed gas separation performance of asymmetric Matrimid and CA membranes, resulting in a relative large loss of selectivity. PPO membranes appeared to be less susceptible to plasticization, but gave low mixed gas CO_2/CH_4-selectivities. The mixed gas separation performance of asymmetric PES/Matrimid membranes was not very sensitive for CO_2-plasticization due to relative strong competitive sorption effects. Although it enhanced the plasticization resistance, blending PES with Matrimid resulted in membranes with a lower selectivity compared to pure Matrimid membranes. On the other hand, the addition of P84 to a Matrimid-based blend resulted in higher selectivity and increased plasticization resistance. However, this was only valid for CO_2-feed gas concentrations below 80 vol.%. Above this

CO_2-feed gas concentration plasticization effects started to dominate the mixed gas separation performance of P84/Matrimid membranes above this CO_2-feed gas concentration.

Acknowledgement

The authors want to acknowledge professor W.J. Koros (Georgia Institute of Technology at Atlanta, U.S.A.) for fruitful discussions on the research covered in this paper.

4.5. References

1. M. Wessling, et al., *Plasticization of gas separation membranes*, Gas Separation & Purification **5** (1991), 222-228.
2. C. Staudt-Bickel and W.J. Koros, *Improvement of CO_2/CH_4 separation characteristics of polyimides by chemical crosslinking*, Journal of Membrane Science **155** (1999), 145-154.
3. T. Visser and M. Wessling, *Sorption-induced relaxation phenomena in a glassy polyimide*, submitted to Macromolecules.
4. R.W. Baker, *Future directions of membrane gas separation technology*, Industrial Engineering and Chemical Research **41** (2002), 1393-1411.
5. M. Wessling, M. Lidon Lopez, and H. Strathmann, *Accelerated plasticization of thin-film composite membranes used in gas separation*, Separation and Purification Technology **24** (2001), 223-233.
6. W.J. Koros, et al., *Model for permeation of mixed gases and vapors in glassy polymers*, Journal of Polymer Science, Polymer Physics Edition **19** (1981), 1513-1530.
7. R.T. Chern, et al., *Second component effects in sorption and permeation of gases in glassy polymers*, Journal of Membrane Science **15** (1983), 157-169.
8. E. Sada, et al., *Permeation of pure carbon-dioxide and methane and binary-mixtures through cellulose-acetate membranes*, Journal of Polymer Science Part B-Polymer Physics **28** (1990), 113-125.
9. S.Y. Lee, B.S. Minhas, and M.D. Donohue, *Effect of gas composition and pressure on permeation through cellulose acetate membranes*, AiChE Symposium Series **84** (1989), 93-99.
10. M.D. Donohue, B.S. Minhas, and S.Y. Lee, *Permeation behaviour of carbon dioxide-methane mixtures in cellulose acetate membranes*, Journal of Membrane Science **42** (1989), 197-214.
11. T. Visser, G.H. Koops, and M. Wessling, *On the subtle balance between competitive sorption and plasticization effects in asymmetric hollow fiber gas separation membranes*, Journal of Membrane Science **252** (2005), 265-277.

12. A. Bos, et al., *Suppression of gas separation membrane plasticization by homogeneous polymer blending*, AIChE Journal **47** (2001), 1088-1093.
13. S. Gagne, et al., *Optimization of CO_2/CH_4-separation performance of integrally skinned assymetric membranes prepared from poly(2,6-dimethyl-1,4-phenylene oxide) by factorial design*, Journal of Applied Polymer Science **72** (1999), 1601-1610.
14. J. Smid, J.H.M. Albers, and A.P.M. Kusters, *The formation of asymmetric hollow fibre membranes for gas separation, using PPE of different intrinsic viscosities*, Journal of Membrane Science **64** (1991), 121-127.
15. J.H. Hao and S. Wang, *Influence of quench medium on the structure and gas permeation properties of cellulose acetate membranes*, Journal of Applied Polymer Science **68** (1998), 1269-1276.
16. J.J. Krol, M. Boerrigter, and G.H. Koops, *Polyimide hollow fiber gas separation membranes: preparation and the suppression of plasticization in propane/propylene environments*, Journal of Membrane Science **184** (2001), 275-286.
17. T. Visser and M. Wessling, *High-flux integrally skinned P84/Matrimid asymmetric hollow fiber membranes for gas separation*, to be published.
18. G.C. Kapantaidakis and G.H. Koops, *High flux polyethersulfone-polyimide blend hollow fiber membranes for gas separation*, Journal of Membrane Science **204** (2002), 153-171.
19. M.K. Murphy, E.R. Beaver, and A.W. Rice, *Post-treatment of asymmetric membranes for gas application*, AIChE Symposium Series **85** (1989), 34-40.
20. P.H. Pfromm, I. Pinnau, and W.J. Koros, *Gas-Transport through Integral-Asymmetric Membranes - a Comparison to Isotropic Film Transport-Properties*, Journal of Applied Polymer Science **48** (1993), 2161-2171.
21. M. Wessling, et al., *Time-dependent permeation of carbon-dioxide through a polyimide membrane above the plasticization pressure*, Journal of Applied Polymer Science **58** (1995), 1959-1966.
22. H.M. Ettouney and O. Majeed, *Transport and permeation properties of a ternary gas mixture in a medium-size polysulfone hollow fiber permeator*, Separation Science and Technology **31** (1996), 1573-1596.
23. J.N. Barsema, et al., *Preparation and characterization of highly selective dense and hollow fiber asymmetric membranes based on BTDA-TDI/MDI co-polyimide*, Journal of Membrane Science **216** (2003), 195-205.
24. J.M.S. Henis and M.K. Tripodi, *Composite hollow fiber membranes for gas separation: the resistance model approach*, Journal of Membrane Science **8** (1981), 233-246.
25. W.R. Vieth, J.M. Howell, and J.H. Hsieh, *Dual sorption theory*, Journal of Membrane Science **1** (1976), 177.
26. M. Al-Juaied and W.J. Koros, *Performance of natural gas membranes in the presence of heavy hydrocarbons*, Journal of Membrane Science **274** (2006), 227-243.

27. A. Bos, et al., *CO_2-induced plasticization phenomena in glassy polymers*, Journal of Membrane Science **155** (1999), 67-78.
28. H. Lin, et al., High-performance polymer membranes for natural-gas sweetening, Advanced Materials **18** (2006), 39-44.

Chapter 5

Plasticization of asymmetric Matrimid-based hollow fiber membranes in C_3-separations

Abstract

This paper reports the stability of asymmetric hollow fiber membranes prepared from Matrimid-based blends towards C_3-plasticization. The C_3H_6/C_3H_8-mixed gas separation performance of asymmetric membranes of a 50/50 wt.% P84/Matrimid-blend is highly influenced by plasticization effects, as the selectivity significantly decreases with increasing propylene partial pressure. Plasticization effects are mainly caused by propylene, although kinetic sorption experiments revealed that propylene and propane both induce sorption relaxations. Sorption experiments also showed that the mixed gas selectivity is mainly based on diffusion selectivity, because the solubility selectivity was relatively small. The mixed gas permeance of propane was highly affected by the presence of propylene, while the mixed gas permeance of propylene was almost unchanged when compared to single gas permeation experiments. Propylene causes more pronounced plasticization effects than propane. Plasticization effects did influence the separation performance of asymmetric Matrimid membranes as well, but the effect is less pronounced. The addition of a third component to the feed mixtures (CH_4) hardly

changes the C_3H_6/C_3H_8-separation performance of P84/Matrimid asymmetric hollow fiber membranes. Competitive sorption effects are less pronounced to those observed in CO_2/CH_4-separations due to the relatively large magnitude of C_3-hydrocarbon induced plasticization effects.

Keywords: C_3-hydrocarbon separation, plasticization, gas separation, hollow fiber membranes, sorption relaxations.

5.1. Introduction

During the past two decades, polymer gas separation membranes have demonstrated to be a new viable technology contributing to sustainable chemical processing. For the next decades, a large market potential is predicted for the employment of such membranes in the petrochemical industry for separation of e.g. gas mixtures containing highly condensable gases, like the separation of olefins and paraffins or C_3-hydrocarbons from light gases such as CH_4 or H_2 [1]. However, the separation performance of polymer membranes is often deteriorated due to irreversible relaxations in the material caused by the sorption-induced swelling of highly condensable penetrants. This penetrant-induced phenomenon is generally called plasticization. The presence of plasticization causes the transport rates of all penetrants in a mixture to increase, which may result in significant selectivity losses. Polyimide-based gas separation membranes are considered to be promising candidates for C_{3+}-separation due to their often high separation performance, as they exhibit high single gas olefin/paraffin selectivities as a result of high diffusion selectivities [2, 3]. However, the diffusion selectivity for mixed gases generally decreases due to C_{3+}-hydrocarbon induced plasticization. In C_3H_6/C_3H_8-separation, mixed gas selectivity losses of more than 40% have been reported for dense films of 6FDA-based polyimides due to plasticization by propylene [4, 5]. Okamoto et al. [6] reported a high degree of C_4H_6-plasticization of several dense polyimide membranes resulting in a significant decrease of the $C_4H_6/n\text{-}C_4H_{10}$-mixed gas selectivity. Also Chan et al. [7] observed significant C_3H_6-plasticization in a series of 6FDA-based polyimide films, although only single gas experiments were carried out. These examples show that dense polyimide-based flat sheet membranes are highly susceptible to plasticization by C_{3+}-hydrocarbons.

The plasticization behavior of asymmetric membranes in the separation of C_{3+}-gas mixtures has been scarcely investigated. Little is known but the transport is generally entirely different from the behavior commonly observed in dense thick films [8, 9]. Krol et al. [10] studied single gas permeation of propylene and propane in asymmetric Matrimid polyimide membranes and observed significant plasticization, especially by propylene. The permeance of propylene showed a continuous increase with increasing pressures and was highly time-dependent, whereas the permeance of propane did not change much and showed a steady-state permeance within 8 hours of permeation. No mixed gas experiments were conducted. Lee et al. [11] investigated the C_3H_6/C_3H_8-mixed gas separation performance of asymmetric hollow fiber membranes of a BPDA-based copolyimide. They did not observe any plasticization effects, although their mixed gas selectivity was much lower than the ideal selectivity from single gas experiments, which was related to the relatively low pressure ratio used. Yoshino et al. [12] reported the mixed gas separation performance of asymmetric hollow fiber membranes of the copolyimide 6FDA/BPDA (1/1)-DDBT in the separation of C_3- and C_4-gas mixtures. Surprisingly, no evidence of the presence of plasticization effects was found in the separation of the C_3-hydrocarbon mixture. However, a poor C_3-hydrocarbon stability was reported for thin film composite membranes of the polyimide BPDA-TMPD in C_{3+}-separation [13].

The stability of asymmetric gas separation membranes can often be increased by chemical or physical cross-linking of the polymer network [14-20]. Generally these methods are used to reduce CO_2-plasticization in CO_2/CH_4-separations. Recently, Hess et al. [21] reported plasticization resistant dense 6FDA-based polyimide membranes in C_3-separation by chemical cross-linking. There is hardly any information known about the effect of crosslinking on the C_3-induced plasticization behavior in asymmetric gas separation membranes. Krol et al. [10] showed that the plasticization resistance to propylene can also be enhanced by thermally treating asymmetric Matrimid polyimide membranes at 220°C. Another alternative and easy way to suppress or reduce CO_2-plasticization effects is homogeneous polymer blending [22]. Recently it was found that plasticization effects in CO_2/CH_4-separations are less pronounced when asymmetric membranes consisting of blends of Matrimid with either polyethersulfone (PES) or the co-polyimide P84 are used [23].

Polymer blending may also improve the stability of asymmetric gas separation membranes to C_3-hydrocarbons. No detailed data are so far reported on the mixed gas plasticization behavior of polymer blends in C_3-separations. Therefore, the main goal of this paper is to investigate the stability of asymmetric membranes consisting of a polymer blend towards C_3-hydrocarbons. The mixed gas separation performance of asymmetric hollow fiber membranes consisting of a 50/50 wt.% P84/Matrimid-blend is investigated in C_3H_6/C_3H_8-separation and compared to the performance of Matrimid asymmetric hollow fiber membranes. Furthermore, the separation of a ternary mixture of $CH_4/C_3H_6/C_3H_8$ is measured to investigate the influence of a third component on the C_3H_6/C_3H_8-mixed gas performance. Single gas permeation experiments with propylene and propane are performed to support the obtained mixed gas permeation results. The kinetic sorption behavior of propylene and propane in dense films of the P84/Matrimid-blend is studied to further clarify plasticization effects induced by C_3-hydrocarbons.

5.2. Experimental

5.2.1. Materials

Asymmetric hollow fiber membranes investigated were prepared of commercially available Matrimid 5218 polyimide (BTDA-AAPTMI, Vantico AG, Switzerland) and of a 50/50 wt.% blend of Matrimid 5218 polyimide and P84 co-polyimide (BTDA-TDI/MDI, HP Polymer GmbH, Austria). Details of the spinning processes are reported elsewhere [10, 23, 24]. The rubbery polymer polydimethylsiloxane (PDMS, Sylgard 184), obtained from Dow Corning (The Netherlands), was used as coating material to plug surface defects (5 wt.% PDMS-solution in n-hexane). Gases (purity > 99.5%) and pre-calibrated gas mixtures were obtained from Praxair (The Netherlands) and used as received.

Dense flat-sheet membranes were prepared by casting polymer solutions of 15 or 20 wt.% in NMP on a glass plate using a 0.3 mm casting knife. Solvent was evaporated in a nitrogen atmosphere for 3 days. After removal of the films from the glass plates they were dried for at least 2 days in vacuum at 150°C. Finally, dry films with a thickness of 30-40 μm were obtained.

5.2.2. Permeation characteristics

All permeation characteristics were determined using the variable pressure method as described by Kapantaidakis and Koops [25]. Five fibers of each ~20 cm long were potted into 3/8 inch stainless steel holders, while sealing the other side using an epoxy resin. The hollow fiber membrane modules were pressurized from the shell side. All measurements were performed at a temperature of 35°C. Single gas permeance values were calculated from the pressure increase in time in a calibrated volume at the permeate side. Steady-state O_2 and N_2-permeance values were measured to verify the quality of the hollow fiber membranes before and after exposure to hydrocarbons. The ideal O_2/N_2-separation factor was calculated from the ratio of single gas permeance values. The thickness of the asymmetric skin was calculated as the ratio of the intrinsic O_2- and N_2-permeability coefficients and the permeance values for the asymmetric membranes. The single gas permeance of propylene and propane for asymmetric P84/Matrimid hollow fiber membranes were measured in time at different feed pressures (1.3, 2.0, 2.5 and 4.0 bar). The ideal selectivity was calculated from the ratio of these single gas permeance values after ~15 hours of permeation. For asymmetric Matrimid hollow fiber membranes, single gas permeation characteristics of propylene and propane at different pressures were reported before [10].

The separation performance of P84/Matrimid asymmetric hollow fiber membranes in the separation of a 50/50 vol.% C_3H_6/C_3H_8-feed gas mixture was measured at feed gas pressures of 1.6, 2.5, 4.0 and 5.0 bar. For comparison, also the C_3H_6/C_3H_8-separation performance of plain Matrimid asymmetric hollow fiber membranes was measured at a feed pressure of 4.0 bar. Furthermore, the influence of a third, inert component on the C_3H_6/C_3H_8 -separation behavior was studied. Therefore, the separation of a 50/40/10 vol.% $CH_4/C_3H_6/C_3H_8$-feed gas mixture was measured using P84/Matrimid membranes at three different feed pressures (2.0, 3.0 and 4.0 bar). The separation performance of the binary mixture was always measured for at least 15 hours, while the separation performance of the ternary mixture was measured for 6 to 8 hours at all feed pressures.

The experiments were always conducted on two membrane modules simultaneously. To avoid discrepancies in the mixed gas transport behavior, membrane modules were used without any permeation history and that were completely aged [26, 27]. The feed and

permeate compositions were analyzed by means of a Perkin-Elmer gas chromatograph (GC) equipped with an Alumina F-1 column. The retentate flow rate was kept constant at 15 ml/min to provide stage-cuts < 1%. To trace residual conditioning the N_2-permeance decay was measured in time after exposure to the hydrocarbon gas mixtures [8]. Subsequently, the O_2-permeance value was measured to examine the effect of hydrocarbon conditioning on the ideal O_2/N_2-selectivity.

5.2.3. High pressure gas sorption

The kinetic sorption behavior of propylene and propane at 35°C in dense films of a 50/50 wt.% P84/Matrimid-blend (~40 μm thick) was investigated using a gravimetric sorption balance. Before each experiment, the samples were degassed for at least 24 hours. Incremental pressure steps of 1 bar were taken up to a maximum pressure of 5 bar. The electronic signal shows always large drifts in the first few minutes of sorption as a result of temperature increases (Joule-Thomson effect) upon pressurization of the sorption balance. For this reason, the first minutes were disregarded in the analysis of the kinetic sorption behavior. The measured weight w_t was corrected for buoyancy according to Archimedes' principle. Based on the exact volume V_t (m^3) and the initial weight w_0 (g) of the sample and the density ϱ_{gas} (g/m^3) of the surrounding gas, the mass gain m_t (g) can be calculated by taking into account the buoyancy effect:

$$m_t = \left(w_t + V_t \rho_{gas}\right) - w_0 \qquad (1)$$

The gas density was estimated using the Peng-Robinson equation of state [28]. The density of the polymer sample was determined at room temperature using a Micromeritics AccuPyc 1330 pycnometer. The gas concentration in the polymer (cm^3 (STP) gas per cm^3 of polymer) was calculated using the molar volume at standard temperature and pressure (STP, 1 bar and 273.15 K), the polymer volume, and the molecular weight of the specific gas.

5.3. Results and discussion

5.3.1. O_2/N_2-single gas permeation characteristics

Table 1 shows the single gas permeation characteristics of 50/50 wt.% P84/Matrimid and of Matrimid flat sheet and asymmetric hollow fiber membranes. The values are an average of four different measurements (standard deviation < 15%). All modules were post-treated with silicone rubber in order to cure surface defects. One Barrer equals $1{\cdot}10^{-10}{\cdot}cm^3{\cdot}cm/cm^{2.}{\cdot}s{\cdot}cmHg$ and one GPU (gas permeation unit) equals $1{\cdot}10^{-6}{\cdot}cm^3(STP)/cm^2{\cdot}s{\cdot}cmHg$.

Table 1: Single gas permeation characteristics of 50/50 wt.% P84/Matrimid and of Matrimid membranes.

Membrane material	*Flat sheets*			*Asymmetric hollow fibers*				
	Permeability (Barrer)		*Selectivity (-)*	*Permeance (GPU)*		*Selectivity (-)*	*Skin thickness (μm)*	
	N_2	O_2	O_2/N_2	N_2	O_2	O_2/N_2	N_2	O_2
P84/Matrimid	0.055	0.42	7.7	0.52	4.0	7.7	0.11	0.11
Matrimid	0.15	1.03	7.0	0.41	2.8	6.9	0.36	0.37

P84/Matrimid membranes have intrinsically much lower O_2- and N_2-permeabilities compared to plain Matrimid membranes. However, the O_2- and N_2-permeance values are relatively similar, as the thickness of the skin layer of P84/Matrimid asymmetric hollow fiber membranes is approximately three times smaller than of Matrimid asymmetric hollow fiber membranes. After post-treatment, the ideal O_2/N_2-selectivity of both P84/Matrimid and of Matrimid asymmetric membranes are similar to the intrinsically values found for dense films.

5.3.2. C_3H_6/C_3H_8-single gas permeation characteristics

Figure 1 shows the single gas permeance of propylene as a function of time for P84/Matrimid membranes at four different pressures. The permeance increases with increasing pressure. At a feed pressure of 1.3 bar, the permeance appears to reach a steady-state relatively fast, while at higher pressures it continues to increase as a function of time. A time-dependent increase in permeance is typically associated with plasticization effects

[27]. The increasing rate at which the permeance increases in time with increasing pressure, suggests an increasing magnitude of plasticization effects.

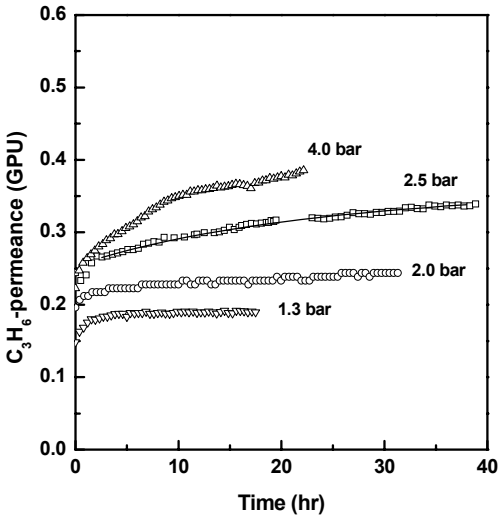

Figure 1: C_3H_6-permeance of P84/Matrimid membranes as a function of time for four different pressures.

Figure 2 shows the single gas permeance of propane as a function of time for P84/Matrimid membranes at four different pressures. The permeance of propane decreases with increasing the pressure up to 2.0 bar, which is a typical behavior of many glassy polymers [29]. However, the permeance increases when the pressure is further increased to 2.5 and 4.0 bar. This minimum in permeance can be attributed to the onset of plasticization effects [29]. The permeance of propane is much less time-dependent than propylene, suggesting a reduced effect of plasticization.

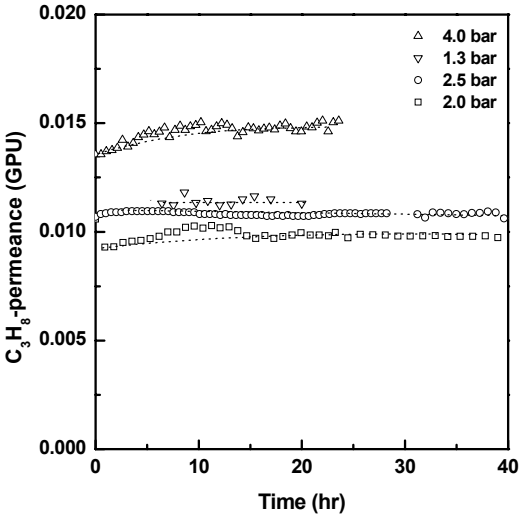

Figure 2: C_3H_8-permeance of P84/Matrimid membranes as a function of time for four different pressures.

Figure 3 shows the single gas permeances of propylene and propane and the ideal calculated C_3H_6/C_3H_8-separation factor as a function of pressure after ~15 hours of permeation. It should be noted that the ideal separation factor does not reflect reality as it is over predicted due to plasticization effects, but it gives at least insights in the order of magnitude of the selectivity. The solid and dotted lines in Figure 3 are trend lines and are only shown to guide the eye. The permeance of propylene shows a continuous increase with increasing pressures, which is a typical effect of plasticization in integrally skinned asymmetric membranes [8]. Due to swelling of the polymer matrix, the segmental mobility of the polymer chains is enhanced resulting in enhanced diffusivity and thus increasing permeance [29]. The permeance of propane initially decreases with increasing pressure and shows an upward inflection starting at a pressure of 2.5 bar. This minimum in the permeance of propane as a function of pressure is generally called the plasticization pressure. The ideal selectivity initially increases with increasing pressure, until the pressure where the C_3H_8-permeance also starts to increase.

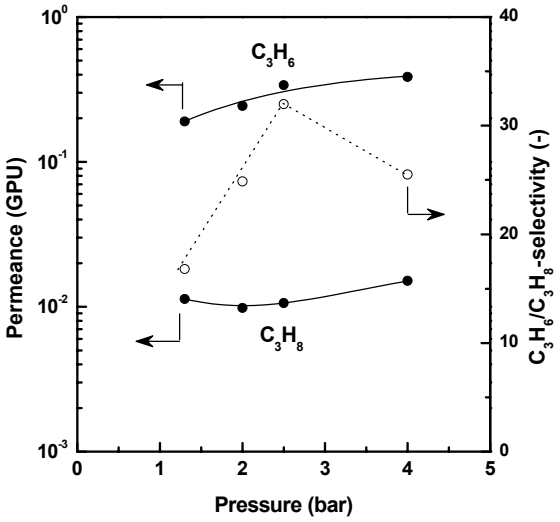

Figure 3: Ideal separation characteristics of C_3H_6- and C_3H_8-permeation in P84/Matrimid asymmetric hollow fiber membranes.

Similar gas permeation characteristics have been reported for propylene in Matrimid asymmetric hollow fiber membranes: the permeance continuously increased with increasing pressure and was time-dependent as well [10]. However, the permeance of propane continuously decreased with increasing pressure, suggesting the absence of plasticization effects. A steady-state permeance was observed within 8 hours of permeation. The ideal separation factor increased from 13 at a pressure of 1 bar to 34 at a pressure of 4 bar. These single gas permeation experiments may suggest that P84/Matrimid membranes are more susceptible to plasticization by hydrocarbons than Matrimid membranes.

5.3.3. C_3H_6- and C_3H_8-kinetic sorption behavior in dense films of a 50/50 wt.% P84/Matrimid-blend

Kinetic sorption behavior provides insights into the plasticization behavior of gases in polymers. Figure 4 shows the kinetic sorption behavior of propylene at different pressures for dense films of a 50/50 wt.% P84/Matrimid-blend. Incremental pressure steps of 1 bar were taken to enhance the visibility of sorption relaxations [30]. Ideal Fickian sorption is typically recognized as a linear weight increase leveling off to equilibrium when plotted as the square root of time [31]. Generally, kinetic sorption behavior becomes non-Fickian

upon extensive swelling, represented by an additional weight increase in time due to polymer chain relaxation [32].

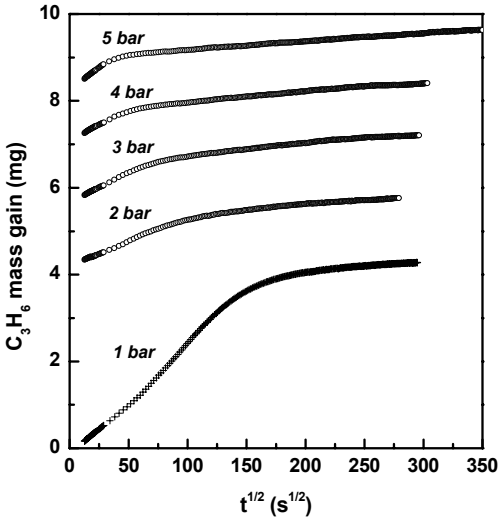

Figure 4: C_3H_6-mass gain as a function of the square root of time in a dense film of a 50/50 wt.% P84/Matrimid blend.

Figure 4 shows that equilibrium is not reached within the time-scale of the experiments. Mass uptake continues to increase after building up the diffusion profile. This is attributed to sorption induced relaxations. With the aid of an empirical model [33, 34], able to separate contributions of diffusion and relaxational sorption, it was found that the magnitude of the relaxational part of the kinetic sorption behavior appears to increase with increasing pressure, suggesting higher levels of plasticization with increasing pressure. This confirms the results obtained with the single gas permeation experiments with propylene that plasticization effects are more pronounced at higher pressures resulting in an increase of the permeance of propylene.

Figure 5 shows the kinetic sorption behavior of propane for dense films of a 50/50 wt.% P84/Matrimid blend, using incremental pressure steps of 1 bar. Although the curves seem linear at first instance, a slight upward inflection can be observed after a certain time (shown by dotted lines at $t^{1/2} \sim 150\text{-}200\ s^{1/2}$), suggesting the presence of sorption-induced relaxations. Due to a relative low diffusion coefficient for propane, the rates of diffusion and relaxation become very similar, resulting in a superposition of the two contributions to

the sorption process [33]. The upward inflection is more pronounced at higher pressures, suggesting an increasing magnitude of polymer chain relaxation. It demonstrates that propane causes sorption-induced relaxations at all pressures investigated. However, single gas permeation experiments showed that a minimum pressure of ~2.5 bar was required to cause an upward inflection in the permeance of propane. Probably at low pressures, the diffusivity of propane is altered due to polymer chain relaxation, but not sufficiently yet to cause an increase in permeance with increasing pressure. We also need to point out that in permeation experiments a concentration gradient exists due to the use of a vacuum at the permeate side of the membrane, while in sorption experiments no gradient exists upon the appearance of relaxations.

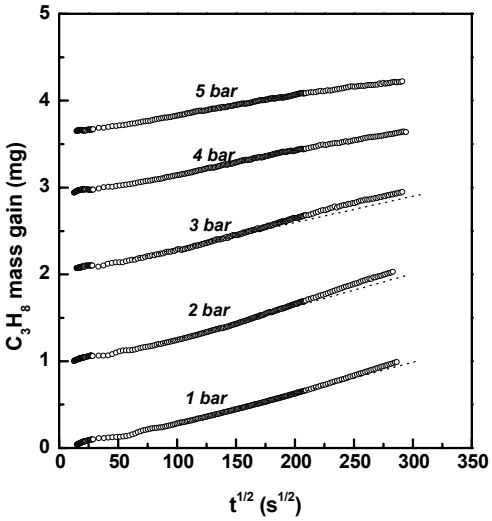

Figure 5: C_3H_8-mass gain as a function of the square root of time in a dense film of a 50/50 wt.% P84/Matrimid-blend.

Figure 6 shows the sorption isotherms of propylene and propane and the C_3H_6/C_3H_8-solubility ratio for dense films of a 50/50 wt.% P84/Matrimid-blend determined from Figures 4 and 5. As equilibrium was not reached within the experimental time-scales due to the time dependency of relaxation phenomena, a 'pseudo'-equilibrium was assumed after 24 hours of sorption.

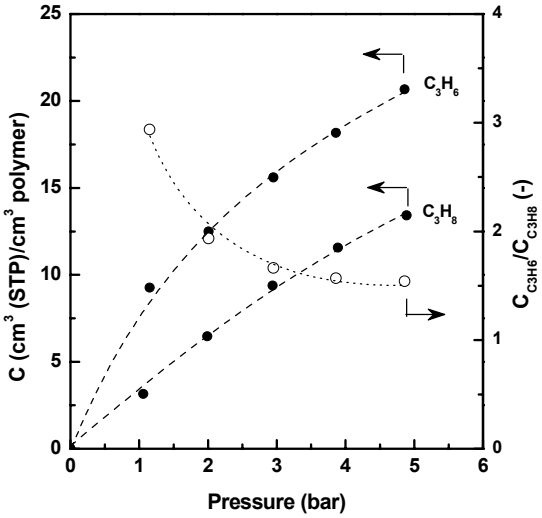

Figure 6: Sorption isotherms of C_3H_6 and C_3H_8 and solubility ratio in films of 50/50 wt.% P84/Matrimid polyimide up to 5 bar.

The concentration of propylene is significantly higher in P84/Matrimid compared to propane. This difference in solubility can be mainly attributed to specific interactions between the unsaturated bond of propylene and the polymer matrix [3]. The solubility ratio represents the solubility selectivity of the polymer blend and decreases with increasing pressure. These values highly depend on the experimental time scale and are only used to estimate the order of magnitude in solubility selectivity. The concentrations of propylene and propane in dense Matrimid films at a pressure of 4 bar were much higher; 31.7 and 19.0 cm^3 (STP)/cm^3 polymer, respectively, resulting in a solubility ratio of 1.67 [34]. The solubility selectivity of Matrimid and a 50/50 wt.% P84/Matrimid-blend are comparable.

5.3.4. Separation of a binary mixture of 50/50 vol.% C_3H_6/C_3H_8

The C_3H_6/C_3H_8-separation performance of asymmetric P84/Matrimid membranes was investigated at four different feed pressures (1.6, 2.5, 4.0 and 5.0 bar) and that of asymmetric Matrimid membranes at one feed pressure (4.0 bar). Figure 7 shows the mixed gas permeance values of (a) propylene and (b) propane as a function of time for these experiments.

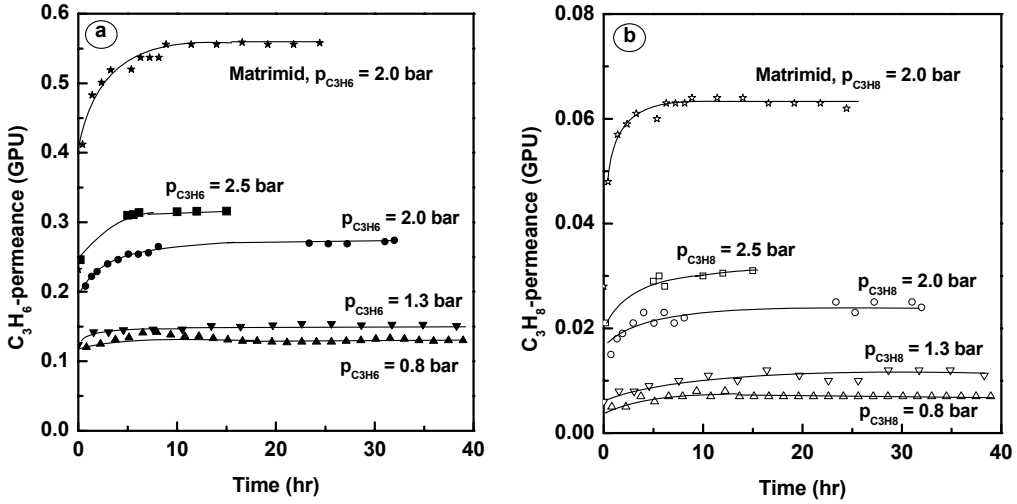

Figure 7: (a) C_3H_6- and (b) C_3H_8-permeance as a function of time in the separation of a 50/50 vol.% feed gas mixture using P84/Matrimid membranes at four different feed gas pressures or Matrimid membranes at one feed gas pressure. The solid lines illustrate the observed trend and are only used to guide the eye.

Figure 7a shows that the mixed gas permeance of propylene values increase with increasing pressure initially, in agreement with the single gas permeation experiments with propylene shown in Figure 1. In contrast to the single gas experiments the permeance values level off to an apparent steady-state value after a rapid initial increase. The mixed gas permeance values of propylene for Matrimid membranes give the same trend as observed for P84/Matrimid membranes: an initially rapid increase in permeance leveling of to a steady-state value, although it was reported that the single gas permeance of propylene continued to increase in time due to significant plasticization [10]. The permeance values of propylene for the P84/Matrimid membranes are approximately two times lower than the corresponding values for Matrimid membranes (at a propylene partial pressure of 2 bar), even though the P84/Matrimid membranes have a much thinner separation layer (Table 1). This can be attributed to a much lower intrinsic permeability of propylene for P84 than for Matrimid.

Figure 7b shows that the mixed gas permeance of propane shows a different behavior compared with the single gas permeation experiments with propane. The mixed gas permeance of propane increases significantly with increasing feed pressure, while minor pressure dependence was observed in the single gas permeation experiments. Furthermore, the permeance of propane shows initially a relative large increase in time before leveling off, while the single gas permeance was almost time-independent. It takes a relatively long time before steady-state is reached. Similar trends can be observed in the mixed gas permeance of propane for Matrimid, although a steady-state is achieved earlier. The rates at which the mixed gas permeance of propane is built up, are significantly higher compared to the single gas experiments, suggesting a significant increase in mobility of propane [31]. This can be attributed to plasticization by propylene only.

Figure 8 shows the C_3H_6/C_3H_8- mixed gas selectivity as a function of time for P84/Matrimid membranes at four different feed gas pressures and for Matrimid membranes at one feed gas pressure. To obtain better visualization, the selectivity data are plotted on a logarithmic scale.

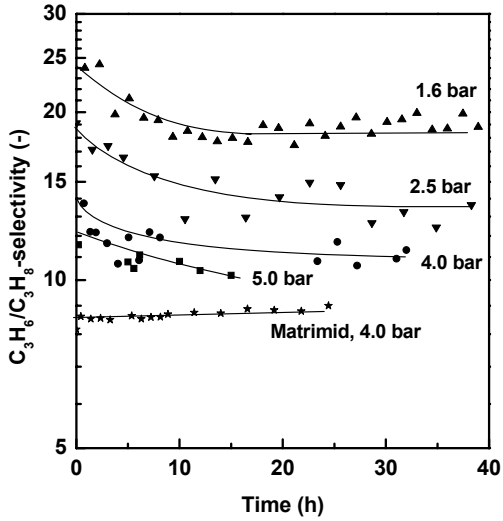

Figure 8: Mixed gas selectivity as a function of time for the separation of a 50/50 vol.% C_3H_6/C_3H_8-feed gas mixture using P84/Matrimid membranes at four different feed gas pressures and Matrimid membranes at one feed gas pressure. The solid lines illustrate the observed trend and are only used to guide the eye.

For asymmetric P84/Matrimid membranes, it takes a relatively long time before reaching steady-state mixed gas selectivity. This is caused by the lower rate at which the permeance of propane changes in time compared to that of propylene. Because these rates are similar and probably much faster for Matrimid membranes, almost no change in mixed gas selectivity is observed in time for these membranes. The mixed gas selectivity of P84/Matrimid membranes significantly decreases with increasing feed gas pressure, which can be related to an increasing magnitude of plasticization effects. However, the mixed gas selectivity of P84/Matrimid membranes at a feed pressure of 4.0 bar is significantly higher than of Matrimid membranes. The experimentally determined mixed gas selectivity of Matrimid membranes (α_{mix} = 8.5) is lower than the ideal selectivities reported for dense Matrimid films [10, 35], which may be related to C_3-hydrocarbon plasticization.

Figure 9 shows an overview of the permeance values of propylene and propane for the single and mixed gas experiments as a function of propylene partial pressure for P84/Matrimid asymmetric hollow fiber membranes. The values were recorded after ~15 hours of permeation. It should be noted that the experiments were conducted with three different membrane modules having slight differences in permeation behavior.

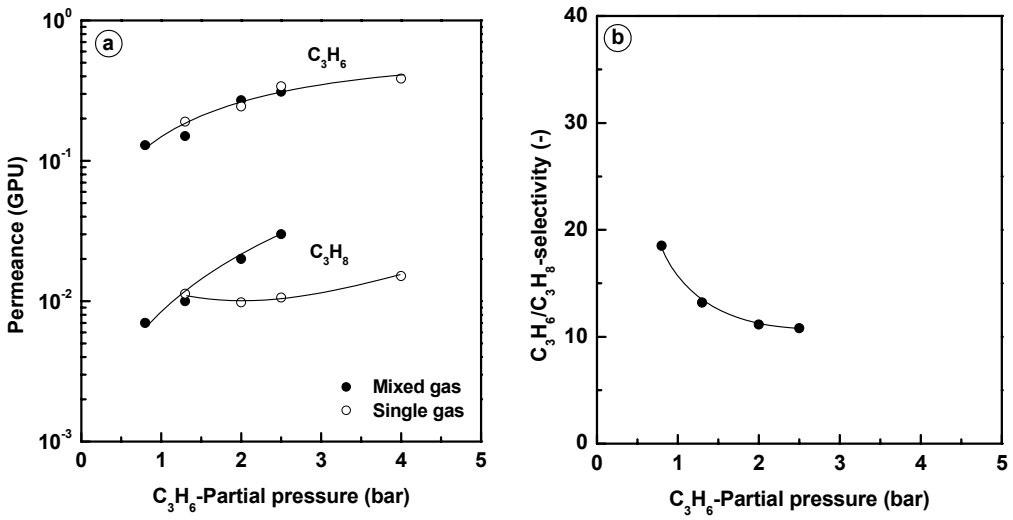

Figure 9: (a) mixed and single gas permeance and (b) mixed gas C_3H_6/C_3H_8-selectivity as a function of C_3H_6-partial pressure for P84/Matrimid asymmetric hollow fiber membranes in the separation of a 50/50 vol.% C_3H_6/C_3H_8-feed gas mixture. The solid lines illustrate the observed trend and are only used to guide the eye.

The mixed gas permeance of propylene is hardly influenced by the presence of a second component (propane), as the single gas and mixed gas values coincide. This is especially surprising since it was shown in single gas sorption and permeation experiments that propane induces plasticization effects as well. In contrast to propylene, the mixed gas permeation behavior of propane is highly affected by the second component. The mixed gas permeance of propane shows a continuous increase in permeance with increasing propylene partial pressure, whereas a minimum in the permeance was observed for single gas experiments with propane. This was attributed to C_3-hydrocarbon plasticization and suggests that it affects the mobility of propane more than that of propylene. The permeability of a penetrant is reduced by the presence of a second penetrant due to competitive sorption effects [9]. As the single and mixed gas permeance values of propylene coincide and the mixed gas permeance of propane is much higher compared to the single gas permeance, it suggests either the absence of competition effects or relatively weak competition effects. However, it has been reported for C_3H_6/C_3H_8-separation in dense polyimide flat sheet membranes that mixed gas permeabilities of propylene were much lower than the corresponding single gas permeabilities, suggesting significant competition effects [3]. This suggests competition effects should also be present in C_3-separtion with P84/Matrimid asymmetric hollow fiber membranes, but are probably entirely masked by dominating plasticization effects.

At a propylene partial pressure of 0.8 bar, the steady-state mixed gas selectivity is still relatively high (~20). As the solubility selectivity of P84/Matrimid membranes is less than two, the mixed gas selectivity is mainly based on diffusion selectivity. A high diffusion selectivity is common for olefin/paraffin-separation in glassy polymer membranes [3]. The mixed gas selectivity is significantly decreasing with increasing propylene partial pressure, as a result of propylene-induced plasticization effects. The diffusion selectivity is higher for P84/Matrimid membranes because Matrimid membranes have comparable solubility selectivity but lower mixed gas selectivity. We conclude that the loss in mixed gas selectivity can be attributed to a loss in diffusion selectivity as a result of C_3-plasticization.

The effect of plasticization induced by C_3-hydrocarbon-conditioning during the mixed gas permeation experiments is quantified afterwards by measuring the N_2-permeance decay in time [8, 9]. Figure 10 shows the N_2-permeance decay as a function of time for P84/Matrimid and for Matrimid asymmetric hollow fiber membranes.

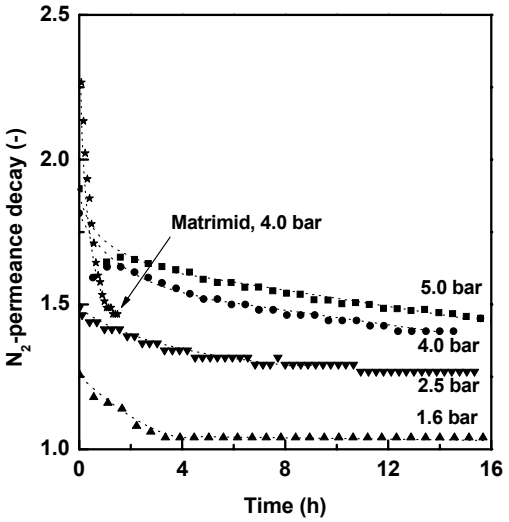

Figure 10: N_2-permeance decay as a function of time after mixed gas experiments for Matrimid and P84/Matrimid membranes. The dashed lines illustrate the observed trend and are only used to guide the eye.

Both membrane materials show a significant amount of residual C_3-hydrocarbon conditioning after performing the mixed gas experiments. For P84/Matrimid membranes, the amount of residual conditioning is increasing with increasing pressure, showing the increased effect of plasticization. Although initially a larger conditioning effect is observed for Matrimid compared to P84/Matrimid asymmetric hollow fiber membranes, the decline in time is much more rapid for Matrimid. This is consistent with the fact that the C_3-hydrocarbon mixed gas permeances reached relatively fast steady-state values during permeation experiments. After the N_2-permeance decay experiments (~16 hours of permeation), the O_2-permeance was measured as well to observe the effect of plasticization on the ideal O_2/N_2-separation factor. The O_2-permeance for Matrimid asymmetric hollow fiber membranes was already measured after 2 hours of N_2-permeation. Table 2 shows the single gas O_2- and N_2-permeation characteristics before and after mixed gas experiments.

Table 2: Single gas O_2- and N_2-permeation characteristics before and after separation of a 50/50 vol.% C_3H_6/C_3H_8-feed gas mixture for P84/Matrimid and for Matrimid asymmetric hollow fiber membranes.

Membrane material	p_{feed} *(bar)*	*(P/l)* N_2 *(GPU)*	*(P/l)* O_2 *(GPU)*	O_2/N_2 *(-) After*	O_2/N_2 *(-) Before*	*% decrease in* O_2/N_2*-selectivity*
Matrimid	4.0	0.66	4.60	7.0	6.9	<1
P84/Matrimid	1.6	0.52	4.07	7.8	7.8	<1
	2.5	0.73	5.25	7.2	7.9	9
	4.0	0.77	4.84	6.3	7.5	15
	5.0	0.77	4.47	5.8	7.6	24

The single gas O_2/N_2-selectivity is unchanged for Matrimid membranes, while the C_3H_6/C_3H_8-separation performance was affected by plasticization effects. The P84/Matrimid membranes used at a feed pressure of 1.6 bar appear not be affected by C_3-plasticization as well. At higher feed pressures, the O_2/N_2-selectivity of P84/Matrimid membranes is clearly affected and shows a strong decrease with increasing C_3-hydrocarbon mixture feed gas pressure. These results suggest that asymmetric Matrimid membranes are less susceptible to C_3-induced plasticization effects compared to asymmetric membranes of a P84/Matrimid-blend and suggests that blending Matrimid with P84 does not improve the stability to C_3-induced plasticization effects although it was reported to be effective in CO_2/CH_4-separations [22].

5.3.5. Separation of a ternary mixture of 50/40/10 vol.% $CH_4/C_3H_6/C_3H_8$

The separation of a ternary mixture of 50/40/10 vol.% $CH_4/C_3H_6/C_3H_8$ was investigated at three different feed gas pressures using asymmetric P84/Matrimid membranes. Figure 11 shows the mixed gas permeance values as a function of time for CH_4, C_3H_6 and C_3H_8 at three different feed pressures. Figure 12 shows the corresponding mixed gas selectivity values.

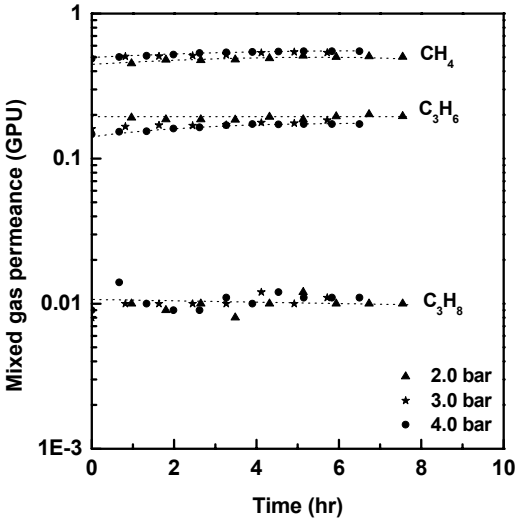

Figure 11: Mixed gas CH_4-, C_3H_6- and C_3H_8-permeance as a function of time for P84/Matrimid asymmetric hollow fiber membranes in the separation of a 50/40/10 vol.% $CH_4/C_3H_6/C_3H_8$-feed gas mixture. The dashed lines illustrate the observed trend and are only used to guide the eye.

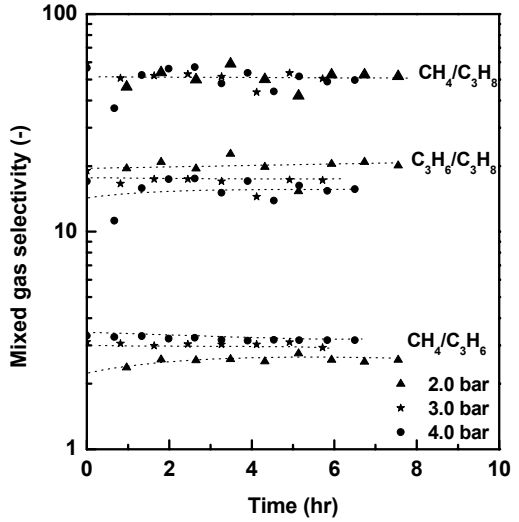

Figure 12: Mixed gas selectivities as a function of time for P84/Matrimid asymmetric hollow fiber membranes in the separation of a 50/40/10 vol.% $CH_4/C_3H_6/C_3H_8$-feed gas mixture. The dashed lines illustrate the observed trend and are only used to guide the eye.

The obtained data show slight scattering due to the very low permeate concentration of propane (~0.3 vol.%), which was close to the detection limit of the gas chromatograph.

Nonetheless, trends in the separation performance can be clearly distinguished. The highest permeance is obtained for CH_4, followed by propylene and propane. Consequently, CH_4 is preferentially permeating through P84/Matrimid membranes compared to propylene and propane, while propylene is preferentially permeating compared to propane. These differences can be attributed to the fact that the mixed gas selectivity of P84/Matrimid asymmetric hollow fiber membranes is based on diffusion selectivity. The mixed gas permeance and selectivity values change just slightly as a function of time, while the obtained results at comparable propylene partial pressures with the binary C_3-mixture showed significant changes, especially in the first hours of permeation. Although the C_3H_6/C_3H_8-selectivity decreases with increasing feed pressure probably due to propylene plasticization, the CH_4/C_3H_8-mixed gas selectivity seems to be unaffected, while the CH_4/C_3H_6-selectivity increases. Additional experiments at higher pressures should be carried out to further clarify these results.

Figure 13 shows the N_2-permeance decay as a function of time after the mixed gas experiments with the ternary gas mixture.

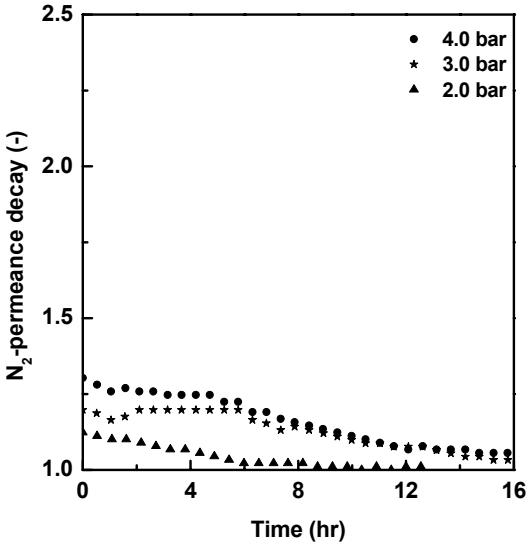

Figure 13: N_2-permeance decay as a function of time after mixed gas experiments for Matrimid and P84/Matrimid asymmetric hollow fiber membranes. The dashed lines illustrate the observed trend and are only used to guide the eye.

As C_3-hydrocarbon partial pressures of only maximum 2 bar were used, the P84/Matrimid asymmetric hollow fiber membranes show afterwards just minor conditioning effects. The amount of residual conditioning is similar to that observed in Figure 10 for the separation of binary mixtures at comparable C_3-hydrocarbon partial pressures.

Figure 14 compares the pressure dependence of the C_3H_6/C_3H_8-mixed gas separation performance of P84/Matrimid membranes in the separation of the binary C_3H_6/C_3H_8-feed gas mixture and the ternary $CH_4/C_3H_6/C_3H_8$-feed gas mixture after 8 hours of permeation.

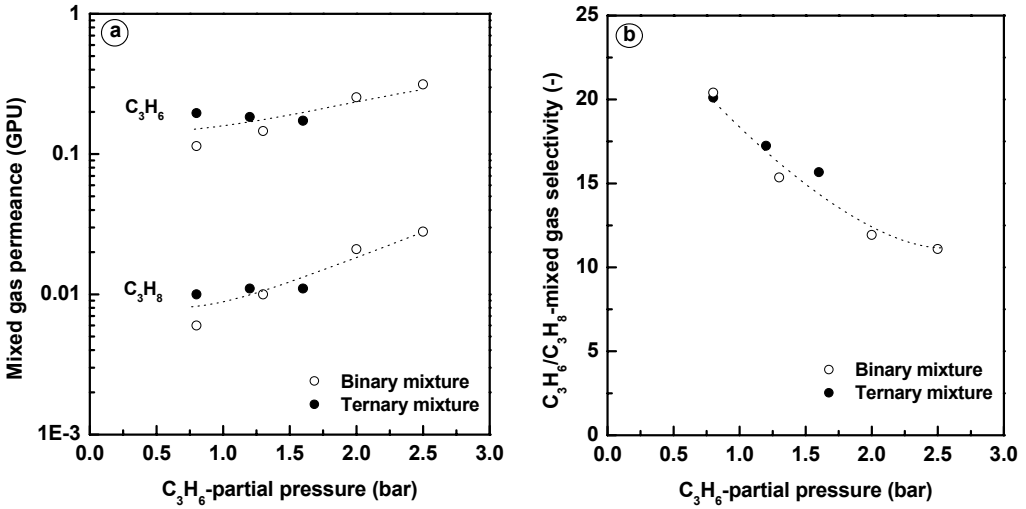

Figure 14: C_3H_6/C_3H_8-mixed gas (a) permeance and (b) selectivity for P84/Matrimid membranes in the separation of a binary and ternary mixture.

Surprisingly, the mixed gas permeance of propylene and propane and the C_3H_6/C_3H_8-mixed gas selectivity data of the binary and ternary mixtures coincide almost with the same trend line, even though different membrane modules were used for the binary and ternary mixed gas experiments. It suggests that the C_3H_6/C_3H_8-mixed gas separation performance is hardly influenced by the presence of CH_4 or by the different C_3H_6/C_3H_8-feed gas ratio (4/1 in stead of 1/1). It was previously reported that in CO_2/CH_4-separations with P84/Matrimid asymmetric hollow fiber membranes the mixed gas separation performance was very sensitive towards the concentration of a second component [23]. With increasing

CH_4-concentration the reduction in CO_2-permeance as a function of pressure was more pronounced, which was related to competitive sorption effects. CO_2-plasticization was less pronounced because the competition effect dominated the mixed gas transport behavior. In the present work competition effects do not seem to have affected the mixed gas separation performance of P84/Matrimid asymmetric hollow fiber membranes in the separation of the C_3-mixtures, which suggests that plasticization is the dominating effect. This agrees also well with the picture of the magnitude of dilation-induced swelling stresses being large for C_3-hydrocarbons, but less dominant for CO_2 [34].

5.4. Conclusions

The mixed gas separation performance of asymmetric hollow fiber membranes of Matrimid polyimide and a 50/50 wt.% blend of Matrimid and the co-polyimide P84 was investigated using binary and ternary C_3-mixtures to study the effect of polymer blending on the mixed gas plasticization behavior of asymmetric membranes.

The C_3H_6/C_3H_8-mixed gas separation performance of asymmetric membranes of the P84/Matrimid-blend is highly affected by plasticization effects, as the selectivity significantly decreases with increasing propylene partial pressure. The loss in mixed gas selectivity was attributed to a loss in diffusion selectivity. The mixed gas permeance of propane was highly affected by the presence of propylene, while the mixed gas permeance of propylene was almost unchanged when compared to single gas permeation experiments. Plasticization effects are mainly caused by propylene, although kinetic sorption experiments revealed that propylene and propane both induce sorption relaxations. Sorption experiments also showed that the mixed gas selectivity is mainly based on diffusion selectivity, because the solubility selectivity was relatively small. The separation performance of Matrimid asymmetric hollow fiber membranes was sensitive to plasticization as well, but the effects were less pronounced. The addition of a third, inert component to the feed mixtures (CH_4) hardly changed the C_3H_6/C_3H_8-separation performance of P84/Matrimid asymmetric hollow fiber membranes. It was suggested that competitive sorption effects are less pronounced to those observed in CO_2/CH_4-separations due to the relatively large magnitude of C_3-hydrocarbon induced plasticization effects. It was concluded that blending Matrimid polyimide with the co-polyimide P84 does not improve the C_3-hydrocarbon stability of P84/Matrimid asymmetric hollow fiber

membranes in the separation of C_3H_6/C_3H_8-gas mixtures although it does in CO_2/CH_4-separations.

5.5. References

1. R.W. Baker, *Future directions of membrane gas separation technology*, Industrial Engineering and Chemical Research **41** (2002), 1393-1411.
2. A. Shimazu, et al., *Relationships between the chemical structures and the solubility, diffusivity, and permselectivity of propylene and propane in 6FDA-based polyimides*, Journal of Polymer Science Part B-Polymer Physics **38** (2000), 2525-2536.
3. S.I. Semenova, *Polymer membranes for hydrocarbon separation and removal*, Journal of Membrane Science **231** (2004), 189-207.
4. C. Staudt-Bickel and W.J. Koros, *Olefin/paraffin gas separations with 6FDA-based polyimide membranes*, Journal of Membrane Science **170** (2000), 205-214.
5. K. Tanaka, et al., *Permeation and separation properties of polyimide membranes to olefins and paraffins*, Journal of Membrane Science **121** (1996), 197-207.
6. K. Okamoto, et al., *Permeation and separation properties of polyimide membranes to 1,3-butadiene and n-butane*, Journal of Membrane Science **134** (1997), 171-179.
7. S.S. Chan, et al., *Gas and hydrocarbon(C_2 and C_3) transport properties of co-polyimides synthesized from 6FDA and 1,5-NDA (naphthalene)/Durene diamines*, Journal of Membrane Science **218** (2003), 235-245.
8. P.H. Pfromm, I. Pinnau, and W.J. Koros, *Gas-Transport through Integral-Asymmetric Membranes - a Comparison to Isotropic Film Transport-Properties*, Journal of Applied Polymer Science **48** (1993), 2161-2171.
9. T. Visser, G.H. Koops, and M. Wessling, *On the subtle balance between competitive sorption and plasticization effects in asymmetric hollow fiber gas separation membranes*, Journal of Membrane Science **252** (2005), 265-277.
10. J.J. Krol, M. Boerrigter, and G.H. Koops, *Polyimide hollow fiber gas separation membranes: preparation and the suppression of plasticization in propane/propylene environments*, Journal of Membrane Science **184** (2001), 275-286.
11. K.-R. Lee and S.-T. Hwang, *Separation of propylene and propane by polyimide hollow-fiber membrane module*, Journal of Membrane Science **73** (1992), 37-45.
12. M. Yoshino, et al., *Olefin/paraffin separation performance of asymmetric hollow fiber membrane of 6FDA/BPDA-DDBT copolyimide*, Journal of Membrane Science **212** (2003), 13-27.
13. I. Pinnau, et al., *Gas separation using C_3+ hydrocarbon resistant membranes*, US 6.361.582 B1 (2002)
14. C. Cao, et al., *Chemical cross-linking modification of 6FDA-2,6-DAT hollow fiber membranes for natural gas separation*, Journal of Membrane Science **216** (2003), 257-268.

15. Y. Liu, et al., *Chemical cross-linking modification of polyimide/poly(ether sulfone) dual-layer hollow-fiber membranes for gas separation*, Industrial & Engineering Chemistry Research **42** (2003), 1190-1195.
16. L. Shao, et al., *The effects of 1,3-cyclohexanebis(methylamine) modification on gas transport and plasticization resistance of polyimide membranes*, Journal of Membrane Science **267** (2005), 78-89.
17. L. Shao, et al., *Polyimide modification by a linear aliphatic diamine to enhance transport performance and plasticization resistance*, Journal of Membrane Science **256** (2005), 46-56.
18. J.D. Wind, et al., *Solid-state covalent cross-linking of polyimide membranes for carbon dioxide plasticization reduction*, Macromolecules **36** (2003), 1882-1888.
19. T.-S. Chung, et al., *Development of asymmetric 6FDA-2,6DAT hollow fiber membranes for CO2/CH4 separation: Part 2. Suppression of plasticization*, Journal of Membrane Science **214** (2003), 57-69.
20. A.F. Ismail and W. Lorna, *Suppression of plasticization in polysulfone membranes for gas separations by heat-treatment technique*, Separation and Purification Technology **30** (2003), 37-46.
21. S. Hess, C. Staudt-Bickel, and R.N. Lichtenthaler, *Propene/propane separation with copolyimide membranes containing silver ions*, Journal of Membrane Science **275** (2006), 52-60.
22. A. Bos, et al., *Suppression of gas separation membrane plasticization by homogeneous polymer blending*, AIChE Journal **47** (2001), 1088-1093.
23. T. Visser and M. Wessling, *Material dependency of mixed gas plasticization behavior of asymmetric membranes*, Submitted to Journal of Membrane Science.
24. T. Visser and M. Wessling, *High-flux integrally skinned P84/Matrimid asymmetric hollow fiber membranes for gas separation*, to be published.
25. G.C. Kapantaidakis and G.H. Koops, *High flux polyethersulfone-polyimide blend hollow fiber membranes for gas separation*, Journal of Membrane Science **204** (2002), 153-171.
26. P.H. Pfromm and W.J. Koros, *Accelerated physical ageing of thin glassy polymer films: evidence from gas transport measurements*, Polymer **36** (1995), 2379-2387.
27. M. Wessling, et al., *Time-dependent permeation of carbon-dioxide through a polyimide membrane above the plasticization pressure*, Journal of Applied Polymer Science **58** (1995), 1959-1966.
28. S.I. Sandler, *Chemical and engineering thermodynamics*, 3rd ed., 1999: Jonh Wiley & Sons, Inc.
29. A. Bos, et al., *CO_2-induced plasticization phenomena in glassy polymers*, Journal of Membrane Science **155** (1999), 67-78.
30. M. Wessling, et al., *Dilation kinetics of glassy, aromatic polyimides induced by carbon-dioxide sorption*, Journal of Polymer Science Part B-Polymer Physics **33** (1995), 1371-1384.

31. J. Crank, *The mathematics of diffusion*, 2nd ed., 1975, Oxford: Clarendon Press.
32. H.L. Frisch, *Sorption and transport in glassy polymers - a review*, Polymer Engineering and Science **20** (1978), 2-13.
33. A.R. Berens and H.B. Hopfenberg, *Diffusion and relaxation in glassy polymer powders: 2. Separation of diffusion and relaxation parameters*, Polymer **19** (1978), 489-496.
34. T. Visser and M. Wessling, *Sorption-induced relaxation phenomena in a glassy polyimide*, submitted to Macromolecules.
35. R.L. Burns and W.J. Koros, *Defining the challenges for C_3H_6/C_3H_8 separation using polymeric membranes*, Journal of Membrane Science **211** (2003), 299-309.

Chapter 6

Sorption-induced relaxations in Matrimid polyimide

Abstract

This study presents the kinetic sorption behavior of six different gases (CO_2, Xe, C_3H_8, C_3H_6, Kr and Ar) in films of the glassy polyimide Matrimid using a magnetic suspension balance. Frequently, it is believed that only highly soluble gases (e.g. CO_2, higher hydrocarbons) have the ability to induce sorption relaxations in glassy polymers. We demonstrate that any gas may induce irreversible sorption relaxations upon reaching a critical amount of volume dilation. Above this critical amount of volume dilation, kinetic sorption behavior becomes non-Fickian. The kinetic sorption behavior was analyzed using a kinetic model quantifying separate contributions of diffusion and relaxations. The model provides a better insight in the different onsets and relative magnitudes of sorption relaxations. The diffusion coefficient was concentration dependent for all gases investigated, which was interpreted in terms of a theoretical framework assuming continuous distribution of sorption site energies. The relative changes in the diffusion coefficient for the gases investigated scaled with the square of the partial molar volume. The concentration dependence of the diffusion coefficient is related to the elastic response of the polymer glass upon sorption only.

Keywords: Gas sorption, plasticization, glassy polymers, non-Fickian sorption, diffusion-relaxation model

6.1. Introduction

In membrane-based gas separation, the membranes separation performance is often deteriorated due to plasticization of the polymer matrix by highly sorbing penetrants [1-3]. These penetrants cause an increase of the motion of polymer segments, which consequently results in enhanced transport rates of all components diffusing. Upon plasticization of glassy polymers, irreversible morphological alterations take place in the polymer matrix, which can be visualized as non-ideal Fickian transport behavior. This non-Fickian transport behavior often can be observed as additional mass uptake in vapor sorption experiments, or as excessive volume changes in dilation experiments with glassy polymers [4-7].

The solubility of a gas mainly depends on its relative ease to condense and its molecular interactions with the polymer matrix (e.g. polar groups). Frequently, it is believed that only gases having very high solubilities have the ability to induce plasticization effects in polymers. Often such gases are falsely coined 'interacting' ignoring the better knowledge that any molecule dissolved in a solid or liquid interacts with its surrounding. Therefore, noble gases are commonly considered as non-plasticizers. Bos et al. [3] suggest the existence of a critical gas concentration required to induce plasticization effects. Others found contradicting results for a series of polyimides as much higher CO_2-concentrations were required to induce plasticization effects [8]. It was suggested that the onset of plasticization is more closely related to a threshold value of the partial molar volume rather than to a critical gas concentration. This critical partial molar volume allows for a specific magnitude of segmental motion, sufficient to cause dramatic effects in the separation performance of glassy polymer membranes. It would suggest that gases having similar values for the partial molar volume have the same ability to plasticize a glassy polymer. The onset of plasticization effects can not be attributed to a critical partial molar volume or a gas concentration alone, although both parameters clearly contribute to the ability to plasticize.

In this paper we use a magnetic suspension balance to very precisely measure weight uptake enabling to distinguish between diffusion and relaxation kinetics. The kinetic

sorption behavior of CO_2, Xe, C_3H_8, C_3H_6, Kr and Ar is investigated in the glassy polyimide Matrimid. We want to demonstrate that non-Fickian sorption behavior is closely related to a critical amount of absolute volume dilation. This observation unites the contributions of partial molar volume [8] and gas solubility [3].

6.2. Characterization of kinetic sorption behavior

6.2.1. Ideal Fickian sorption

Crank [4] shows that the sorption of a penetrant in a polymer matrix is proportional to the square root of time, assuming a constant diffusion coefficient. This behavior is called ideal Fickian sorption and the mass uptake (g) in time ($M(t)$) can be described with the following equation:

$$\frac{M(t)}{M_\infty} = 1 - \frac{8}{\pi^2}\sum_{m=0}^{\infty}\frac{1}{(2m+1)^2}\exp\left\{-\frac{D(2m+1)^2\pi^2 t}{L^2}\right\} \qquad (1)$$

where M_∞ is the amount of mass (g) sorbed by Fickian sorption at infinite time, D is the diffusion coefficient (m^2/s), t is the time (s), and L is the sample thickness (m). Fitting of the sorption data into this equation leads to the diffusion coefficients.

6.2.2. Diffusion-relaxation model

Non-Fickian kinetic sorption behavior can be empirically described using a model proposed by Berens and Hopfenberg [9]. The model considers sorption processes to comprise of two distinct sorptive regimes, a Fickian sorption regime (M_F) and a relaxational regime (M_R):

$$M(t)_{Total} = M(t)_F + M(t)_R \qquad (2)$$

Because the diffusion-controlled regime is often far more rapid than the long term relaxational regime, the two sorption processes can be separated. Consequently, the overall sorption process can be considered as a sum of phenomenological independent contributions from Fickian diffusion and polymer relaxation:

$$\frac{M(t)}{M_\infty} = M_{F,\infty}\left[1 - \frac{8}{\pi^2}\sum_{m=0}^{\infty}\frac{1}{(2m+1)^2}\exp\left\{-\frac{D(2m+1)^2\pi^2 t}{L^2}\right\}\right] - \sum_{i=1}^{\infty} M_{R_i}\left[1 - \exp\left\{-\frac{t}{\tau_{R_i}}\right\}\right] \quad (3)$$

where $M_{F,\infty}$ and M_{Ri} are the infinite sorbed mass of the Fickian part and the relaxational parts of sorption (g), respectively, of which the sum in principle should equal one upon complete relaxation. τ_{Ri} is the characteristic time for relaxation (s). Often it is sufficient to describe non-Fickian sorption behavior by the sum of Fickian and two relaxational sorption regimes [6, 7]. The first, fast relaxation follows diffusion kinetics [7]. The second relaxation is much slower and is considered as irreversible relaxation of the excess free volume resulting from polymer network dilation. The fractions of Fickian and fast and slow relaxational sorption are represented as m_F, m_{R1} and m_{R2}, respectively.

The diffusion-relaxation model can only be used when the two contributions to sorption, Fickian diffusion and polymer relaxation, are well separated in the sorption kinetics, which implies that the diffusion rate should be much higher than the relaxation rate. The relative magnitude of the rates of diffusion and relaxation is quantified as the Deborah number and is defined as the ratio of the diffusion rate of a penetrant to the relaxation rate of the polymer matrix with a dimension L. The sorption processes of diffusion and relaxation are well separated when the Deborah number is much larger than unity. The appendix further illustrates the importance of film thickness on the description of sorption kinetics using the diffusion-relaxation model.

6.3. Experimental

6.3.1. Materials and film preparation

Thick dense polymer films were prepared by solvent evaporation of a 15 wt.% Matrimid 5218 (Vantico AG) polyimide in NMP, cast on a glass plate using 0.3 or 1 mm casting knifes. After preparation, the wet films were stored in a closed container flushed with N_2 gas for three days to evaporate the solvent. To remove any residual solvent, the films were stored in a vacuum oven at 150°C for 2 more days. The dry thickness of the film was 30 or 100 μm. All gases used were purchased from Praxair (The Netherlands) and were used without further purification.

6.3.2. Gravimetric sorption balance

Gas sorption in glassy polymers is typically measured using pressure decay or gravimetric methods. The principle of the pressure decay method is based on the measurement of a pressure difference in time due to sorption between two cells with one containing the sample and the other being an empty reference cell. The total pressure decay typically is small compared to the absolute pressure used (<5%). Analysis of the kinetic behavior is often difficult due to limitations in experimental accuracy as well as time-dependent boundary conditions for the pressure in the cell. Gravimetric sorption techniques maintain their accuracy at long time scales and are therefore more suitable to accurately record small weight changes occurring as a result of sorption-induced relaxations.

Therefore, the kinetic sorption behavior of the different gases in the polymer films was determined gravimetrically, using a magnetic suspension balance (MSB, Rubotherm), equipped with a vacuum pump ($p_{vac}<10^{-3}$ mbar), thermostat bath and gas supply. The temperature was kept constant at 35°C (308 K) throughout all experiments. Before each experiment, the samples were degassed for at least 24 hours. Mass uptake was measured with incremental pressure steps in a sorption/desorption cycle. The electronic signal shows always large instabilities in the first few minutes of sorption as a result of temperature increases (Joule-Thomson effect) upon pressurization of the sorption balance. For this reason, the first minutes were disregarded in the analysis of the kinetic sorption behavior. The measured weight w_t (g) was corrected for buoyancy according to Archimedes' principle. Based on the exact sample volume V_t (m^3) and the initial weight w_0 (g) of the sample and the density ϱ_{gas} (g/m^3) of the surrounding gas, the mass gain m_t (g) can be calculated by taking into account the buoyancy effect:

$$m_t = \left(w_t + V_t \rho_{gas}\right) - w_0 \tag{4}$$

The gas density was estimated using the Peng-Robinson equation of state [10]. The density of the polymer sample was determined at room temperature using a Micromeritics AccuPyc 1330 pycnometer. The gas concentration in the polymer (cm^3 (STP) gas per cm^3 of polymer) was calculated using the molar volume at standard temperature and pressure (STP, 1 bar and 273.15 K), the polymer volume, and the molecular weight of the specific

gas. Data fitting with the diffusion-relaxation model was carried out using graphing and data analysis software from Originlabs (Origin Pro 7).

6.4. Results

6.4.1. Kinetic sorption behavior of carbon dioxide

Figure 1 shows the incremental pressure steps in a pressurization/depressurization cycle measured for CO_2-sorption in a dense Matrimid polyimide film. Pressure steps of 3, 5 and 10 bar were taken upon pressurization and steps of 10 and 20 bar upon depressurization.

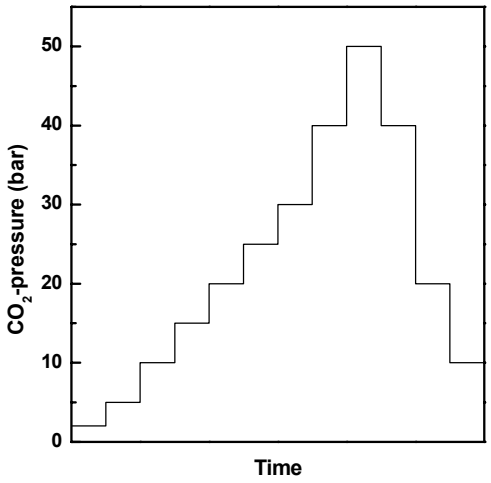

Figure 1: Incremental pressure steps used in a carbon dioxide pressurization/depressurization cycle.

Figure 2 shows the weight gain of the polymer film (m_t-m_0) as a function of time for pressures between 2 and 30 bar. It can be observed that the weight gain per pressure step decreases with increasing pressure.

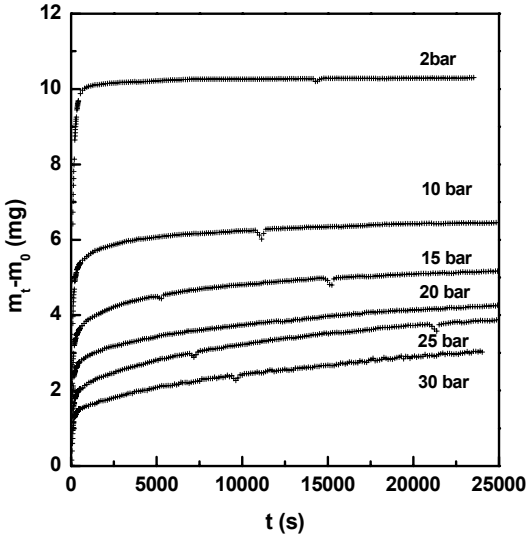

Figure 2: Weight gain per pressure step as a function of time for sorption of CO_2 in Matrimid polyimide.

Figure 3 shows the CO_2-concentration as a function of time for six different pressures. The data are plotted as a function of the logarithm of time intentionally to improve visualization of the different sorption regimes.

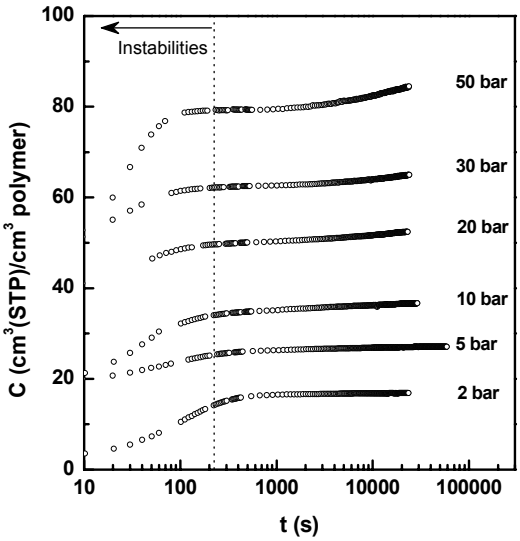

Figure 3: The CO_2-concentration in Matrimid polyimide as a function of the logarithm of time for different pressures. Only a selection of experimental pressures is shown.

At 2 bar CO_2, only one distinctive sorption regime is observed representing ideal Fickian sorption: an initial fast increase (build-up diffusion profile) and subsequent leveling off to equilibrium. Above 2 bar, a second regime emerges, which becomes more pronounced at higher pressures. This additional increase in concentration at higher pressures is due to the onset of irreversible volume relaxations.

Figure 4 replots Figure 3 and shows the weight divided by the weight at 'infinite' time (m_t/m_{inf}) as a function of the logarithm of time. Therefore, a pseudo-'infinite' weight was chosen after 240 minutes of sorption. Plotting the data as shown in Figure 4 provides a better picture of the extent of the different contributions of diffusion and relaxation.

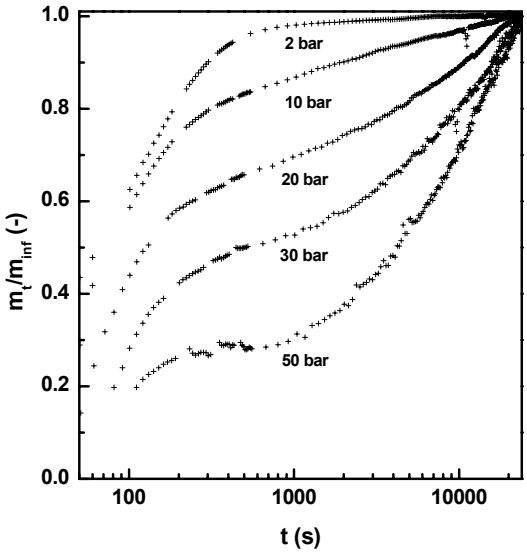

Figure 4: Weight divided by 'infinite' weight gain (m_t/m_{inf}) for CO_2 in Matrimid polyimide as a function of the logarithm of time for 5 different pressures.

As previously mentioned, the first minutes of sorption were disregarded due to drift in the balance signal. However, the first few minutes completely cover the build-up of the diffusion profile, especially at higher pressures. To be able to obtain diffusion coefficients, the CO_2-sorption kinetics of a 100 μm film were measured as well, as this increases the time for diffusion. Since the separation of the different sorption regimes is better defined with relatively thin films, the kinetic data obtained for the 30 μm film is used to obtain the five other fitting parameters used in the diffusion-relaxation model (see Appendix). Table

1 shows the fitting parameters obtained with the diffusion-relaxation model (fit confidence > 98%). The total fraction of the Fickian and relaxational sorption processes is set to one ($m_F + m_{R1} + m_{R2} = 1$) after 240 minutes, although the relaxation process is not completed yet.

Table 1: Fitting results for sorption of CO_2 in Matrimid polyimide obtained from the diffusion-relaxation model.

Pressure (bar)	$\mathbf{m_F}$	$\mathbf{m_{R1}}$	$\mathbf{m_{R2}}$	$\mathbf{D_{Fick}}$ **(·1·10^{-8}) (cm^2/s)**
2	0.94	0.06	-	0.67
5	0.87	0.10	0.03	0.93
10	0.77	0.14	0.09	1.25
15	0.63	0.18	0.19	1.75
20	0.59	0.19	0.31	2.35
25	0.43	0.13	0.44	2.60
30	0.44	0.10	0.46	3.48
40	0.31	0.11	0.52	4.60
50	0.22	0.06	0.72	5.80

The following trends for sorption of carbon dioxide in Matrimid polyimide can be observed from Figure 4 and Table 1:

- Ideal Fickian sorption is only observed at 2 bar CO_2. At higher pressures the kinetic sorption behavior is non-Fickian due to the onset of irreversible secondary volume relaxations.
- The fraction of slow relaxational sorption (m_{R2}) increases with increasing pressure, while the fraction of Fickian sorption (m_F) decreases with increasing pressure. The magnitude of the fraction of fast relaxational sorption (m_{R1}) appears to be independent of pressure.
- The diffusion coefficient is concentration dependent and increases with increasing pressure.
- The relaxation times are typically about $\tau_{R1} = 1{\cdot}10^3$ s and $\tau_{R2} = 1{\cdot}10^5$ s and are pressure or concentration independent within the accuracy of the experiment.

Figure 5 shows the CO_2-sorption isotherm upon a pressurization/depressurization cycle. Since equilibrium is not reached within the time-scale of the experiment above a pressure of 2 bar, pseudo-equilibrium values after 180 minutes of sorption and desorption were taken to calculate the sorbed concentration. The desorption isotherm is higher than the sorption isotherm. Secondary volume dilation introduced during sorption cannot consolidate rapidly enough during desorption elevating the sorption isotherm to higher values.

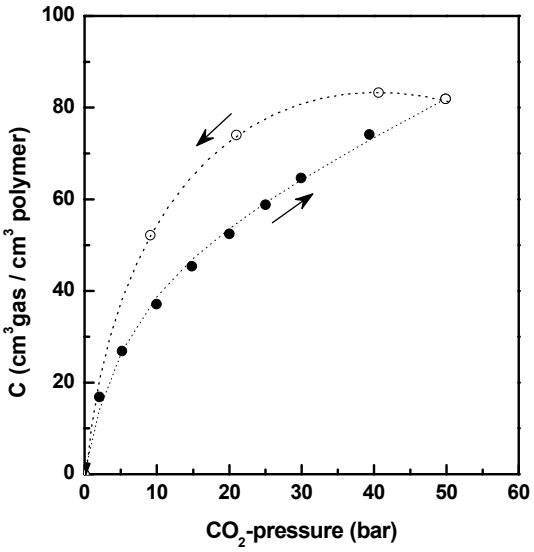

Figure 5: CO_2-sorption isotherm in Matrimid polyimide in a pressurization/depressurization cycle. Values were obtained after 180 minutes of sorption.

6.4.2. Kinetic sorption behavior of xenon

Figure 6 shows the incremental pressure steps used in a pressurization/depressurization cycle for Xe-sorption in Matrimid polyimide.

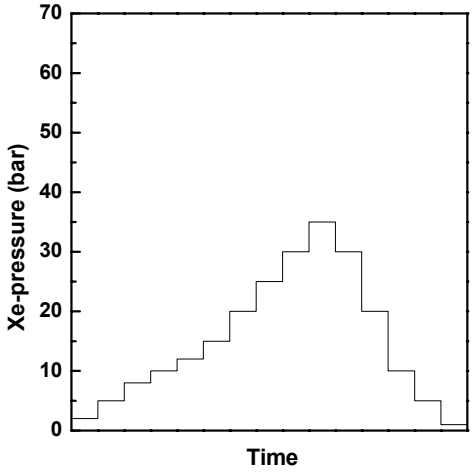

Figure 6: Incremental pressure steps used in a xenon pressurization/depressurization cycle.

Figure 7 shows the xenon concentration as function of the logarithm of time for several pressures in Matrimid polyimide (small fluctuations are visible in the curves at 15, 20 and 25 bar, which are caused by temperature fluctuations during sorption). Xenon shows a similar kinetic sorption behavior as carbon dioxide: at 2 bar, almost ideal Fickian sorption is observed, while at higher pressures the kinetic sorption behavior becomes non-Fickian due to the onset of secondary relaxations. This is surprising as it is commonly assumed that inert gases such as noble gases show ideal Fickian behavior.

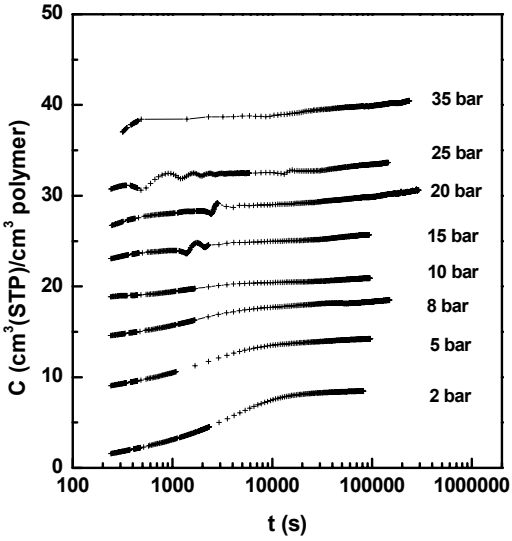

Figure 7: Kinetic sorption behavior of xenon in Matrimid polyimide for incremental pressure steps.

Table 2 shows the fitting results of the kinetic sorption behavior of xenon in Matrimid polyimide obtained with the diffusion-relaxation model. The weight after 2400 minutes of sorption was taken as the pseudo-'infinite' weight. The observed trends are comparable to the phenomena observed for CO_2, although the data fitting was less reproducible due to temperature fluctuations (visible in Figure 7).

Table 2: Fitting results for xenon sorption obtained with the diffusion-relaxation model.

Pressure (bar)	$\mathbf{m_F}$	$\mathbf{m_{R1}}$	$\mathbf{m_{R2}}$	$\mathbf{D_{Fick}}$ **(·1·10^{-8}) (cm^2/s)**
2	0.94	0.06	-	0.023
5	0.84	0.05	0.11	0.031
8	0.79	0.02	0.19	0.036
10	0.71	0.04	0.25	0.045
15	0.65	0.04	0.31	0.060
20	0.60	0.05	0.35	0.080
25	0.56	0.05	0.39	0.095
35	0.43	0.08	0.49	0.170

The following trends for sorption of xenon in Matrimid polyimide can be distinguished from Figure 7 and Table 2:

- Ideal Fickian sorption is observed at 2 bar Xe, while non-Fickian sorption is observed at higher pressures.
- The fraction of slow relaxational sorption (m_{R2}) increases, while the fraction of Fickian sorption (m_F) decreases with increasing pressure. The magnitude of the fraction of slow relaxational sorption (m_{R2}) is smaller than the value found for CO_2. The fraction of fast relaxational sorption (m_{R1}) appears to be independent of pressure and is smaller than the value found for CO_2 as well.
- The diffusion coefficient is concentration dependent and increases with increasing pressure. It is two orders of magnitude smaller than the diffusion coefficient found for CO_2.
- The relaxation times are typically about $\tau_{R1} = 5{\cdot}10^2$ s and $\tau_{R2} = 8{\cdot}10^5$ s and are pressure or concentration independent within the accuracy of the experiment.

Figure 8 shows the xenon sorption isotherm in a pressurization/depressurization cycle. The data points shown in Figure 8 are pseudo-equilibrium values (above 2 bar) obtained after 180 minutes of sorption or desorption. The desorption isotherm is higher than the sorption isotherm, as a result of secondary volume dilation during sorption.

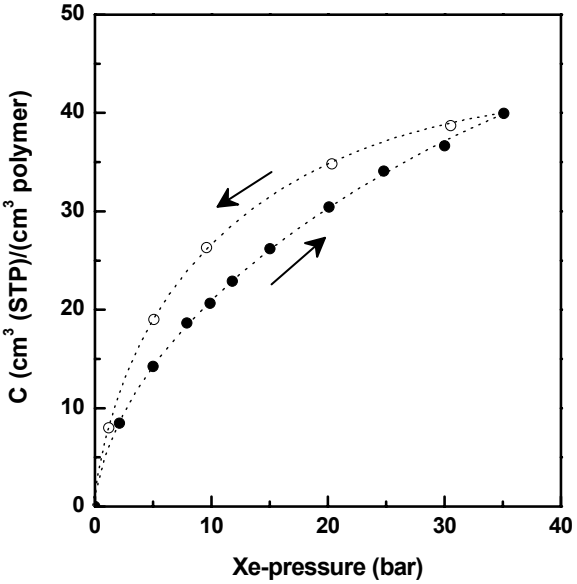

Figure 8: Xe-sorption isotherm in Matrimid polyimide in a pressurization/depressurization cycle. Values were obtained after 180 minutes of sorption.

6.4.3. Kinetic sorption behavior of propane and propylene

Propane

Figure 9 shows the sorbed propane concentration in Matrimid polyimide as a function of the square root of time for four incremental pressure steps. In this case the data are plotted as a function of the *square root* of time in stead of a *logarithmic* time-axis, as it better visualizes the non-ideal sorption behavior of propane. In case of Fickian sorption one should find a linear increase in time, leveling off to an equilibrium value [4].

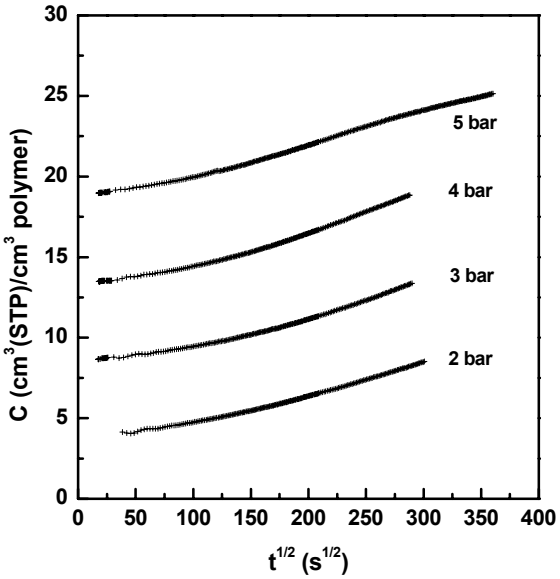

Figure 9: Kinetic sorption behavior of sorption of propane in Matrimid polyimide as a function of the square root of time.

Regular Fickian weight uptake can not be distinguished. The kinetic sorption behavior shows an upward inflection for all pressures, suggesting a non-Fickian sorption behavior. Apparently, the rates of diffusion and polymer chain relaxation are almost identical, which is often interpreted as case III or anomalous non-Fickian diffusion [11]. Unfortunately, the diffusion-relaxation model fails when diffusion and relaxation processes are coupled [12]. Reduction of the time scale for the diffusion process would in principle allow the separation of the two sorption processes. Practically this may be achieved by using thinner polymer films (see Appendix). However, these experiments were not performed as the drift in the balance signal during the first few minutes makes the analysis too inaccurate. It remains an experimental challenge to separate the two contributions to sorption, Fickian diffusion and polymer relaxation, when the time scale of diffusion overlaps with relaxational sorption.

Propylene

Figure 10 shows the sorbed propylene concentration in Matrimid polyimide as a function of the square root of time for five different pressures. Also these data are plotted as a function of the *square root* of time to enhance visualization of non-idealities in the sorption

behavior. As in the case with propane sorption, also propylene shows a clearly non-Fickian kinetic sorption behavior, especially at higher pressures.

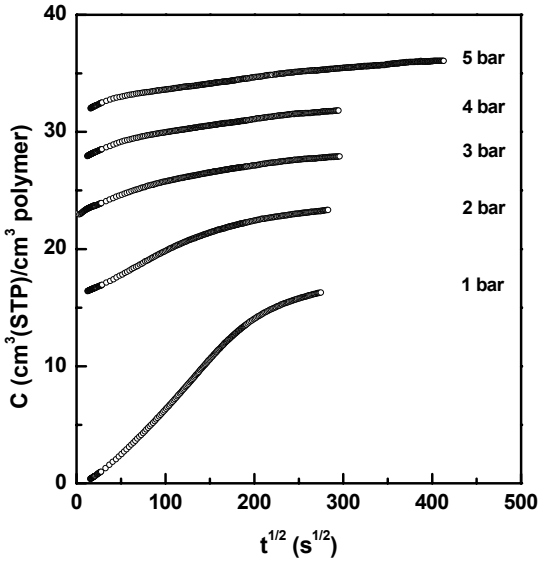

Figure 10: Kinetic sorption behavior for sorption of propylene in Matrimid polyimide as a function of the square root of time.

The sorption processes of diffusion and relaxation using propylene are better separated as was the case using propane, which can probably be attributed to a higher diffusion coefficient for propylene. Consequently, the diffusion-relaxation model could be applied for propylene, whereas this was not possible for propane. The weight after 1400 minutes of sorption was taken as the pseudo-'infinite' weight. Table 3 shows the fitting results of propylene sorption in Matrimid polyimide.

Table 3: Fitting results for propylene sorption in Matrimid polyimide obtained with the diffusion-relaxation model.

Pressure (bar)	m_F	m_{R1}	m_{R2}	D_{Fick} ($\cdot 1 \cdot 10^{-8}$) (cm^2/s)
1	0.53	0.25	0.22	0.003
2	0.35	0.26	0.39	0.010
3	0.21	0.21	0.58	0.037
4	0.17	0.23	0.60	0.078
5	0.13	0.27	0.60	0.249

The following trends for sorption of propylene in Matrimid polyimide can be distinguished from Figure 10 and Table 3:

- At all pressures investigated a highly non-Fickian sorption behavior is observed.
- The fraction of Fickian sorption (m_F) decreases rapidly with increasing pressure, while the fraction of slow relaxational sorption (m_{R2}) increases rapidly with increasing pressure. Apparently, propylene causes very strong sorption-induced relaxations in Matrimid polyimide. Furthermore, the magnitude of the fraction of fast relaxational sorption (m_{R1}) appears to be independent of pressure and is higher compared to CO_2 and Xe.
- The magnitude of the secondary volume relaxations (m_{R2}) is larger than the corresponding values for CO_2 and Xe.
- The diffusion coefficient is highly concentration dependent and increases with increasing pressure. It is three orders of magnitude smaller than the values found for CO_2 at a pressure of 1 bar and only one order of magnitude at a pressure of 5 bar.
- The relaxation times are typically about $\tau_{R1} = 2.5 \cdot 10^3$ s and $\tau_{R2} = 4 \cdot 10^5$ s and are pressure independent within the accuracy of the experiment.

Sorption isotherms

Figure 11 shows the sorption isotherms for propane and propylene in Matrimid polyimide up to a pressure of 5 bar. The pseudo-equilibrium concentrations were calculated with data points taken after 1400 minutes (24 hours) of sorption. The sorption isotherm for propylene has a concave shape with respect to the pressure axis, which is consistent with dual-mode sorption theory for glassy polymers. However, propane surprisingly shows a slight convex shaped isotherm. This unusual behavior is probably the result of a very large fraction of relaxational sorption compared to Fickian sorption resulting in an anomalous increase in solubility.

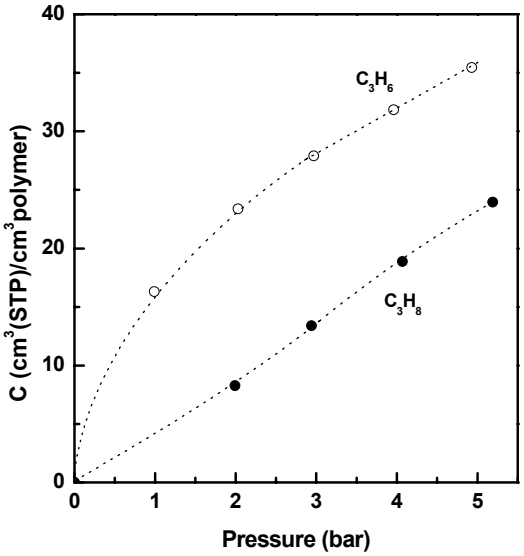

Figure 11: Sorption isotherms for C_3H_6 and C_3H_8 in Matrimid polyimide. Values were obtained after 2400 minutes of sorption.

6.4.4. Kinetic sorption behavior of krypton

Figure 12 shows the incremental pressure steps used in a pressurization/depressurization cycle for sorption of krypton in Matrimid polyimide.

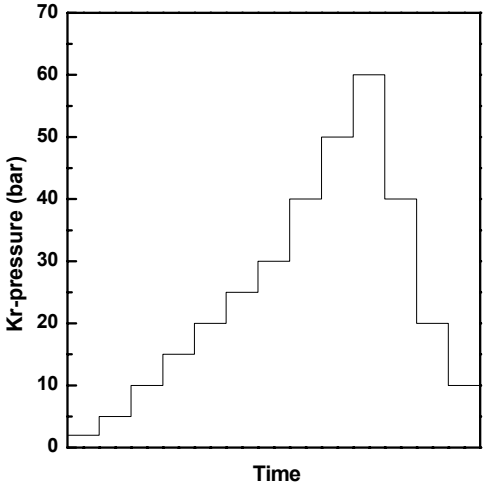

Figure 12: Incremental pressure steps used in a krypton pressurization/depressurization cycle.

Figure 13 shows the concentration krypton in Matrimid polyimide as a function of the logarithm of time up to pressures of 60 bar. Not all experimentally investigated pressures are shown to maintain better visualization of the data.

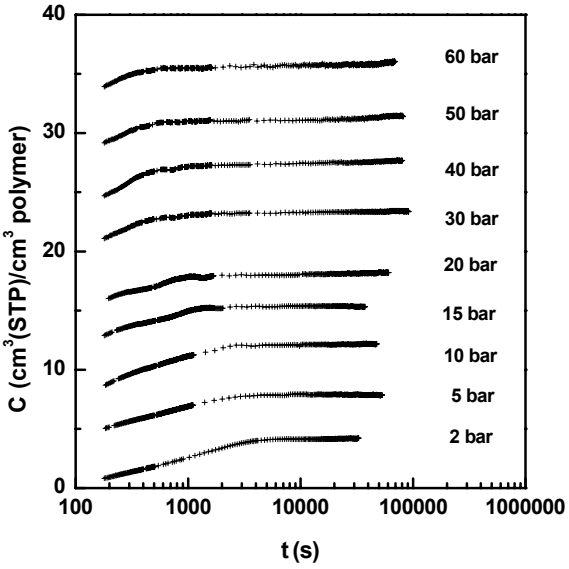

Figure 13: Kinetic sorption behavior of krypton in Matrimid polyimide for incremental pressure steps.

At first sight, the kinetic sorption behavior seems to be ideal Fickian at all pressures; an initial steep increase continued by a leveling off to equilibrium. However, at higher pressures ($\geq$ 20 bar), the concentration further increases slightly after ~3 hours of sorption, suggesting the onset of slow sorption relaxations. Table 4 shows the fitting results at different pressures obtained with the diffusion-relaxation model for the kinetic sorption behavior of krypton in Matrimid polyimide. The weight after 1400 minutes of sorption was taken as the pseudo-'infinite' weight. The fitting results confirm the presence of sorption-induced relaxations above a krypton pressure of 20 bar.

Table 4: Fitting results for krypton sorption obtained with the diffusion-relaxation model.

Pressure (bar)	m_F	m_{R1}	m_{R2}	D_{Fick} ($\cdot 1 \cdot 10^{-8}$) (cm^2/s)
2	1	-	-	0.07
5	1	-	-	0.10
10	1	-	-	0.12
15	1	-	-	0.19
20	0.93	0.01	0.06	0.24
25	0.87	0.03	0.10	0.28
30	0.87	0.04	0.09	0.28
40	0.85	0.03	0.12	0.38
50	0.86	0.02	0.12	0.46
60	0.85	0.04	0.11	0.54

The following trends for the sorption of krypton in Matrimid polyimide can be observed from Figure 13 and Table 4:

- Ideal Fickian sorption is observed up to a pressure of 15 bar. Above this pressure the kinetic sorption behavior shifts towards non-Fickian due to the onset of secondary volume relaxations.
- The fraction of Fickian sorption (m_F) decreases slightly with increasing pressure, while the fraction of slow relaxational sorption (m_{R2}) increases slightly with increasing pressure. The fraction of fast relaxational sorption (m_{R1}) seems to be independent of pressure. The magnitude of the relaxations is much smaller compared to CO_2, Xe and C_3H_6 sorption.
- The diffusion coefficient is concentration dependent and increases with increasing pressure. Furthermore, it is only one magnitude smaller compared to CO_2.
- The relaxation times are typically about $\tau_{R1} = 5 \cdot 10^2$ s and $\tau_{R2} = 4 \cdot 10^5$ s and are pressure or concentration independent within the accuracy of the experiment.

Figure 14 shows the krypton concentration in Matrimid polyimide as a function of pressure in a pressurization/depressurization cycle. The data points shown in Figure 14 were obtained after 300 minutes of sorption. The desorption isotherm is slightly higher than the sorption isotherm, confirming the non-Fickian sorption kinetics as a result of

secondary volume dilation during sorption. The hysteresis is smaller when compared to Xe and CO_2, which is attributed to the lower magnitude of relaxational sorption.

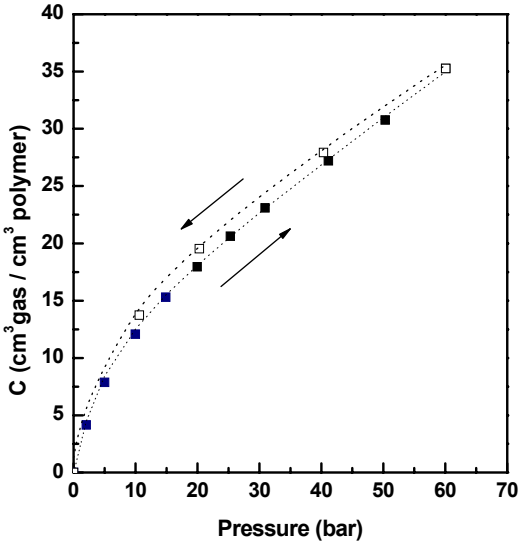

Figure 14: Kr-sorption isotherm in Matrimid polyimide in a pressurization/depressurization cycle. Values were obtained after 300 minutes of sorption.

6.4.5. Kinetic sorption behavior of argon

Figure 15 shows the incremental pressure steps used in a pressurization/depressurization cycle for Ar-sorption in Matrimid polyimide. Initially, incremental sorption measurements were performed only up to a maximum pressure of 50 bar argon. In a second set, sorption experiments with a new film were carried out starting at 50 bar argon (integral) and subsequently increasing the pressure to 60 bar.

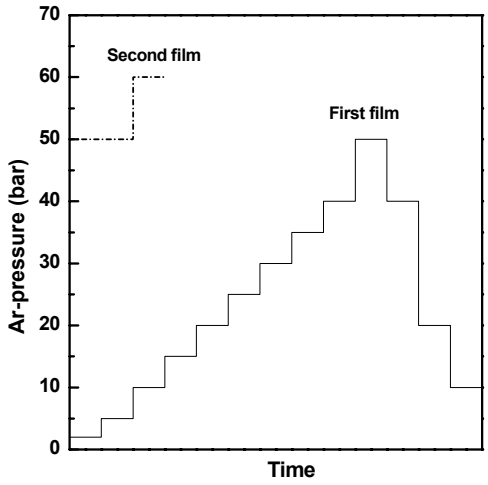

Figure 15: Incremental pressure steps used in an argon pressurization/depressurization cycle.

Figure 16 shows the argon concentration in Matrimid polyimide as a function of the logarithm of time for pressures up to 50 bar for the first film and up to 60 bar for the second film (closed dots, indicated as 2nd). The total argon concentration sorbed at a pressure of 50 bar remains the same irrespective of incremental or integral pressure steps.

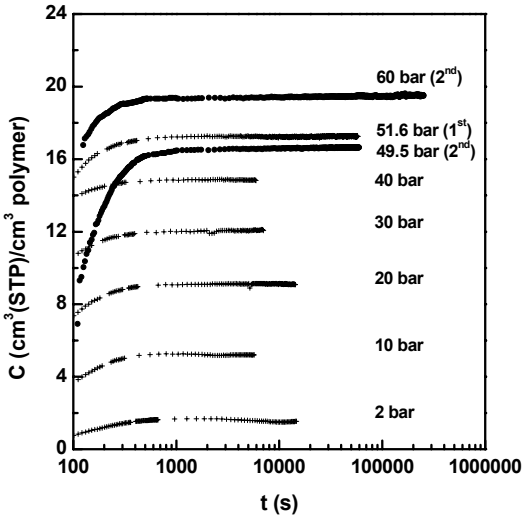

Figure 16: Kinetic sorption behavior of argon in Matrimid polyimide.

For pressures up to 50 bar the kinetic sorption behavior is clearly ideal Fickian. However, at a pressure of 60 bar, the argon concentration in the polymer film appears to increase slightly at times of ~3 hours of sorption. This was confirmed using the diffusion-

relaxation model which gave a 6% additional increase in concentration (m_{R2} = 0.06) after build-up of the diffusion profile (pseudo-'infinite' time of 4000 minutes). The relaxation time was determined to be ~$1 \cdot 10^6$ s. The kinetic sorption behavior of lower pressure (< 60 bar) were fitted using regular Fickian sorption (Equation 1). The determined diffusion coefficients are shown in Table 5. It can be observed that the argon diffusion coefficient is concentration dependent and increases with increasing pressure.

Table 5: Argon diffusion coefficients in Matrimid polyimide determined using regular Fickian sorption (Equation 1).

Pressure (bar)	**D_{Fick} ($\cdot 1 \cdot 10^{-8}$) (cm^2/s)**
2	0.48
5	0.50
10	0.57
15	0.61
20	0.55
25	0.62
30	0.60
40	0.65
50	0.75
60	0.79

Figure 17 shows the argon sorption isotherm in a pressurization/depressurization cycle carried out up to a pressure of 50 bar (visualized as dots). The values obtained for the second film are included as well (visualized as stars). As expected, for the first film no hysteresis is observed up to a pressure of 50 bar. As relaxations are observed at a pressure of 60 bar, it is expected that depressurization would have caused some hysteresis. However, probably the effect is too small to be visible in Figure 17.

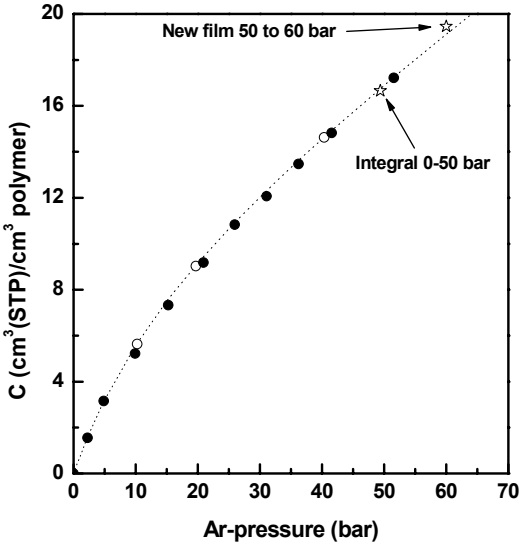

Figure 17: Argon sorption isotherm in Matrimid polyimide in a pressurization (closed dots)/depressurization (open dots) cycle.

6.5. Discussion

6.5.1. Energy distribution of sorption sites

Kirchheim developed a theoretical framework describing the sorption of gases in polymers assuming a continuous distribution of dissociation energies (rather than 2 populations only, as suggested by the Dual-Mode sorption model) [13, 14]. During sorption of penetrant molecules, the polymer network dilates, yielding different elastic distortion energies (G_{el}) which depend on the volume distribution of intermolecular space into which sorption occurs:

$$G_{el} = \frac{2}{3}\mu_s \frac{\left(V_g^2 - V_h^2\right)}{V_h} \quad \text{and} \quad V_p = V_g - V_h \tag{5}$$

where μ_s is the shear modulus of the polymer at a certain temperature (GPa), V_g is the volume of a gas molecule (cm^3) and V_h is the volume of a hole or site (cm^3). Sites are part of normal interstices between macromolecules and part of the free volume of the polymer. The partial molar volume or the volume change of a polymer induced by introducing a gas

molecule V_p (cm^3/mol) is defined as the difference between the volume of a gas molecule and that of a site. The free energy G of dissolution of molecules into the sites of a glassy polymer can be described by a Gaussian distribution $n(G)$:

$$n(G) = \frac{1}{\sigma\sqrt{\pi}} \exp\left[-(G - G_0)^2 / \sigma^2\right] \quad (6)$$

where σ is the width of the site distribution and reflects the magnitude of sorption isotherms and G_0 is the average free energy corresponding to the free energy change to transfer a gas molecule into an average site of the polymer matrix. Sorption isotherms are described well by using a Gaussian distribution of sorption energies and Fermi-Dirac statistics [13]. Within the framework, σ correlates with the difference of the square of the volume of a gas molecule and that of a site in the polymer and hence is directly related to the partial molar volume:

$$\sigma = \frac{2\left(V_g^2 - V_{h0}^2\right)\mu_s}{3V_{h0}} \sqrt{\frac{2RT}{BV_{h0}}} \quad (7)$$

Where μ_s is the shear modules of the polymer at a certain temperature T, B is the bulk modulus in the liquid state at the glass transition temperature T_g, V_g is the volume of a gas molecule and V_{h0} is the average site volume.

6.5.2. *Concentration dependence diffusion coefficients*

Figure 18 presents the diffusion coefficients as a function of gas concentration in Matrimid polyimide for C_3H_6, CO_2, Xe, Kr and Ar and clearly illustrates the concentration dependence of the diffusion coefficient for these gases. It also shows that the determination of the selectivity of glassy polymer membranes based on diffusion selectivity is highly dependent on the feed pressure and hence gas concentration in the glassy polymer matrix.

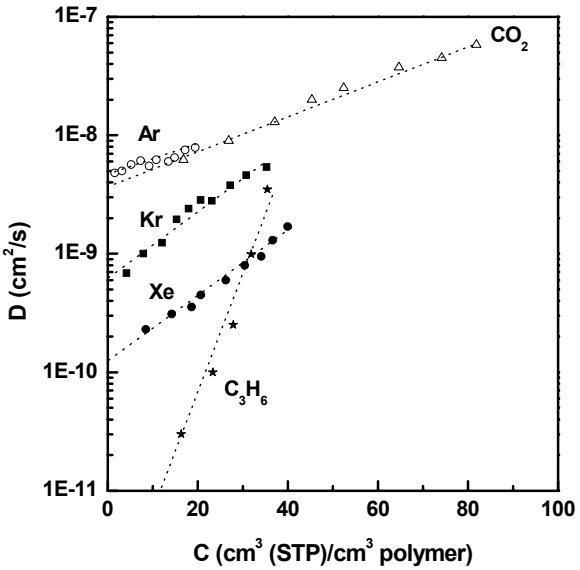

Figure 18: Diffusion coefficient (D) as a function of gas concentration (C) of C_3H_6, CO_2, Xe, Kr and Ar in Matrimid polyimide.

The concentration dependent diffusion coefficient for all gases investigated is in line with the theoretical framework of Kirchheim. The description of gas sorption using a distribution of site energies causes the diffusion coefficient to be strongly concentration dependent because the average activation energy of diffusion decreases when higher energy sites are filled [13, 15]. The experimental concentration dependence can be linearized assuming an exponential relation in which the intersection with the y-axis represents the diffusion coefficient at infinite dilution (D_0) and the slope ($d(\ln(D/D_0))/dc$) the magnitude of the relative change in the diffusion coefficient. Figure 19 plots the relative change of the diffusion coefficient with respect to the diffusion coefficient at infinite dilution D_0 as a function of penetrant concentration. The logarithmic y-axis indicates the exponential increase of the diffusion coefficient as a function of concentration.

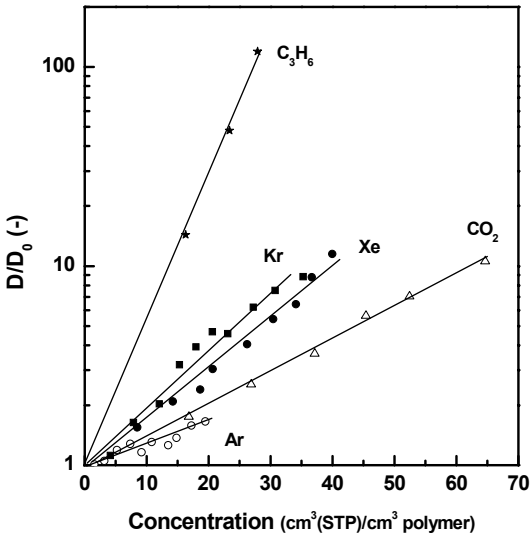

Figure 19: Diffusion coefficients (D) as a function of gas concentration normalized for diffusion coefficients at infinite dilution (D_0) for C_3H_6, Xe, Kr, CO_2 and Ar in Matrimid polyimide.

The slope of the curve varies significantly for different penetrant molecules showing a larger slope for larger penetrant molecules. Since the width of the sorption site distribution (Γ) scales with the square of the partial molar volume of a gas, Figure 20 plots the slope of the concentration dependent diffusion coefficient as a function of the square of the partial molar volume in the rubbery polymer poly(dimethylsiloxane) (PDMS).

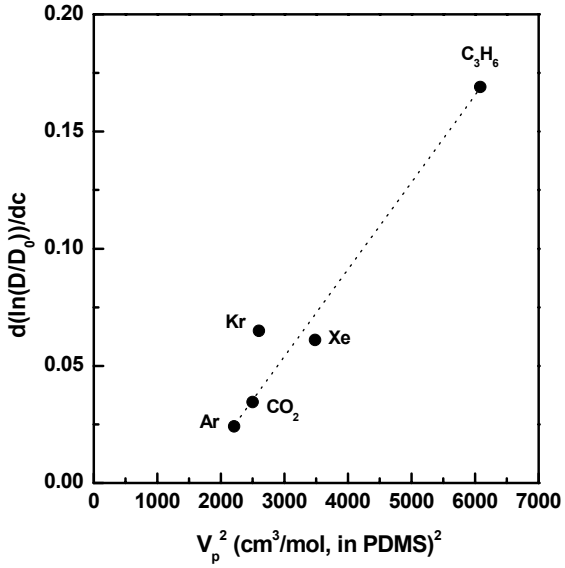

Figure 20: The slopes of curves presented in Figure 18 ($d(\ln(D/D_0))/dc$) as a function of the square of the partial molar volume $(V_p)^2$ in PDMS [16].

Since values for the partial molar volume of gases in Matrimid polyimide are not known, corresponding values for PDMS were used [16], as it reflects similar interactions between gas molecules and the polymer matrix. The values are typically smaller in glassy polymers due to the presence of excess free volume, which is not mobile enough to cause dilation after occupation of a sorption site [17]. Table 6 shows the values for the partial molar volume of the gases investigated in PDMS [18], the diffusion coefficients at infinite dilution D_0 and the slope of the relative change in the diffusion coefficient obtained from Figure 19.

Table 6: Partial molar volumes in PDMS at 25°C for gases investigated [18], values for the slopes of Figure 19 ($d\ln(D/D_0)/dc$) and the diffusion coefficient at infinite dilution (D_0).

Gas	**V_p (cm^3/mol)**	**$d(\ln(D/D_0))/dc$ (-)**	**D_0 ($\cdot 1 \cdot 10^{-9}$) (cm^2/s)**
Ar	47	0.024	4.75
Kr	51	0.065	0.61
Xe	59	0.061	0.13
CO_2	50	0.035	3.55
C_3H_6	78	0.17	0.002
C_3H_8	85	n.a.	n.a.

Figure 20 and Table 6 show there exists a linear relationship between the slopes of Ar, CO_2, Xe and C_3H_6 and the square of the values of the partial molar volume, although it is unclear why Kr shows a divergent behavior. Nonetheless, it qualitatively supports the partial molar volume dependence of the concentration dependent diffusion coefficient for the gases investigated. Further detailed measurements are required to support the Kirchheim framework. For now, we conclude that the elastic response of the polymer glass upon sorption is able to describe the sorption isotherm as well the concentration dependent diffusion coefficients.

6.5.3. Overall sorption and predicted dilation isotherm

Gas solubility in a polymer is influenced by: (1) specific molecular interactions and (2) gas condensability. Polymer modifications (the introduction of for example polar groups) can drastically alter gas solubility [19]. For different gases, gas solubility increases with an increase in relative condensability. The condensability of a gas increases with increasing values for its the Lennard-Jones force constant (ε/k) or critical temperature (T_c), of which values are presented in Table 7 for the gases investigated [20].

Table 7: Values for the Lennard-Jones force constant (ε/k) or its critical temperature (T_c) of the gases investigated.

Gas	T_c (K)	ε/k (K)
Ar	151	93
Kr	209	179
Xe	290	231
CO_2	304	195
C_3H_6	365	249
C_3H_8	370	237

Figure 21 shows the overall sorption isotherm for all experimentally used gases at 35°C. C_3H_6 has the highest solubility in Matrimid polyimide, followed by CO_2, C_3H_8, Xe, Kr and Ar. This order in magnitude of gas solubility reflects the differences in relative condensability well, based on the values in Table 7. As the relative condensability of Xe is higher than those of Ar and Kr, Xe has the higher solubility in Matrimid polyimide. On the other hand, the gases CO_2 and Xe have similar condensability, although the solubility of CO_2 is significantly higher. This can be attributed to specific molecular interactions between CO_2 and Matrimid polyimide.

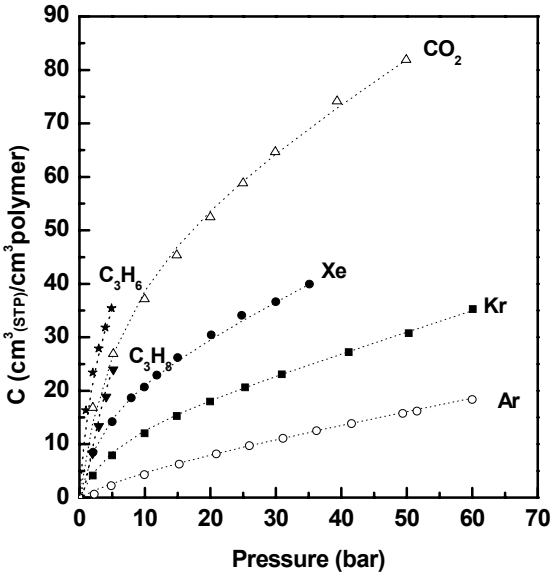

Figure 21: Gas concentration in Matrimid polyimide as a function of pressure for all gases investigated.

Higher gas solubilities do not automatically result in lower pressures required to induce secondary volume relaxations. The sorption of propylene and propane causes slow relaxations at much lower pressures and concentrations than CO_2 and Xe. Besides, the solubility of propylene in Matrimid polyimide is higher than of propane, while they appeared to induce relaxations at more or less the same pressure. Also the onset of relaxations in the case of CO_2 and Xe occurred at more or less the same pressure, but the concentration of sorbed gas at this pressure was significantly different. At a pressure of 50 bar Ar, Matrimid polyimide contains the same concentration of gas as at 1 bar propylene or 4 bar propane. The sorption kinetics of argon only starts to show secondary relaxations at very high pressures.

The results show that sorption relaxations are induced at different gas concentrations, while it was postulated that the onset of plasticization effects is related to a certain critical gas concentration [3]. Others related the onset of plasticization effects to a threshold value of the partial molar volume [8]. Table 6 showed that the partial molar volumes of Ar, Kr and Xe in PDMS do not differ significantly from that of CO_2, while completely different pressures were required to observe the onset of sorption relaxations. The ability of CO_2 to plasticize Matrimid polyimide can be mainly attributed to the fact that it has much higher gas solubility than the noble gases, as shown in Figure 21. The solubility of C_3H_8 was slightly lower than that of CO_2, while the onset of sorption relaxations was observed at a lower pressure. This can be attributed to the higher value of the partial molar volume of C_3H_8 compared to CO_2. These results show that the onset of relaxations is not determined by a critical value of the partial molar volume or concentration alone, but by both parameters simultaneously. The volume dilation ($\Delta V/V_0$) of a polymer exposed to a gas is defined as the product of penetrant concentration c (cm^3 (STP)/cm^3 polymer) and partial molar volume V_p of penetrants (cm^3/mol) [16]:

$$\frac{\Delta V}{V_0} = c \cdot V_p \cdot 22{,}400 \qquad (8)$$

Dilation isotherms for Matrimid polyimide can be estimated using Equation 8, the experimental sorption data and an assumed partial molar volume in Matrimid. Values for the partial molar volume in glassy polymers can be estimated from corresponding values in

organic liquids or rubbery polymers as it is known that the partial molar volume scales exponentially with the glass transition temperature of a polymer [21]. In this way, the values in Matrimid polyimide, which has a T_g of 313°C, are estimated to be ~30% of those in PDMS. Figure 22 shows the predicted volume dilation as a function of gas pressure in Matrimid polyimide for the gases investigated.

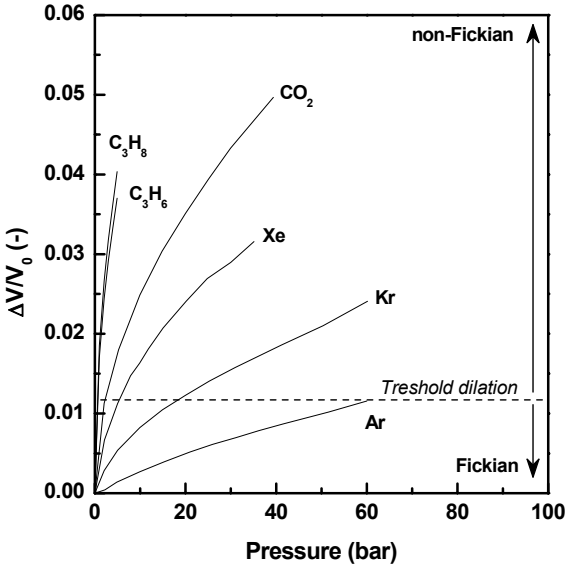

Figure 22: Predicted dilation isotherms in Matrimid polyimide for the gases investigated. The dashed line represents a threshold amount of dilation required to induce non-Fickian sorption kinetics.

The different gases investigated show relaxation phenomena at different pressures. In Figure 22, these pressures correlate with one single value for the amount of volume dilation. This illustrates that for any gas investigated the same critical threshold amount of volume dilation is required to induce sorption relaxations. Below the threshold, only elastic reversible distortion of the glassy polymer occurs resulting in ideal Fickian sorption, while plastic irreversible distortion occurs above the threshold resulting in non-Fickian sorption phenomena. CO_2 causes much more volume dilation than Kr, Ar and Xe, as a result of a much higher solubility in Matrimid polyimide, while C_3H_8 causes more volume dilation than CO_2 due to its higher partial molar volume. It demonstrates that the critical threshold depends on both the gas solubility and the partial molar volume of a gas. Based on this we conclude that the ability of a gas to induce irreversible changes in polymer

glasses can be estimated from the sorption isotherm of the gas in the polymer and the glass transition temperature of the polymer.

6.6. Conclusions

The kinetic sorption behavior of six different gases (CO_2, Xe, C_3H_6, C_3H_8, Kr and Ar) in Matrimid polyimide was investigated using a gravimetric sorption balance. The empirical diffusion-relaxation model allows to quantify that the fractions of relaxational sorption increase, whereas the fractions of Fickian sorption decreases with increasing pressure. The diffusion coefficient is concentration dependent for all gases investigated, which can be understood by a theoretical framework assuming continuous distribution of sorption site energies. The concentration dependence of the diffusion coefficient is related to the elastic response of the polymer glass upon sorption only. The relative changes in the diffusion coefficient for the gases investigated scaled with the square of the partial molar volume.

The work demonstrates that the combination of the partial molar volume and the solubility of a gas in a glassy polymer allow the prediction of a certain critical threshold amount of volume dilation upon which sorption relaxations are induced. Above this threshold, kinetic sorption behavior becomes non-Fickian.

Acknowledgement

The authors want to acknowledge Ole Hölck (BAM, Berlin) for fruitful discussions and his help in the data fitting with the diffusion-relaxation model.

Appendix: Influence of film thickness on CO_2-kinetic sorption behavior

The relaxation process occurring in glassy polymers upon sorption is independent of the polymer dimensions. Diffusion-controlled sorption on the other hand, varies with the square of the polymer dimensions [1]. Therefore, the sample thickness affects the overlap in time of diffusion and relaxation in sorption kinetics. To discriminate between the kinetics of Fickian and relaxational weight uptake, one desires to use relative thin polymer samples. Thinner films reduce the time scale for diffusion so that the analysis of the diffusion coefficient becomes impossible because the rapid weight uptake can not be measured accurately. On the other hand, thicker films may result in a superposition of the two sorption processes. To apply the diffusion-relaxation model there should be a distinct separation of the two sorption processes [12, 22, 23]. The relative magnitude of the rates

of diffusion and relaxation is often characterized by the diffusion Deborah number (DEB_D), which is defined as [23]:

$$(DEB)_D = \frac{\tau_R \cdot D}{L_0^2} \qquad \text{(A1)}$$

Where τ_R is the characteristic relaxation time and L_0^2 / D is the characteristic diffusion time, with L_0 the sample thickness and D the diffusion coefficient. For $(DEB)_D >> 1$ the rate of diffusion is much faster than the response of polymer relaxation, while for $(DEB)_D \approx 1$, the rates of diffusion and relaxation are equal resulting in a superposition of the two processes. When the Deborah number is smaller than unity, the rate of relaxation is faster than that of diffusion.

Figure A1 shows the effect of film thickness on the kinetic sorption behavior at 20 bar CO_2 for 30 and 100 μm Matrimid polyimide films. The symbols represent the experimental values while the solid lines represent the calculated fits from the diffusion-relaxation model. At a film thickness of 100 μm diffusion and relaxation kinetics start to overlap, while the diffusion profile is relatively short at a film thickness of 30 μm. A Deborah number of ~25 for the 30 μm film and less than 3 for the 100 μm film was calculated.

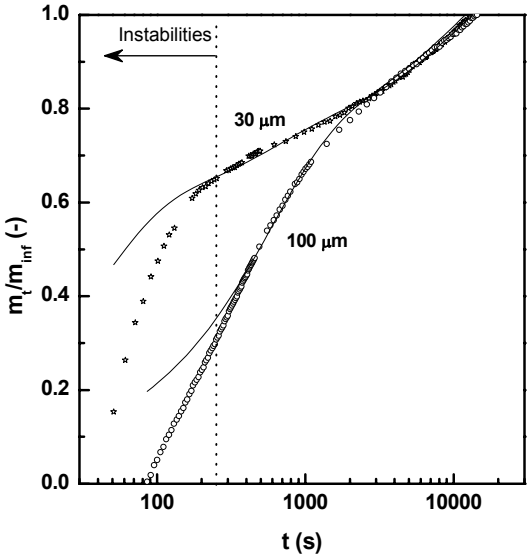

Figure A1: Film thickness dependence on the kinetic sorption behavior at 20 bar CO_2.

Figure A1 shows that the contributions of diffusion and relaxation are well separated in the case of the 30 μm film. However, the first 240 seconds of the experimental measurements were not taken into account due to significant disturbance of the electronic signal (temperature fluctuation), which causes deviations between model and experimental data. As a result, 30 μm films can not be used to determine diffusion coefficients. In the case of the 100 μm the build up of the diffusion profile is long enough to provide a good determination of the diffusion coefficient. As relaxation parameters are independent on the sample dimensions, this diffusion coefficient calculated from the 100 μm film can be used for the 30 μm as well. This allows the calculation of the other fitting parameters based on the 30 μm film. Figure A1 shows that the calculated fits (solid lines) have good agreement with the experimental data, but it also shows that the choice for the right film thickness for kinetic gas sorption experiments is essential, to be able to distinguish between Fickian and non-Fickian kinetic sorption behavior.

6.7. References

1. E.S. Sanders, S.M. Jordan, and R. Subramanian, *Penetrant-plasticized permeation in polymethylmethacrylate*, Journal of Membrane Science **74** (1992), 29-36.
2. M. Wessling, et al., *Plasticization of gas separation membranes*, Gas Separation & Purification **5** (1991), 222-228.
3. A. Bos, et al., *CO_2-induced plasticization phenomena in glassy polymers*, Journal of Membrane Science **155** (1999), 67-78.
4. J. Crank, *The mathematics of diffusion*, 2nd ed., 1975, Oxford: Clarendon Press.
5. A.C. Newns, *Sorption and diffusion in polymers*, Nature **218** (1968), 355-356.
6. M. Wessling, et al., *Dilation kinetics of glassy, aromatic polyimides induced by carbon-dioxide sorption*, Journal of Polymer Science Part B-Polymer Physics **33** (1995), 1371-1384.
7. M. Boehning and J. Springer, *Sorptive dilation and relaxational processes in glassy polymer/gas systems - I. Poly(sulfone) and poly(ether sulfone)*, Polymer **39** (1998), 5183-5195.
8. J.D. Wind, et al., *Carbon dioxide-induced plasticization of polyimide membranes: Pseudo-equilibrium relationships of diffusion, sorption, and swelling*, Macromolecules **36** (2003), 6433-6441.
9. A.R. Berens and H.B. Hopfenberg, *Diffusion and relaxation in glassy polymer powders: 2. Separation of diffusion and relaxation parameters*, Polymer **19** (1978), 489-496.
10. S.I. Sandler, *Chemical and engineering thermodynamics*, 3rd ed., 1999: Jonh Wiley & Sons, Inc.

11. H.L. Frisch, *Sorption and transport in glassy polymers - a review*, Polymer Engineering and Science **20** (1978), 2-13.
12. Y.-M. Sun, *Sorption/desorption properties of water vapour in poly(2-hydroxyethyl methacrylate): 2. Two-stage sorption models*, Polymer **37** (1996), 3921-3928.
13. R. Kirchheim, *Sorption and partial molar volume of small molecules in glassy polymers*, Macromolecules **25** (1992), 6952-6960.
14. R. Kirchheim, *Partial molar volume of small molecules in glassy polymers*, Journal of Polymer Science, Part B: Polymer Physics **31** (1993), 1373-1382.
15. P. Pekarski, et al., *Effect of aging and conditioning on diffusion and sorption of small molecules in polymer glasses*, Macromolecules **33** (2000), 2192-2199.
16. Y. Kamiya, et al., *Sorptive dilation of polysulofne and poly(ethylene terephtalate) films by high-pressure carbon dioxide*, Journal of Polymer Science, Part B: Polymer Physics **26** (1988), 159-177.
17. J.-S. Wang, Y. Kamiya, and Y. Naito, *Effects of CO_2-conditioning on sorption, dilation, and transport properties of polysulfone*, Journal of Polymer Science, Part B: Polymer Physics **36** (1998), 1695-1702.
18. Y. Kamiya, et al., *Volumetric properties and interaction parameters of dissolved gases in poly(dimethylsiloxane) and polyethylene*, Macromolecules **33** (2000), 3111.
19. G.J. van Amerongen, *Influence of structure of elastomers on their permeability to gases*, Journal of Polymer Science **5** (1950), 307-332.
20. B.E. Poling, J.M. Prausnitz, and J.P. O'Connell, *The properties of gases and liquids*, 5 ed., 2001, New York: Mc Graw Hill.
21. J.G. Wijmans, *The role of permeant molar volume in the solution-diffusion model transport equations*, Journal of Membrane Science **237** (2004), 39.
22. H. Hopfenberg, *The effects of film thickness and sample history on the parameters describing transport in glassy polymers*, Journal of Membrane Science **3** (1978), 215-230.
23. J.S. Vrentas, C.M. Jarzebski, and J.L. Duda, *Deborah number for diffusion in polymer-solvent systems*, AIChE Journal **21** (1975), 894.

Chapter 7

Outlook

Abstract

Suggestions for further research are discussed based on the research presented in this thesis, covering multi-component plasticization phenomena in asymmetric membranes, single and dual layer hollow fiber spinning and the use of alternative techniques to analyze plasticization effects.

7.1. Introduction

A major part of this thesis focuses on the plasticization behavior of asymmetric hollow fiber membranes in the separation of binary gas mixtures. One of the most important findings is the existence of a subtle balance between competitive sorption and plasticization effects in CO_2-separations. For asymmetric membranes this balance is highly dependent on the membrane material used. Asymmetric hollow fiber membranes consisting of homogeneous Matrimid-based blends have very good gas separation properties in CO_2-separations. The presence of plasticization in balance with competitive sorption may even improve the separation performance at elevated CO_2-feed gas pressures. Asymmetric membranes of a P84/Matrimid-blend are susceptible to C_3-hydrocarbon plasticization in the separation of C_3H_6/C_3H_8-feed gas mixtures. Kinetic sorption experiments in Matrimid showed that C_3H_6 and C_3H_8 are much stronger plasticizers than CO_2. The presence of competitively absorbing CH_4 does not counteract C_3-plasticization, as determined in ternary mixed gas separation experiments. The ability to induce

plasticization effects is dependent on the partial molar volume and gas solubility. Since the partial molar volumes are much larger for C_3H_6 and C_3H_8 compared to CO_2, they are considered as much stronger plasticizers. The results described in this thesis shows that Matrimid-based asymmetric hollow fiber membranes can potentially be very interesting for industrial gas separation processes. To verify the potential of asymmetric hollow fiber membranes of Matrimid-based blends to be employed in industrial applications with highly plasticizing gas mixtures, future research should be focused on:

- Physics of mixed gas plasticization,
- Plasticization behavior in separation of multi-component mixtures,
- Optimization of spinning process of asymmetric P84/Matrimid hollow fiber membranes ,
- Co-extrusion of thin separating layers of expensive high-performance polymers.

7.2. Physics of mixed gas plasticization

To our knowledge, studies on mixed gas plasticization behavior are always carried out by gas permeation experiments. However, gas permeation experiments provide only an indirect measurement of morphological alterations occurring in the polymer matrix upon plasticization. Besides, membrane separation performance in permeation experiments may be affected by other transport effects (e.g. stage-cut, pressure ratio, pressure drop, temperature changes due to the Joule-Thomson effect) which may mask plasticization induced effects. Therefore, it is important to employ other techniques that are able to study directly the complex behavior of mixed gas plasticization effects in polymer membranes. In general such techniques should meet the following criteria:

- Simultaneously measurement of sorption kinetics or permeation of gases and the morphological alterations occurring in the glassy polymer;
- Direct and in-situ measurement;
- Applicable to thin polymer films (preferably < 1 μm);
- Use of (high) pressure and gas mixtures.

Table 1 displays potential techniques able to analyze effects of plasticization in glassy polymers and also indicates to which extent the technique meets the requirements. It is assumed that with proper equipment (pressure vessels) all techniques can work under high pressure mixed gas conditions. Of course, techniques that do not fulfill the mentioned

criteria may be useful in cases where other plasticization phenomena are studied (e.g. thickness dependent plasticization behavior).

Table 1: Overview of alternative methods to analyze gas induced plasticization effects.

Technique	Sorption kinetics	In-situ	Thin samples	Ref.
Sorption/dilation or force sensor	Y	Y	N	[1-3]
Infrared spectroscopy (ATR/FT-IR)	Y	Y	N	[4-7]
Ellipsometry	Y	Y	Y	[8-10]
Waveguide spectroscopy	Y	Y	Y	[11]
Positron Annihilation Lifetime Spectroscopy (PALS)	N	N	Y	[12-15]
Nuclear Magnetic Response (NMR)	N	Y	N	[16, 17]
Dynamic Mechanical Analysis (DMA)	N	N	N	[18]
Differential Scanning Calorimetry (DSC)	N	Y	Y	[19, 20]
Wide Angle X-ray Diffraction (WAXD)	N	Y	Y	[21]
Dielectric relaxation spectroscopy	N	Y	Y	[22-24]

Only four techniques (IR-spectroscopy, sorption combined with dilation or force sensor, ellipsometry and waveguide spectroscopy) are able to measure in-situ the sorption of gases while analyzing alterations in the polymer matrix. The combination of sorption and dilation using an automated spring balance equipped with a very sensitive digital camera seems to be promising [1]. However, the measurement of dilation-induced geometrical changes of a very thin polymer film will be very difficult. The combination of sorption by pressure decay measurements and a vibrating wire force sensor to measure changes in the sample volume seem a more suitable technique, although a large amount of sample is required to obtain sufficient resolution.

With infrared (IR) spectroscopy the competitive sorption behavior inside a polymer may be directly studied, as the sorption of CO_2 and CH_4 can both be measured quantitatively by determining their absorbance in the IR-spectrum [25]. Preliminary experiments were

carried out at the facilities of Dr. Kazarian at Imperial College in London to investigate the applicability of high-pressure ATR-IR spectroscopy to simultaneously measure CO_2-sorption and swelling in Matrimid polyimide. Figure 1 shows IR-spectra of the change in absorbance of CO_2 at a wave number of 2335 cm^{-1} and a Matrimid polyimide film at a wave number of 1725 cm^{-1} with increasing CO_2-pressure using ATR-IR spectroscopy. The solid grey lines are the base lines and represent the spectrum of the polymer before CO_2-exposure.

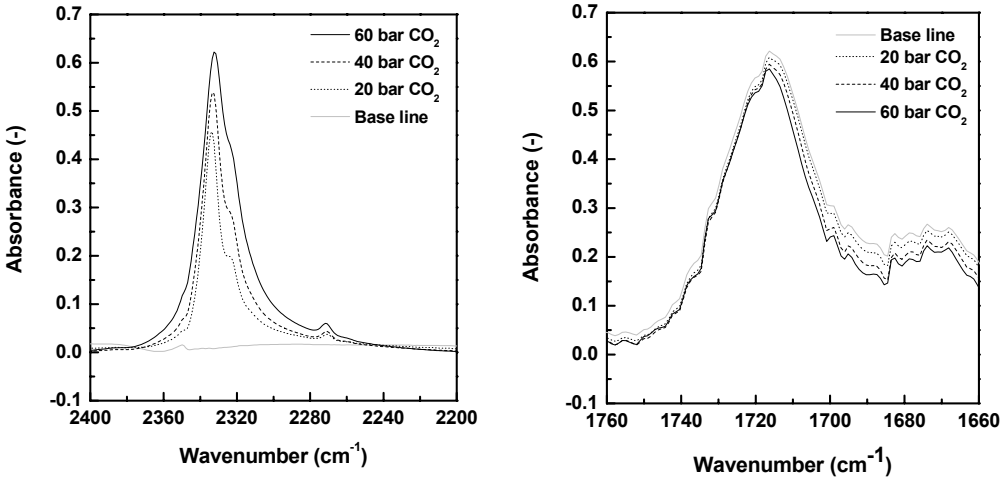

Figure 1: Absorbance of (a) CO_2 and (b) Matrimid polyimide as a function of the wavenumber for CO_2-sorption at three different pressures in Matrimid polyimide using ATR-IR spectroscopy.

With increasing CO_2-pressure the CO_2-absorbance increases indicating an increase of CO_2-concentration in Matrimid polyimide. The absorbance of the polymer decreases with increasing CO_2-pressure illustrating CO_2-induced dilation of the glassy polymer network. It demonstrates that IR-spectroscopy is able to simultaneously study sorption and swelling in polymer films. Unfortunately, it is not applicable to thin polymer films, as the sample thickness should be at least ~10 μm to provide sufficient absorbance signal in the spectra.

Ellipsometry and waveguide spectroscopy are the only techniques capable to simultaneously analyze in-situ sorption and swelling of thin polymer samples. The samples are typically spin-coated as a very thin layer on silicon wafers. The techniques are currently

only used for pure gas experiments until now. Expanding the techniques to the use of gas mixtures will be a significant step forward.

7.3. Plasticization behavior in the separation of multi-component mixtures

The research presented in this thesis mainly focuses on the separation of binary mixtures. Obviously, industrial feed streams consist of more than two components. The presence of additional components, either plasticizing or not, will certainly alter the separation behavior of asymmetric membranes. Natural gas typically contains significant amounts of different C_{3+}-hydrocarbons and water vapor, while a typical feed in the petrochemical industry may additionally consist of aromatics besides C_{3+}-hydrocarbons, water vapor and light gases (e.g. H_2, CH_4). Very few scientific publications discuss the separation performance of asymmetric membranes in the presence of these often strong plasticizing penetrants [26-28]. Asymmetric hollow fiber membranes of Matrimid-based blends have good separation performance using binary CO_2/CH_4-feed gas mixtures (Chapter 4), while they have a promising separation performance for gas mixtures containing CH_4 and higher saturated hydrocarbons (Chapter 5). Future research should focus on the transport behavior of these membranes in the separation of multi-component feed gas mixtures in order to further investigate their industrial potential.

One preliminary mixed gas separation experiment is performed with P84/Matrimid asymmetric hollow fiber membranes in the separation of a ternary mixture of 20/79/1 vol.% $CO_2/CH_4/n\text{-}C_4H_{10}$. Figure 2 shows the CO_2-permeance and mixed gas CO_2/CH_4-selectivity as a function CO_2-fugacity using asymmetric P84/Matrimid membranes in the separation of this ternary mixture. For comparison the results obtained for a 20/80 vol.% CO_2/CH_4-feed gas mixture are also shown. Mixed gas selectivities for $n\text{-}C_4H_{10}$ are not shown as $n\text{-}C_4H_{10}$ could not be detected in the permeate gas stream due to limitations in the analytical technique.

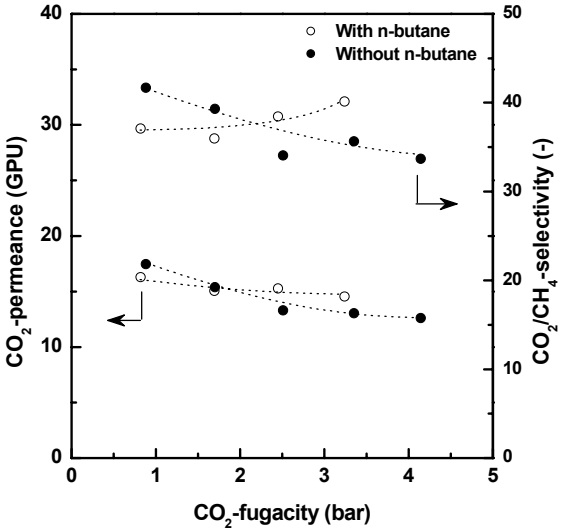

Figure 2: CO_2/CH_4-separation performance as a function of CO_2-fugacity using asymmetric P84/Matrimid membranes in the separation of a ternary feed gas mixture of 20/79/1 vol.% $CO_2/CH_4/n\text{-}C_4H_{10}$ and a binary feed gas mixture of 20/80 vol.% CO_2/CH_4.

The addition of 1 vol.% nC_4H_{10} does not result in an additional loss of mixed gas selectivity when compared to the 20/80 vol.% CO_2/CH_4-feed gas mixture, not even after 100 hours of permeation, but results in a slight increase of the CO_2/CH_4-mixed gas selectivity with increasing CO_2-fugacity. It remains unclear what causes the increase in separation factor with increasing CO_2-fugacity and requires much more experiments. Future mixed gas experiments should focus on CO_2/CH_4-separations with different n-C_4H_{10}-feed gas concentrations or other C_{3+}-hydrocarbons added to further study the effect of a third component on the CO_2/CH_4-separation performance, since the magnitude of plasticization effects would be larger. It would also be interesting to investigate changes in the CO_2/CH_4-separation behavior of P84/Matrimid asymmetric membranes using ternary feed gas mixtures at higher CO_2-fugacities.

7.4. Optimization of P84/Matrimid hollow fiber spinning process

The prepared asymmetric P84/Matrimid hollow fibers membranes described in this thesis have very good separation performances, even at plasticizing conditions (Chapter 3 and 4). However, to be employed in potential applications and to compete with existing commercial asymmetric polyimide hollow fiber membranes (e.g. Ube Industries Ltd. and

L'Air Liquide/MEDAL™), they require much better geometrical properties and especially require much higher mechanical strength (resistance to high burst/collapse pressures), next to having good separation properties. Due to the limitations in mechanical strength, the maximum pressure tested in this thesis is only 20 bar, while pressures of industrial gas streams generally are much higher.

Significant improvements in mechanical properties can be achieved by improving the dope formulation, studying its rheological behavior and the spinneret design. The addition of a non-solvent to spinning dopes often suppresses the formation of macrovoids and typically results in an open interconnected porous substructure. The addition of poly(vinyl pyrrolidone) (PVP) to a spinning dope of PES and NMP resulted in a macrovoid free ultrafiltration (UF)-type of asymmetric membrane [29]. However, the addition of polymeric additives like PVP also inhibits the formation of a dense gas separation skin [30]. Other non-solvents have to be considered in order to obtain a dense gas separation skin and a macrovoid-free open porous substructure. Ekiner and Vassilatos [30] discussed the influence of several different swelling agents, polymeric and inorganic additives on the structure of a polyaramide fiber. Table 2 shows some examples of additives that can be used in fiber spinning to improve the overall performance of hollow fiber membranes [30].

Table 2: Different swelling agents, polymeric and inorganic additives to improve hollow fiber structure properties [30].

Swelling agent	**Polymeric additives**	**Inorganic additives**
Tetrahydrofuran	Polyvinylpyrrolidone	NaI
Triethylamine	Polyvinylpyridine	LiCl, LiBr
Tetramethylensulfone	Polyethyleneglycol	$CaCl_2$, $CaBr_2$
Acetonitrile	Polypropyleneglycol	$MgCl_2$
Formamide		$ZnCl_2$
Diethyleneglycoldimethylether		

L'Air Liquide uses the swelling agent tetramethylenesulfone in spin dopes to improve fiber properties of asymmetric hollow fiber membranes of P84-blends [31]. Others add diethylene glycol dimethyl ether (DGDE) to obtain hyper-thin skin layers and macrovoid-

free substructures in the formation of asymmetric hollow fiber membranes of a 6FDA-based polyimide [32].

The rheological behavior (shear and elongational viscosity) of a spinning dope is a critical factor in the final mechanical properties and separation performance of fibers and is a key variable in the hollow fiber spinning process. The shear viscosity determines the maximum pressure drop during pumping through tubing and spinneret, while elongational viscosity determines the stability of the spinning line and the maximum draw ratio (ratio of take-up speed and dope velocity at spinneret exit). Change of shear and elongational viscosity can result in enhanced selectivities of asymmetric polyimide membranes due to shear and elongation stress induced orientation of the skin [33-35], but it can reduce the mechanical properties [36]. Several methods have been developed to measure shear and elongation viscosity directly or to approximate it by semi-empirical models [37]. For example, a dual-bore capillary rheometer using a capillary and an orifice die in the bores can measure both the shear and elongational viscosity [38].

The rheological behavior of a spinning dope also depends on the spinneret design, which may affect separation and mechanical properties of hollow fiber membranes [39]. Usually, spinnerets contain straight annular channels with a high annulus length/flow ratio, which typically results in high shear stresses. Wang et al. [39] reported that macrovoid formation in asymmetric UF-type polyethersulfone (PES) hollow fibers can be suppressed by altering the flow angle using a conical spinneret.

7.5. Co-extrusion of thin layers of expensive high performance polymers

Single step dual-layer spinning technology (co-extrusion) offers a way to use expensive high performance polymers as separating layer. The application of thin layers of a high performance polymer, having potentially superior plasticization resistance, on a cheap porous support only requires small amounts of polymer (~ 1 g/m^2 surface area). Additionally, dual-layer fiber spinning offers the opportunity to optimize the properties of both layers separately. This also gives the opportunity to study the thickness dependent plasticization behavior of high-performance polymers. The technology of single step dual layer fiber spinning or co-extrusion was developed by Ube Industries Ltd. [40] and Du Pont [41] in the beginning of the 1990s.

A few scientific papers report the preparation of single step dual-layer hollow fiber membranes [42-44]. Most researchers encounter problems with delamination of the top layer due to different shrinkage rates of the two layers during drying. Jiang et al. [45] described the preparation of dual layered hollow fiber membranes with PES as the porous inner layer and Matrimid as the selective outer layer. The adhesion of the two layers is determined by inter-layer diffusion phenomena. Interlayer diffusion may be increased by improving the interaction between the two layers. The addition of the inner layer material, PES, to the Matrimid solution of the outer layer improves the interaction between the two layers. Chapter 2 of this thesis shows that PES/Matrimid-blending results in improved CO_2/CH_4-separation properties. Therefore we prepared dual-layered hollow fiber membranes consisting of a 20/80 wt.% PES/Matrimid-blend as the outer layer and PES as the inner layer. Spinning parameters were chosen according to the paper of Jiang et al. [45], except for the velocity of the inner layer solution, which was 1.0 ml/min or 1.5 ml/min. Figure 3 shows the overall and outside cross-sections of dual-layered fibers spun at an inner layer velocity of (a) 1.0 ml/min and (b) 1.5 ml/min.

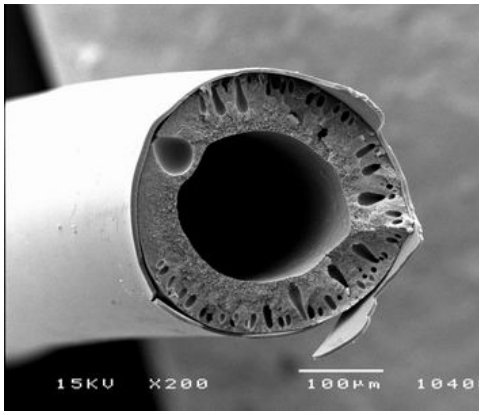

(a) Magnification: 200x

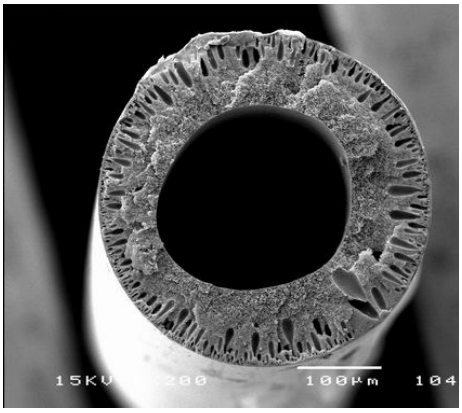

(b) Magnification: 200x

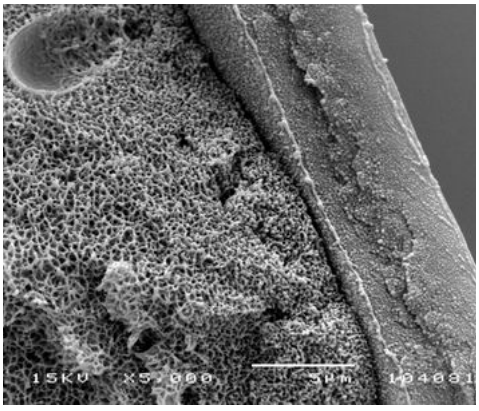

(a) Outside, magnification: 5000x

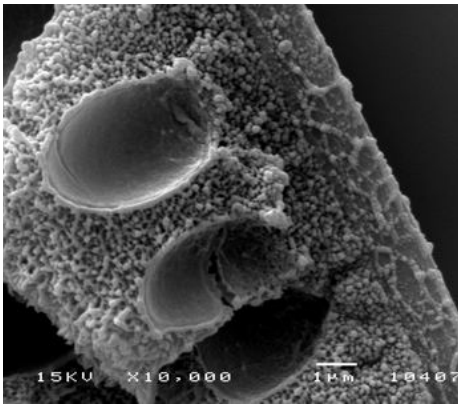

(b) Outside, magnification: 10.000x

Figure 3: Cross-sections of asymmetric dual-layered PES/Matrimid-PES hollow fibers prepared with (a) an inner layer velocity of 1.0 ml/min and (b) an inner layer velocity of 1.5 ml/min.

No delamination is observed with dual-layer hollow fibers spun at a velocity of the inner layer solution of 1.5 ml/min and it seems that both layers are fairly well interconnected. The thickness of the outer layer decreases from ~7 µm to ~1.5 µm by increasing the velocity from 1.0 ml/min to 1.5 ml/min. Further, it results in a significant increase in the amount of macrovoids near the second layer as well, which suggests the presence of a dense skin at the inner layer [46]. This suggests that the velocity of the inner layer solution is an important factor to eliminate delamination. Gas permeation experiments show that the hollow fibers spun at an inner layer velocity of 1.5 ml/min exhibit an O_2/N_2-selectivity of 6.0 with an O_2-permeance of ±1.3 GPU. The obtained O_2/N_2-selectivity is within 90% of the intrinsic value for single layer PES/Matrimid hollow fibers (⟨ = 6.7, see Chapter 2).

However, the selectivity did not improve after plugging surface defects with silicone rubber, which suggests that the outer layer does not contain a dense skin and the selectivity is not determined by the outer PES/Matrimid layer, but by the inner PES-layer. Significant improvements can be made in the recipes of the solutions of both layers. The inner layer should be more open and porous without a skin layer at the outside, which may be achieved by adding high amounts of non-solvents (see Table 2). The outer layer should be denser, which can be obtained by increasing the polymer concentration and adding small amounts of volatile non-solvents (e.g. acetone).

7.6. References

1. E. Piccinini, M. Giacinti Baschetti, and G.C. Sarti, *Use of an automated spring balance for the simultaneous measurement of sorption and swelling in polymeric films*, Journal of Membrane Science **234** (2004), 95-100.
2. A. Rajendran, et al., *Simultaneous measurement of swelling and sorption in a supercritical CO_2-poly(methyl methacrylate) system*, Industrial and Engineering Chemistry Research **44** (2005), 2549-2560.
3. S. Hilic, et al., *Simultaneous measurement of the solubility of nitrogen and carbon dioxide in polystyrene and of the associated polymer swelling*, Journal of Polymer Science, Part B: Polymer Physics **39** (2001), 2063-2070.
4. N.M.B. Flichy, et al., *An ATR-IR study of poly (dimethylsiloxane) under high-pressure carbon dioxide: Simultaneous measurement of sorption and swelling*, Journal of Physical Chemistry B **106** (2002), 754-759.
5. N.H. Brantley, S.G. Kazarian, and C.A. Eckert, *In situ FTIR measurement of carbon dioxide sorption into poly(ethylene terephthalate) at elevated pressures*, Journal of Applied Polymer Science **77** (2000), 764-775.
6. A.M.M. Pereira, et al., *Solvent sorption measurements in polymeric membranes with ATR-IR spectroscopy*, Journal of Membrane Science **260** (2005), 174-180.
7. T. Guadagno and S.G. Kazarian, *High-pressure CO_2-expanded solvents: Simultaneous measurement of CO_2-sorption and swelling of liquid polymers with in-situ near-IR spectroscopy*, Journal of Physical Chemistry B **108** (2004), 13995-13999.
8. S.M. Sirard, et al., *Anomalous properties of poly(methyl methaerylate) thin films in supercritical carbon dioxide*, Macromolecules **35** (2002), 1928-1935.
9. S.M. Sirard, P.F. Green, and K.P. Johnston, *Spectroscopic ellipsometry investigation of the swelling of poly(dimethylsiloxane) thin films with high pressure carbon dioxide*, Journal of Physical Chemistry B **105** (2001), 766-772.
10. J.D. Wind, et al., *Relaxation dynamics of CO2 diffusion, sorption, and polymer swelling for plasticized polyimide membranes*, Macromolecules **36** (2003), 6442-6448.

11. U. Fehrenbacher, et al., *Refractive index and swelling of thin PMMA films in CO2/MMA mixtures at elevated pressures*, Fluid Phase Equilibria **200** (2002), 147-160.
12. G. Dlubek, F. Redmann, and R. Krause-Rehberg, *Humidity-induced plasticization and antiplasticization of polyamide 6: A positron lifetime study of the local free volume*, Journal of Applied Polymer Science **84** (2002), 244-255.
13. D. Cangialosi, et al., *Positron annihilation lifetime spectroscopy for measuring free volume during physical aging of polycarbonate*, Macromolecules **36** (2003), 142-147.
14. J.P. Yuan, et al., *Subnanometer hole properties of CO_2-exposed polysulfone studied by positron annihilation lifetime spectroscopy*, Journal of Polymer Science Part B-Polymer Physics **36** (1998), 3049-3056.
15. X. Hong, et al., *Free-volume hole properties of gas-exposed polycarbonate studied by positron annihilation lifetime spectroscopy*, Macromolecules **29** (1996), 7859-7864.
16. R.A. Assink, *Plasticization of Poly(dimethyl Siloxane) by High-Pressure Gases as Studied by NMR Relaxation*, Journal of Polymer Science Polymer Physics Edition **12** (1974), 2281-2290.
17. M.D. Sefcik and J. Schaefer, *Solid state ^{13}C NMR evidence for gas-polymer interactions in the carbon dioixde-poly(vinyl chloride) system*, Journal of polymer science. Part A-2, Polymer physics **21** (1983), 1055.
18. J.R. Fried, H.C. Liu, and C. Zhang, *Effect of sorbed carbon dioxide on the dynamic mechanical properties of glassy polymers*, Journal of polymer science. Part C, Polymer letters **27** (1989), 385-392.
19. Z.Y. Zhang and Y.P. Handa, *An in situ study of plasticization of polymers by high-pressure gases*, Journal of Polymer Science Part B-Polymer Physics **36** (1998), 977-982.
20. Z.K. Zhong, S.X. Zheng, and Y.L. Mi, *High-pressure DSC study of thermal transitions of a poly(ethylene terephthalate) carbon dioxide system*, Polymer **40** (1999), 3829-3834.
21. A.Y. Houde, S.S. Kulkarni, and M.R. Kulkarni, *Permeation and plasticization behaviour of glassy polymers - a WAXD interpretation*, Journal of Membrane Science **71** (1992), 117-128.
22. Y. Kamiya, K. Mizoguchi, and Y. Naito, *A Dielectric-Relaxation Study of Plasticization of Poly(Ethyl Methacrylate) by Carbon-Dioxide*, Journal of Polymer Science Part B-Polymer Physics **28** (1990), 1955-1964.
23. S.-I. Hirota, et al., *Dielectric relaxation behavior of poly(methyl methacrylate) under high-pressure carbon dioxide*, Journal of Polymer Science Part B: Polymer Physics **43** (2005), 2951-2962.
24. M. Wubbenhorst, C.A. Murray, and J.R. Dutcher, *Dielectric relaxations in ultrathin isotactic PMMA films and PS-PMMA-PS trilayer films*, European Physical Journal E **12** (2003), S109-S112.

25. S.G. Kazarian, *Polymers and supercritical fluids: Opportunities for vibrational spectroscopy*, Macromolecular Symposia **184** (2002), 215-228.
26. M. Al-Juaied and W.J. Koros, *Performance of natural gas membranes in the presence of heavy hydrocarbons*, Journal of Membrane Science **274** (2006), 227-243.
27. L.S. White, et al., *Properties of a polyimide gas separation membrane in natural gas streams*, Journal of Membrane Science **103** (1995), 73-82.
28. J.D. Wind, D.R. Paul, and W.J. Koros, *Natural gas permeation in polyimide membranes*, Journal of Membrane Science **228** (2004), 227-236.
29. R.M. Boom, et al., *Microstructures in phase inversion membranes. Part 2. The role of a polymeric additive*, Journal of Membrane Science **73** (1992), 277-292.
30. O.M. Ekiner and G. Vassilatos, *Polyaramide hollow fibers for hydrogen/methane separation - spinning and properties*, Journal of Membrane Science **53** (1990), 259-273.
31. O.K. Ekiner, *Polyimide blends for gas separation membranes*, WO 2004/050223 A2 (2004)
32. H. Hachisuka, T. Ohara, and K. Ikeda, *New type asymmetric membranes having almost defect free hyper-thin skin layer and sponge-like porous matrix*, Journal of Membrane Science **116** (1996), 265-272.
33. T.S. Chung, W.H. Lin, and R.H. Vora, *The effect of shear rates on gas separation performance of 6FDA-durene polyimide hollow fibers*, Journal of Membrane Science **167** (2000), 55-66.
34. A.F. Ismail, et al., *Direct measurement of rheologically induced molecular orientation in gas separation hollow fibre membranes and effects on selectivity*, Journal of Membrane Science **126** (1997), 133-137.
35. S.J. Shilton, G. Bell, and J. Ferguson, *The rheology of fibre spinning and the properties of hollow-fibre membranes for gas separation*, Polymer **35** (1994), 5327-5335.
36. M.-C. Yang and M.-T. Chou, *Effect of post-drawing on the mechanical and mass transfer properties of polyacrylonitrile hollow fiber membranes*, Journal of Membrane Science **116** (1996), 279-291.
37. C.W. Macosko, *Rheology: principles, measurements, and applications*, 1994, New York: Wiley-VCH.
38. D.W. Wallace, C. Staudt-Bickel, and W.J. Koros, *Efficient development of effective hollow fiber membranes for gas separations from novel polymers*, Journal of Membrane Science **278** (2006), 92-104.
39. K.Y. Wang, et al., *The effects of flow angle and shear rate within the spinneret on the separation performance of poly(ethersulfone) (PES) ultrafiltration hollow fiber membranes*, Journal of Membrane Science **240** (2004), 67-79.
40. Y. Kusuki, T. Yoshinaga, and H. Shimazaki, *Aromatic Polyimide Double Layered Hollow Filamentary Membrane and Process for Producing Same*, US 5.141.642 (1992)

41. O.M. Ekiner, R.A. Hayes, and P. Manos, *Novel multicomponent fluid separation membranes*, US 5.085.676 (1992)
42. D. Li, T.-S. Chung, and R. Wang, *Morphological aspects and structure control of dual-layer asymmetric hollow fiber membranes formed by a simultaneous co-extrusion approach*, Journal of Membrane Science **243** (2004), 155-175.
43. T. He, et al., *Preparation of composite hollow fiber membranes: co-extrusion of hydrophilic coatings onto porous hydrophobic support structures*, Journal of Membrane Science **207** (2002), 143-156.
44. L. Jiang, et al., *Fabrication of Matrimid/polyethersulfone dual-layer hollow fiber membranes for gas separation*, Journal of Membrane Science **240** (2004), 91-103.
45. M. Boehning and J. Springer, *Sorptive dilation and relaxational processes in glassy polymer/gas systems - I. Poly(sulfone) and poly(ether sulfone)*, Polymer **39** (1998), 5183-5195.
46. C.A. Smolders, et al., *Microstructures in phase-inversion membranes. Part 1. Formation of macrovoids*, Journal of Membrane Science **73** (1992), 259-275.

Summary

This thesis describes the thorough investigation of mixed gas transport behavior of asymmetric membranes in the separation of feed streams containing plasticizing gases in order to gain more insights into the complicated behavior of plasticization. To successfully employ gas separation membranes in (new) applications containing plasticizing feed streams, membranes with improved stability have to be developed. Fundamental knowledge on the complicated behavior of plasticization in the separation of these gas streams using asymmetric membranes is an important issue in this development.

In Chapter 2 the mixed gas plasticization behavior of asymmetric hollow fiber membranes consisting of a PES/Matrimid-blend is investigated using CO_2/CH_4- and CO_2/N_2-feed gas mixtures with different feed gas compositions. While typically the CO_2-permeance continuously increases with increasing pressure, the CO_2-permeance showed a continuous decrease after introduction of 2% CH_4 or N_2 to the feed gas mixture. The magnitude of the CO_2-permeance reduction increased with increasing CH_4- or N_2-feed gas concentration. The mixed gas separation factor showed just a moderate decrease as a function of pressure and increased with decreasing CH_4- and N_2-feed gas concentration, suggesting plasticization effects did almost not affect the membrane separation performance. However, N_2-permeance decay experiments, which were performed after exposure to gas mixtures, revealed that plasticization effects were significantly present during the mixed gas experiments. A mixed gas permeation model illustrated that the observed effects can be attributed to the existence of a subtle balance between competition and plasticization effects.

Chapter 3 presents the preparation of asymmetric hollow fiber membranes of a P84/Matrimid-blend for gas separation. Homogeneous polymer blending is an easy way to tune gas separation properties of polymer membranes and it may increase the stability to aggressive feed streams as well. Fibers were prepared from spinning dopes containing different amounts of the volatile additive acetone, which was used to enhance skin formation. At low acetone concentration, high-flux fibers were obtained (skin of ~900 Å)

with an ideal O_2/N_2-selectivity within 80% of the intrinsic value for P84/Matrimid. Low-flux fibers were obtained (skin of ~4000 Å) at high acetone concentration in the spinning dope, having an ideal O_2/N_2-selectivity within 90% of the intrinsic value. Single gas permeation experiments showed that the prepared P84/Matrimid fibers are commercially interesting, as separation properties comparable to those of commercially available membranes for gas separation were obtained.

As presented in Chapter 2 of this thesis, PES/Matrimid asymmetric hollow fiber membranes show a subtle balance between competition and plasticization effects. Therefore in Chapter 4, the mixed gas separation performance of asymmetric CA, PPO, Matrimid and P84/Matrimid membranes in the separation of various CO_2/CH_4-feed gas mixtures was measured in order to study the subtle balance behavior in these membranes. Results showed that a subtle balance exists in all asymmetric membranes, but that this balance highly depends on the magnitude of plasticization and competition effects. Because CO_2-plasticization effects were relatively strong in asymmetric CA and Matrimid membranes, the separation behavior was dominated by plasticization. On the other hand, competition effects dominated the separation behavior of PES/Matrimid, P84/Matrimid and PPO membranes as the effects of competitive sorption were relatively stronger. The highest CO_2/CH_4-mixed gas selectivities were achieved for asymmetric P84/Matrimid membranes, although they were slightly more susceptible to plasticization than PES/Matrimid and PPO membranes, especially at high levels of CO_2 in the feed gas mixture.

Since P84/Matrimid-blending effectively reduces CO_2-plasticization effects, it may improve the stability to C_3-hydrocarbons as well. Chapter 5 investigates the C_3-hydrocarbon separation performance of P84/Matrimid hollow fiber membranes in the separation of a binary and ternary C_3-based feed gas mixture. The C_3H_6/C_3H_8-separation performance of asymmetric P84/Matrimid membranes is significantly affected by plasticization effects induced by ptopylene. The C_3H_6/C_3H_8-mixed gas selectivity decreases with increasing propylene partial pressure due to a relatively strong increase in propane permeance, which can be attributed to plasticization by propylene. The addition of CH_4 to the feed gas mixture in C_3-hydrocarbon separation hardly affects the C_3H_6/C_3H_8-separation behavior of P84/Matrimid, which suggests that plasticization effects are much more pronounced than competition effects. Apparently, P84/Matrimid-

blending does not result in improved stability to feed streams containing significant amounts of C_3-hydrocarbons.

The kinetic sorption behavior of six different gases in the glassy polymer Matrimid polyimide is investigated in Chapter 6 using gravimetric sorption. The results show that any gas can induce sorption relaxations upon reaching a certain threshold amount of volume dilation, which is related to gas solubility and partial molar volume of a gas. Furthermore, the relative change of the concentration dependent diffusion coefficient is related to the square of the partial molar volume, which fits in the theoretical framework of Kirchheim describing the sorption of gases assuming a continuous distribution of dissolution energies.

Chapter 7 suggests future research directions based on the findings presented in this thesis. Some preliminary results of scouting experiments support the proposed research directions.

Samenvatting

Dit proefschrift beschrijft een grondig onderzoek naar het transportgedrag van asymmetrische gasscheidingsmembranen in de scheiding van voedingsstromen die plastificerende gassen bevatten. Dit om meer inzicht te krijgen in het complexe gedrag van plastificering. Gasscheidingsmembranen zullen pas met succes worden toegepast in (nieuwe) toepassingen met plastificerende voedingsstromen wanneer membranen met een verbeterde stabiliteit worden ontwikkeld. Fundamentele kennis in het complexe gedrag van plastificering in de scheiding van deze gasstromen met asymmetrische membranen is een belangrijk punt in deze ontwikkeling.

In Hoofdstuk 2 is het menggasplastificeringsgedrag onderzocht van asymmetrische holle vezelmembranen gemaakt van een PES/Matrimid-mengsel, waarbij CO_2/CH_4- en CO_2/N_2-gasmengsels met verschillende voedingssamenstellingen zijn gebruikt. Terwijl normaal gesproken de CO_2-permeabiliteit continu toeneemt met toenemende druk, werd een continu dalende CO_2-permeabiliteit waargenomen na het toevoegen van 2% CH_4 of N_2 aan het voedingsmengsel. De sterkte van de daling van de CO_2-permeabiliteit als functie van druk nam toe bij toenemende CH_4- of N_2-voedingsgasconcentratie. De menggasselectiviteit daalde licht als functie van druk en nam toe bij afnemende CH_4- of N_2-voedingsgasconcentratie, wat suggereerde dat plastificeringseffecten de scheidingsprestatie van de membranen nauwelijks beïnvloed hebben. N_2-permeabiliteitsmetingen die zijn uitgevoerd na blootstelling aan gasmengsels, brachten echter aan het licht dat plastificeringseffecten significant aanwezig waren tijdens de menggasexperimenten. Een menggaspermeatiemodel illustreerde dat de waargenomen effecten konden worden toegeschreven aan het bestaan van een subtiele balans tussen effecten van competitieve sorptie en plastificering.

Hoofdstuk 3 presenteert de bereiding van asymmetrische holle vezelmembranen bestaande uit een P84/Matrimid-mengsel voor gasscheiding. Het homogeen blenden van polymeren is een gemakkelijke methode om de gasscheidingseigenschappen van polymere membranen aan te passen en kan tevens de stabiliteit verbeteren tot plastificerende voedingsstromen. Vezels werden bereid van polymeeroplossingen met verschillende hoeveelheden van het

vluchtige additief aceton, dat gebruikt werd om het ontstaan van een dichte toplaag te verbeteren. Bij lage concentraties aceton werden vezels verkregen met een zeer hoge flux (toplaag van ~900 Å) en een ideale O_2/N_2-selectiviteit die meer dan 80% van de intrinsieke waarde voor P84/Matrimid bedroeg. Vezels met een lage flux (toplaag van ~4000 Å) en een ideale O_2/N_2-selectiviteit die meer dan 90% van de intrinsieke waarde bedroeg werden verkregen bij het gebruik van een hoge acetonconcentratie in de polymeeroplossing. De gaspermeatiemetingen toonden aan dat de geproduceerde P84/Matrimid-vezels commercieel interessant zijn, gezien het feit dat de gemeten scheidingseigenschappen vergelijkbaar zijn met die van commercieel verkrijgbare gasscheidingsmembranen.

Zoals beschreven in Hoofdstuk 2 bestaat er een subtiele balans tussen competitieve sorptie en plastificering in PES/Matrimid asymmetrische holle vezelmembranen. Om deze reden is in hoofdstuk 4 de menggasscheidingsprestatie van asymmetrische CA-, PPO-, Matrimid- en P84/Matrimid-membranen gemeten in de scheiding van verschillende CO_2/CH_4-voedingsgasmengsels om het gedrag van deze subtiele balans in deze materialen te bestuderen. De resultaten toonden aan dat er een subtiele balans bestaat in alle gebruikte asymmetrische membranen, maar dat deze sterk afhangt van de relatieve sterktes van de effecten van plastificering en competitie. Omdat plastificeringseffecten relatief sterk zijn in asymmetrische membranen van CA en Matrimid, werd het scheidingsgedrag sterk gedomineerd door plastificering. Competitie-effecten daarentegen domineerden het scheidingsgedrag van PES/Matrimid-, P84/Matrimid- en PPO-membranen, omdat dit effect het sterkst aanwezig is. De hoogste CO_2/CH_4-menggasselectiviteiten werden behaald voor P84/Matrimid-membranen, ondanks het feit dat ze licht gevoeliger zijn voor plastificering dan PES/Matrimid- en PPO-membranen, met name bij hoge CO_2-concentratie in het voedingsgasmengsel.

Aangezien het blenden van P84 en Matrimid een effectieve manier is om CO_2-plastificeringseffecten te verminderen, zou het tevens de stabiliteit tot hogere koolwaterstoffen (C_{3+}) kunnen verbeteren. Hoofdstuk 5 onderzoekt de scheidingsprestatie van P84/Matrimid holle vezelmembranen in de scheiding van binaire en ternaire C_3-gebaseerde voedingsgasmengsels. De C_3H_6/C_3H_8-scheidingsprestatie van asymmetrische P84/Matrimid-membranen werd significant beïnvloed door plastificeringseffecten die veroorzaakt zijn door propyleen. De C_3H_6/C_3H_8-menggasselectiviteit daalde met

toenemende partiaaldruk van propyleen door een relatief sterke stijging in de propaanpermeabiliteit, wat gerelateerd kon worden aan plastificering door propyleen. De toevoeging van CH_4 aan een voedingsgasmengsel in de C_3-koolwaterstof gebaseerde scheiding beïnvloedde nauwelijks het C_3H_6/C_3H_8-scheidingsgedrag van P84/Matrimid-membranen, wat suggereerde dat plastificeringseffecten veel sterker aanwezig zijn dan competitieve sorptie-effecten. Blijkbaar resulteert het blenden van P84 en Matrimid niet in een verbeterde stabiliteit tot voedingsstromen die significante hoeveelheden C_3-koolwaterstoffen bevatten.

Het kinetische sorptiegedrag van zes verschillende gassen is onderzocht in het glasachtige polymeer polyimide (Matrimid) met behulp van gravimetrische sorptiemetingen in Hoofdstuk 6. De resultaten toonden aan dat elk gas in staat is om sorptierelaxaties te veroorzaken mits een bepaalde hoeveelheid volumedilatie wordt bereikt. Dit is gerelateerd aan de oplosbaarheid in het polymeer en het partieel molair volume van het gas. Verder bleek dat de relatieve verandering in de concentratie-afhankelijke diffusiecoëfficiënt is gerelateerd aan het kwadraat van het partieel molair volume van een gas. Dit sluit aan bij het theoretische kader van Kirchheim waarin sorptie beschreven wordt als een continue verdeling van energieniveaus.

Hoofdstuk 7 geeft suggesties voor verder onderzoeksmogelijkheden gebaseerd op de bevindingen die gepresenteerd zijn in dit proefschrift. Deze onderzoeksmogelijkheden worden hierbij toegelicht met enkele resultaten van verkennende metingen.

Dankwoord

Na vier jaar oneindig veel modules maken van zelf gesponnen holle vezelmembranen om deze vervolgens oneindig vaak door te meten is het moment dan eindelijk daar: mijn proefschrift is af. Maar dit proefschrift is natuurlijk niet tot stand gekomen zonder de hulp en toewijding van anderen. Daarom wil ik hier alle mensen bedanken die mij geholpen en geïnspireerd hebben tijdens de afgelopen vier jaar.

Allereerst wil ik Matthias Wessling, mijn promotor en gedurende het laatste anderhalf jaar tevens mijn dagelijkse begeleider, bedanken. Jouw enthousiaste en inspirerende manier van spreken deed mij al snel besluiten dat ik verder wilde in de membraanwereld. Gelukkig kreeg ik de kans om na mijn afstuderen verder te gaan met promoveren in het vakgebied membraantechnologie. Samen met Geert-Henk heb je mij de afgelopen vier jaar wegwijs gemaakt in de wereld van gasscheiding. Je gaf me altijd veel vertrouwen. Ik vond het altijd zeer prettig om met je samen te werken.

Geert-Henk Koops is de eerste twee en een half jaar van mijn promotietijd mijn dagelijkse begeleider geweest. Ook bij jou kon ik altijd terecht voor vragen, problemen of een discussie, zelfs als je zeer druk was met het EMI. Ik heb erg veel van je geleerd en wil je daarom bedanken voor alle hulp in de periode dat we hebben samengewerkt.

Kitty Nymeijer was dan niet mijn dagelijks begeleider, toch heb ik dat wel zo gevoeld gedurende de laatste paar maanden van mijn promotie. Vele uurtjes heb je extra gemaakt – zelfs thuis en op congres – om mij van de nodige feedback op mijn proefschrift te voorzien. Daarnaast kon ik gelukkig ook bij jou terecht voor het uiten van frustraties. Ik wil je bedanken voor al je hulp, ondersteuning en de altijd fijne samenwerking.

I should not forget to thank my master students, Nayeli, Koray en Lisanne. The fact that only the work of Nayeli can be found in this thesis (Chapter 4), does not mean that the others did a less good or interesting job.

Arian Nijmeijer (Shell) en Jaap Vente (ECN), bedankt voor jullie actieve inbreng tijdens de besprekingen van de gebruikerscommissie en jullie inzet tot het mogelijk maken van experimenteel werk op jullie laboratoria.

Met een aantal (oud)-collega's heb ik vele discussies gehad over onderwerpen die in dit proefschrift terugkomen. Van deze momenten heb ik erg veel geleerd en ze hebben zeker een positief bijdrage gehad in het tot stand komen van dit boekje. Hylke, Jens, Jorrit, Wilbert, Jonathan en Sybrand: bedankt!

I would like to thank my (former) roommates (Zhang, Olga, Wilbert en Hakan) for the nice time in room 1342. Greet, ik wil je bedanken voor alle (papieren) zaken die niets met wetenschap te maken hebben maar wel gedaan moeten worden tijdens een promotie, maar ook voor de altijd fijne gesprekken. Herman en John, jullie wil ik bedanken voor alle technische hulp rond veel van mijn experimentele werk.

All other MTG-colleagues I would like to thank for the very nice time the past four years. It has always been a great pleasure to work in the membrane group and the atmosphere has always been relaxed and pleasant. The many group activities (go-karting, bowling, soccer and volleyball games, sailing, bicycle tour, borrelen in the Geus, etc.) were a nice break during (and after) work.

Na het werk was er gelukkig altijd nog genoeg tijd over om me sportief uit te leven bij volleybalvereniging Harambee. Ik wil dan ook al mijn (oud)-teamgenoten en vrienden van Harambee bedanken voor de gezellige tijd.

Albert Bokkers en Hylke Sijbesma zullen mij vergezellen op het podium tijdens mijn verdediging. Ik ben jullie hier erg dankbaar voor. Hylke, ik wil je speciaal bedanken voor het feit dat je altijd tijd had tijdens het werk voor een goed gesprek, een discussie, een vraag of hulp bij experimentele problemen. Albert, ik wil je bedanken voor de periode dat we huisgenoten waren, voor de avonden en soms weekenden dat we als gele kanaries op het zand stonden en voor tegenwoordig de gezellige avonden in de Arena bij wedstrijden van Ajax of Oranje.

Ma en Pa, het doen van een promotie, maar ook het volgen van een universitaire studie was niet mogelijk geweest zonder jullie steun. Jullie hebben mij de kans gegeven en mij altijd aangespoord mij verder te ontwikkelen. Ook hebben jullie altijd interesse getoond in mijn werk, ondanks het feit dat het niet altijd even duidelijk zal zijn geweest wat ik nu precies aan het doen was in Twente. Bedankt voor al jullie steun en interesse.

Als laatste wil ik Ingrid bedanken. Thuis kon ik altijd bij jou mijn verhaal kwijt, of het nou over experimentele problemen of over iets ging wat ik niet snapte. Geduldig wachtte je dan mijn verhaal af en probeerde dan daar een zo goed mogelijk antwoord op te geven. Zonder jouw steun, geduld en liefde had ik dit niet gered. Het is nu mijn beurt om jou zo goed mogelijk te ondersteunen bij jouw laatste deel van je promotie. Ik hou van je.

Tymen

Levensloop

Tymen Visser is geboren op 10 december 1977 te Zevenaar. Na de lagere school ('t Scathe te Pannerden) heeft hij in 1996 zijn VWO-diploma gehaald aan het Liemers College te Zevenaar. In hetzelfde jaar begon hij met zijn studie Chemische Technologie aan de Universiteit Twente te Enschede. Zijn stage werd uitgevoerd bij ECN te Petten in het voorjaar van 2001 aan het onderwerp "Applying a mesoporous silica coating on a α_2-alumina support with the dipcoating technique". Zijn afstudeeropdracht met de titel "Stable composite hollow fiber membranes for olefin/paraffin separation" werd uitgevoerd bij de vakgroep Membraantechnologie van Prof. M. Wessling en werd afgerond in juni 2002. In augustus 2002 begon hij binnen dezelfde vakgroep met zijn promotie-onderzoek getiteld "Mixed gas plasticization phenomena in asymmetric membranes". Dit onderzoek is uitgevoerd onder de begeleiding van Prof. M. Wessling die tevens fungeerde als promotor. Het promotie-onderzoek was gericht op het fundamenteel inzicht krijgen in verschijnselen die optreden tijdens het scheiden van gasmengsels met behulp van asymmetrische polymeer membranen. Sinds september 2006 is hij werkzaam als onderzoeker bij het EMI te Enschede.